VNIVERSITAT DE VALÈNCIA

FACULTAD DE CIENCIAS BIOLÓGICAS
Departament de Bioquímica y Biologia Molecular

Doctorado en Biotecnología

Role of TNF-α receptor 2 (TNFR2) in the regulation of adult neural stem cells

Germán Belenguer Sánchez

Directores de la Tesis Doctoral

Isabel Fariñas Gómez
Jose Manuel Morante Redolat

Valencia, mayo de 2017

Dña. Isabel Fariñas Gómez, Profesora Catedrática del Departamento de Biología Celular, Biología Funcional y Antropología Física, de la Facultad de Ciencias Biológicas de la Universidad de Valencia y, D. Jose Manuel Morante Redolat, Profesor Ayudante Doctor del Departamento de Biología Celular, Biología Funcional y Antropología Física, de la Facultad de Ciencias Biológicas de la Universidad de Valencia

INFORMAN QUE:

D. Germán Belenguer Sánchez, licenciado en Biología y Bioquímica por la Universidad de Valencia, ha realizado bajo su dirección el trabajo titulado "*Role of TNF-α receptor 2 (TNFR2) in the regulation of adult neural stem cells*", y que hallándose concluida, autorizan su presentación, a fin de que pueda ser juzgado por el Tribunal correspondiente para la obtención del grado de Doctor por la Universitat de València.

Y para que conste, en cumplimiento de la legislación, firman el presente informe en Burjassot, a 31 de mayo del 2017.

Dra. Isabel Fariñas Gómez

Dr. Jose Manuel Morante Redolat

Este trabajo de Tesis Doctoral ha sido posible gracias a una beca predoctoral del Programa de Formación de Profesorado Universitario (FPU), financiada por el Ministerio de Educación, Cultura y Deporte, un contrato predoctoral financiado por la RETIC de Terapia Celular del ISCIII y un contrato como investigador no doctor financiado por la red "CIBER en Enfermedades Neurodegenerativas" CIBERNED. La investigación ha sido financiada por los siguientes proyectos de investigación:

- "Dinámica celular y auto-renovación en poblaciones de células madre del cerebro adulto". Plan Nacional de I+D+I MINECO, Ministerio de Economía y Competitividad, SAF2011-13332. (2012 - 2014).

- "Estudio de células madre en el ámbito de las investigaciones básicas en terapia celular", Fundación Botín-Banco Santander. (2014 – 2018).

- "CIBER en Enfermedades Neurodegenerativas" (CIBERNED), ISCIII,CB06/05/0086. (2006 - actualidad).

A mis padres,

Miguel Angel y Obdulia

A mi hermano,

Migue

A ti, mi amor,

Jenni

Me gustaría dedicar esta página a todas las personas que con su granito de arena (o la playa entera…) me han ayudado a alcanzar la meta de un maratón que ha durado 6 años.

En primer lugar me siento agradecido contigo, Isabel, por la oportunidad que me concediste en su día, por confiar en mí y por todo lo que ha supuesto realizar una tesis a tu lado. No solo me has puesto la caña en las manos sino que me has enseñado a pescar. Sinceramente, creo que no encontraría un lugar mejor donde formarme personal y profesionalmente. Formar parte de tu equipo es un orgullo por el que siempre estaré agradecido.

Y por supuesto a Jose Manuel. Sabes que no hay suficientes páginas para poder expresar mi agradecimiento a todo lo que has hecho por mí, tanto dentro como fuera del laboratorio, sujetándome en todo momento, impidiendo que me caiga. Simplemente, ¡gracias! Solo espero que sientas este trabajo tan tuyo como mío. Y a Eva. Espero que ambos podáis sentiros orgullosos de vuestro pequeño padawan. Ambos pusisteis las primeras piedras, me disteis todas las herramientas necesarias y me habéis llevado hasta la meta.

Y a mis neuromoles. A todos los compañeros, con los que he compartido alegrías y fracasos, lloros y risas, buenos y malos momentos que quedan grabados también en esta tesis. Y en especial a mi CFN, ¡el motor del lab! Gracias por vuestro apoyo, estando cerca o lejos, os he sentido a mi lado empujando. Y también a nuestros magníficos tecnomoles, que nos allanan cada día el camino, vuestra labor ha sido esencial.

También quiero agradecer al Dr. Luís Parada y a todos los miembros de su laboratorio por abrirme las puertas de su casa en el UTSW Medical Center de Dallas dándome la oportunidad de conocer la ciencia en otros lugares y seguir formándome.

Agradezco también el trabajo de los profesionales de la secretaría del departamento de Biología Celular, Funcional y Antropología Física y de los distintos servicios del SCSIE, en especial al servicio de cultivos celulares y citometría, al servicio de microscopía y a los técnicos del animalario del campus de Burjassot que con su labor han permitido completar este trabajo.

Gracias también a vosotros, mi grupo, mis "monitores" y mis "torres del mar", mis amigos que me habéis ayudado, me habéis animado y habéis estado a mi lado desde el principio. Habéis sido ese oasis necesario para reponer fuerzas y no desfallecer.

A mis padres, Miguel Ángel y Obdulia, y a mi hermano Migue y a Giusy, a los que os dedico esta tesis. Vosotros me habéis dado la base, habéis puesto los cimientos y me habéis convertido en la persona que soy. Gracias por vuestro apoyo incondicional, sabéis que sois mi pilar fundamental. Solo espero que os sintáis la mitad de orgullosos de lo que yo estoy de vosotros. Y a todos los miembros de mi familia, de Gandía y de Alcoy, porque sé que han estado a mi lado durante todo este tiempo. Y así lo he sentido.

Quiero terminar mis agradecimientos contigo, Jenni, con mi columna vertebral, mi guía, mi animadora, mi compañera de vida, mi amor. Gracias por todo. Gracias por tu apoyo incondicional, por tus consejos, por tu paciencia. Gracias por creer y confiar en mí. Sabes que este trabajo es tan tuyo como mío.

Simplemente, ¡gracias!

Index

Abbreviation list

ADAMTS-7	disintegrin and metalloproteinase with thrombospondin type 1 motif 7
aNSC	active NSC
Ara-C	β-D-arabinofuranoside
ASCL1	achaete-scoute homologue 1
BBB	blood-brain barrier
BLBP	brain lipid-binding protein
BMP	bone morphogenetic protein
BSA	bovine serum albumin
CC	corpus callosum
CDK	cyclin-dependent kinases
ChP	choroid plexus
cIAP	cellular inhibitors of apoptosis
CldU	5-Chloro-2'-deoxyuridine
CNS	central nervous system
CSC	cancer stem cell
CSF	cerebrospinal fluid
DAPI	4',6-diamidine-2'-phenylindole dihydrochloride
DCX	doublecourtin
DDAO	Cell Trace Far Red DDAO-SE
DFFDA	Cell trace Oregon Green 488 Carboxy-DFFDA-SE
DKO	TNFR1 and TNFR2 double *knock-out*
DLK1	delta-like homologue 1
DMEM	Dulbeccos modified eagle medium
DNMT3A	DNA methyl transferase 3A
DRC	DDAO retaining cell
EBSS	Earle´s Balanced Salt Solution
ECM	extracellular matrix
EDTA	Ethylenediaminetetraacetic acid
EGF	epidermal growth factor
EGFR	epidermal growth factor receptor
EPO	erythropoietin
ESC	embryonic stem cell
FACS	fluorescence activated cell sorting
FADD	Fas-associated death domain
FBS	foetal bovine serum
FGF	fibroblast growth factor
FSC	forward scatter
FTLD-TDP	frontotemporal lobar degeneration with ubiquitinated TDP-43-positive
GABA	gamma-aminobutyric acid
GCL	granule cell layer
GFAP	glial fibrillary acidic protein
GL	glomerular layer
GLAST	glutamate aspartate transporter
GRN	granulin
GSC	germ stem cell
HB	heparin binding
HBSS	Hanks balanced salt solution
HGF	hepatocyte growth factor
HIF1-α	hypoxia inducible factor-1 alpha
HSC	hematopoietic stem cell
i.p.	intraperitoneal
ICM	inner cell mass
IdU	5-Iodo-2'-deoxyuridine
IFN	interferon
IGF-2	insulin growth factor 2
IkB	inhibitor kB
IKK	IkB kinase complex
IL	interleukin
kDa	kilo daltons
LIF	leukaemia inhibiting factor
LPS	lipopolysaccharide
LRC	label-retaining cells
MACS	magnetic activated cell sorting
MCM	microglia conditioned media
MMP	matrix metalloproteinase
mTOR	mechanistic target of rapamycin
MuSC	muscle stem cell

NFκB	nuclear factor kappa B
NSA	neurosphere assay
NSAID	non-steroidal anti-inflammatory drug
NSC	neural stem cell
NT3	neurotrophin 3
OB	olfactory bulb
PB	phosphate buffer
PBS	phosphate buffer saline
PCR	polimerase chain reaction
PEDF	pigmented epithelium-derived factor
PFA	paraformaldehyde
PGRN	progranulin
PRC1	poly-comb repressive complex 1
PSA-NCAM	polysialylated neural-cell-adhesion molecule
qNSC	quiescent NSC
qRT-PCR	quantitative real-time PCR
R1KO	TNFR1 *knock-out*
R2KO	TNFR2 *knock-out*
RGC	radial glial cell
RIP	receptor interacting protein
RMS	rostral migratory stream
ROS	reactive oxygen species
RT	room temperature
SAPKS	stress-activated protein kinases
SC	stem cell
SDF1	stromal cell-derived factor 1
SDS-PAGE	sodium dodecyl sulfate polyacrylamide gel electrophoresis
SEZ	sub-ependymal zone
SGZ	sub-granular zone
Shh	sonic hedgehog
SOX	sex determining region Y-box
SSC	side scatter
T/E	Trypsin/EDTA
TACE	TNF-α converting enzyme
TAP	transit amplifying progenitor
TBS-T	Tris-buffered saline tween 20
TE	trophectoderm
TF	transcription factor
TFG-β	transforming growth factor
TMZ	temozolomide
TNF	tumor necrosis factor
TNFR1	TNF-α receptor 1
TNFR2	TNF-α receptor 2
TRADD	TNF receptor-associated death domain
TRAF2	TNF receptor-associated factor 2
TX-100	Triton^{TM} X-100
VCAM1	vascular cell adhesion molecule-1
VEGF	vascular endothelium derived factor
V-SVZ	ventricular-subventricular zone
VZ	ventricular zone
WT	wild-type

Introduction

1. Adult stem cells (SCs): functional units of homeostasis and tissue repair

1.1. Tissue-specific SCs

Adult stem cells (SCs) are unique tissue-resident cells with the ability to perpetuate (self-renewal) while producing new tissue-specific differentiated cells (multipotency) and represent the essential component for the maintenance of tissue homeostasis and repair in multicellular organisms (Barker et al., 2010). The totipotent zygote soon starts to divide after fecundation giving rise to the inner cell mass (ICM) and the trophectoderm (TE). During the initial stages of embryonic development, the pluripotent cells from the ICM expand until they generate the three germ layers (endoderm, mesoderm and ectoderm). From here and along the embryonic development, pluripotent cells start a process of increasing commitment losing their pluripotency and generating all the variety of differentiated tissue-specific cell types. However, not all the somatic cells are differentiated and discrete populations of multipotent SCs persist during the adult lifespan to ensure tissue renewal and a certain degree of tissue regeneration in response to injury (Fuchs et al., 2004; Weissman, 2000).

In homeostatic conditions, SCs are relatively quiescent cells that divide infrequently to produce new SCs and non-renewing, rapidly cycling cells or transit amplifying progenitor (TAP) cells that will proliferate for a discrete number of cycles to eventually differentiate into functional cells of the particular tissue. This hierarchical relation represents a conservative mechanism that preserves the SC genomic integrity by limiting the number of times SCs divide thereby preventing their premature differentiation and guaranteeing the availability of SCs during adulthood. However, this process requires a finely regulated equilibrium between self-renewal, proliferation and differentiation to ensure efficient replacement of cells while limiting pathological situations such as cancer (Biteau et al., 2011).

The inherent abilities of SCs for tissue regeneration convert them, together with the use of embryonic pluripotent stem cell (ESC), in fundamental candidates for regenerative medicine and tissue repair. Thus, the identification of *bona fide* SCs and the understanding of their biology and regulation and how organs maintain and repair themselves in the postnatal organism are crucial requirements before a successful cell therapy is achieved. Furthermore, the evidences that cancer stem cells (CSCs) are originated from somatic SCs (Alcantara Llaguno et al., 2009; Barker et al., 2009; Lapouge et al., 2011; Youssef et al., 2010) not only reinforce the idea that a precise control of stem cell proliferation is required to prevent tumour formation, but also opens new perspectives for the identification of molecular similarities between CSCs and tissue-specific SCs that would undoubtedly yield new targets for cancer therapy.

1.2. Dynamics and heterogeneity of adult SCs in homeostasis

In the last decades, different SCs have been identified and proven to act as true stem cells in many tissues. The discovery of hematopoietic stem cells (HSCs) residing at the bone marrow represented the first demonstration about the existence of cells with self-renewal and multipotency properties (Till and Mc, 1961) and, since then, this system has played a leading role in the stem cell field and has greatly helped in setting the standards for the characterization of other tissue-specific SCs (Weissman, 2000). The discovery of SCs in a variety of tissues with different cell replacement dynamics such as the intestinal epithelium, the hair follicles, the peripheral and central nervous system, the skin or the muscles has highlighted the existence of a remarkable diversity of SCs differing in their identifying markers, degree of multipotentiality, or proliferative dynamics and thus, contrary to what it was previously thought, SCs do not constitute a homogeneous population. Instead, they rather represent an ensemble of single cells in different proliferative states (quiescent or active) with different predispositions to respond to external stimuli (Biteau et al., 2011; Chaker et al., 2016; Li and Clevers, 2010)

(Figure 1). Nowadays there are known several tissues were quiescent and active SCs coexist and participate in the long-term cell turnover; however, it is not fully understood whether they represent two states of the same cell or they are rather different pools, being the quiescent SCs a reservoir of the active pool. In any case, in order to maintain tissue homeostasis, the SC activity actually seems to be controlled at different levels: (1) as mentioned above, the balance between self-renewal, proliferation and differentiation; (2) the induction of SC proliferation in response to injury; and (3) return to a quiescent state after regeneration is achieved.

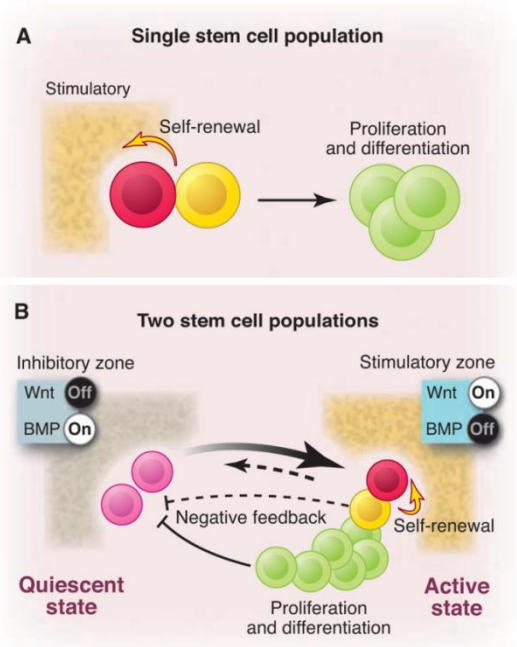

Figure 1. Adult SCs are dynamically heterogeneous. (A) Initially, it was proposed that tissue self-renewal relied on a single relatively quiescent stem cell population which asymmetrically divided to balance self-renewal and differentiation. (B) Instead, SCs co-exist in different proliferative states (quiescent and active) representing separated populations which are maintained by inhibitory and stimulatory cross-signalling. In this currently prevailing model, tissue turnover and regeneration is driven by the interconversion of quiescent and active SCs. Conversely, active stem cells may replace lost quiescent stem cells and, together with the progeny, may contribute to maintain quiescence. The figure depicts the particular situation of intestinal SC as an example. Adapted from Li et al. 2010.

Apart from the heterogeneity in cell dynamics, recent data has evidenced that SCs are also diverse in their self-renewal and differentiation potentials and suggest that different stem cell types co-exist under homeostatic conditions (Dykstra et al., 2007; Ousset et al., 2012; Stange et al., 2013; Van Keymeulen et al., 2011). Furthermore, each SC type seems to have a pre-defined role under normal conditions but they show flexibility after perturbations and can adapt to other functions when required (Goodell et al., 2015). Therefore, the conception of stem cell hierarchy is still currently evolving and new models have been proposed in different tissues such as the hematopoietic and the intestinal stem cell systems (Figure 2). These proposals suggest that SCs initially have different lineage biases to generate specific restricted progenitors that produce a specific differentiated cell. Moreover, the distinct SC types are also progressively committed to a more restricted SC. However, after injury, committed progenitors may revert to a partially-committed stem-like state. Thus, the complexity of this heterogeneous systems with SCs that differ in their dynamics and multipotency has caused that, despite all the progress made since SC discovery, the stem cell regulation is still under thorough study.

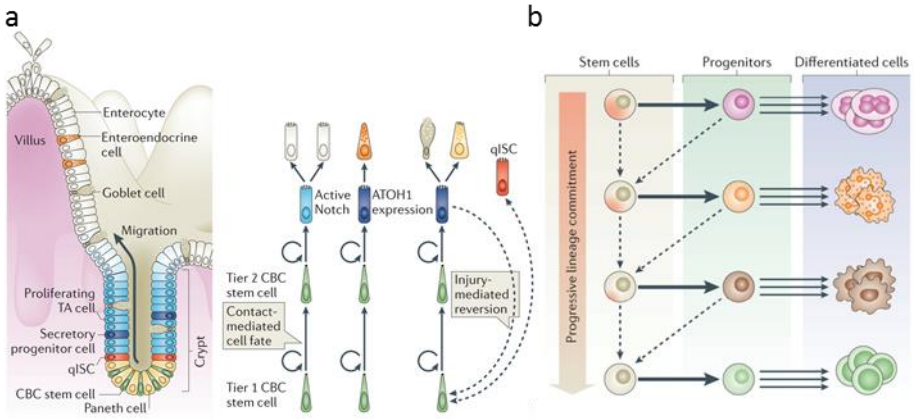

Figure 2. Adult SCs are functionally heterogeneous. Tissue-specific SCs have a pre-defined role under normal conditions and give rise to specific committed progenitors but they show flexibility after perturbations and can adapt to other functions when required**.** Additionally, progenitors may revert to a stem cell state upon extreme injury. Two examples of this are (a) the intestinal and (b) the hematopoietic SC systems. Adapted from Goodell et al. 2015.

1.3. Quiescence in adult SC populations: a novel level of regulation during homeostasis and injury

Quiescence is a reversible cell cycle arrested state (G_0) and, unlike post-mitotic cells, quiescent SCs keep the ability to re-enter cell cycle and proliferate. This property of stem cells represents a key factor in preserving both the stemness for long-term tissue renewal and their DNA integrity to avoid dysregulation of SCs proliferation and tumorigenesis (Orford and Scadden, 2008). Cellular quiescence is characterized by an un-replicated genome, a specific metabolic status characterized by predominant glycolytic activity, a decreased cell size with increased nuclei to cytoplasm ratio and a reversible suppression of global RNA and protein synthesis. Contrary to the traditional view of quiescence as an inactive default cell state, it is currently known that this condition is rather an active regulated state where molecular changes are taking place in response to niche signals (Rumman et al., 2015). In fact, quiescent SCs are maintained by either growth inhibiting signals or absence of growth-promoting signals and loss of quiescence is associated with compromised tissue regeneration (Daynac et al., 2016; Delgado et al., 2014; Fleming et al., 2008; Porlan et al., 2013a). Furthermore, quiescent SC exhibit better survival ability under adverse conditions and, interestingly, they are activated upon injury to generate new SCs and progenitors (Mich et al., 2014; Rodgers et al., 2014; Rossi et al., 2012; Tian et al., 2011). This current knowledge has generated a novel area of research that is gaining biological significance and relevance within the SC field but, unlike regulation of the activation state of SC, the regulation of quiescence is vastly unknown.

Satellite cells are considered the tissue-specific SC in skeletal muscle (MuSCs) and are characterized by an extremely low turn-over rate during homeostasis. However, after injury, this mainly quiescent population dramatically increases proliferation displaying a huge regenerative capacity (Dhawan and Rando, 2005). Additionally, Rodgers et al. have recently found that the quiescent MuSC residing in

a muscle contralateral to a mechanically injured muscle respond to the distant injury displaying cycling properties different to the previously characterized for quiescent and activated pools. This quiescent 'alert' state (G_{alert}) of MuSCs, as it has been defined, and compared to the quiescent 'dormant' state (G_0), shows a higher predisposition to enter proliferation, an accelerated cell-cycle entry, a higher mitochondrial activity and a slightly bigger size. Moreover, global transcription profiles suggest that it represents an intermediate state between G_0 and active SCs (Rodgers et al., 2014). MuSCs appear to adopt this state in response to remote injuries whose impact on the physiology of the tissue is not enough to trigger SC activation and, hence, expansion of the SC population. Additionally, it has also been observed that other SC population, like the fibroadipogenic progenitors and long-term HSCs, adopt similar alert properties upon distant injury indicating that this quiescent transition is not an isolated phenomenon and may represent a general response to injury. Interestingly, the G_{alert} state reverts to the dormant state following resolution of the inducer (Rodgers et al., 2014). Together, all these data has demonstrated that SCs also undergo dynamic transitions between functional phases in the quiescent state stablishing a novel reversible quiescence cycle model (Figure 3). Moreover, this novel functional state also indicates that dormant SCs in different tissues can adopt an adaptive state in response to signals produced in remote regions of the organism, suggesting the existence of a homeostatic control of adult SCs.

The existence of a quiescence cycle that precedes activation opens a new regulatory level of SC dynamics. The signalling through the hepatocyte growth factor (HGF) receptor cMet was found to activate the mTOR complex 1 (mTORC1) signalling pathway to mediate the G_0-G_{alert} transition in MuSCs. Furthermore, inhibition of mTORC1 completely abolished the acquisition of a G_{alert} state indicating that this pathway may play a central role in the "quiescence cell cycle" (Rodgers et al., 2014) and indicates that this transition must also be a regulated process. Nevertheless, the relevance of the quiescence cycle regulation in tissue

homeostasis and repair or the nature of effectors that control the acquisition of an alert or a dormant state are not already known.

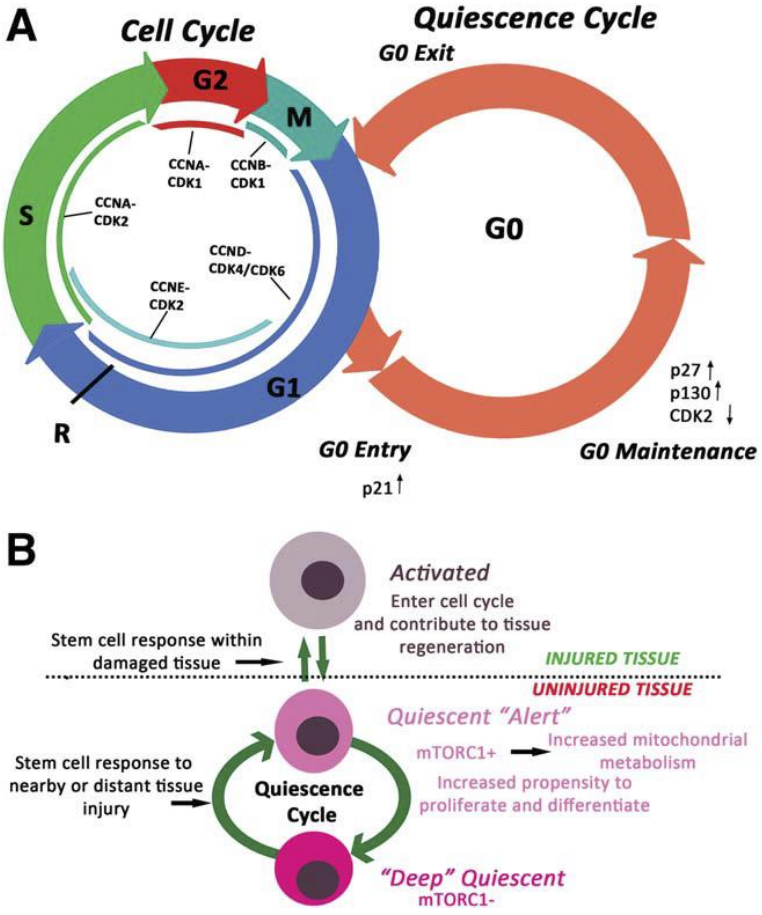

Figure 3. The quiescence SC cycle. (A) In the activated state, SCs progress through the different cell cycle phases to achieve cell division. Once accomplished, cells may enter G_0 quiescent state. This state may be also be regulated for maintenance or release by both intrinsic and extrinsic signals. (B) A quiescence cell cycle has been proposed that would be characterized by two distinct phases: deep or dormant state and alert or primed state. Enrty into the alert phase can be induced by injury signals and is regulated by mTORC1 signalling pathway. The cycle takes into account the reversibility of the alert state indicated by the experimental data. Adapted from Rumman et al. 2015.

1.4. Adult SC niches

SCs reside on specific well-organized neighbourhoods termed 'niches'. The SC niche refers to the specialized microenvironment that surrounds, interact and regulate the SC behaviour to keep a proper balance between quiescence or activation and self-renewal or differentiation, thus playing a fundamental role in tissue homeostasis. The term was initially proposed by R. Schofield in 1978 after observing that HSC proliferative potential differed depending on the location they were isolated from: the spleen or the bone marrow (Schofield, 1978). From there, the hypothesis has been vastly supported by a variety of co-culture experiments (Dexter et al., 1977; Moore et al., 1997; Rios and Williams, 1990) or by SC transplantation into niches in which its components were previously removed through irradiation or drug administration (Brinster and Zimmermann, 1994; Li and Xie, 2005). Schofield proposed that a niche would act as "*an environment… to explain the unlimited proliferation and failure to mature of …stem cells*" by regulating restriction on stem cell entry into cell cycle and differentiation programs, integration of signals reflecting tissue and organismal state, mechanisms for limiting "mutational errors", and imposition of stem cell features on daughter cells. Experimental evidence gathered since then has provided strong support to Schofield´s postulates.

Invertebrate models with simpler stem cell-microenvironment relation like germ stem cells (GSC) in the gonad tips of *Drosophila* and *C. elegans* provided the first examples of discrete niches and their characterization has greatly helped to the identification of SC niches in vertebrates (Morrison and Spradling, 2008; Voog and Jones, 2010). So far, different SC niches have been identified in many tissues, including the germline, bone marrow, skeletal muscle, skin and hair follicles, mammary gland, and digestive, respiratory or central and peripheral nervous systems and their current characterization is starting to resolve the critical components in the SC niche (Wagers, 2012) (Figure 4).

Cell-to-cell interactions between SCs and mesenchymal, vascular, neuronal, glial or inflammatory cells participate in the structural support of the niche, regulates adhesion of SC and produce soluble and membrane-bound signals that control SC function (Wagers, 2012). In particular, adhesion molecules such as integrins or cadherins and signalling molecules such as Sonic hedgehog (Shh), Wnt, bone morphogenetic factors (BMPs), Noggin, Notch, fibroblast growth factors (FGFs) or transforming growth factor-β (TGF-β) have been implicated in the regulation of SCs in tissues like the intestinal epithelium, bone marrow or hair follicles (Li and Xie, 2005). Vasculature, for example, is tightly associated to SC in bone marrow or brain were it plays an important role both in secreting and transporting factors that mediate stem cell self-renewal and proliferation such as vascular endothelium derived factor (VEGF) or pigmented epithelium-derived factor (PEDF) (Bautch, 2011; Ramirez-Castillejo et al., 2006) (see Rafii et al., 2016 for a review). Cells from the immune system are increasingly gaining relevance as an essential stem cell niche component that regulates SCs upon injury but also during homeostasis (Aurora and Olson, 2014) and, due to the topic of this thesis, it requires an independent section that will be later extensively introduced.

Aside the cellular components, SCs interact with non-cellular components like the extracellular matrix (ECM) which participates as a mechanical signal by itself, but also as a reservoir of growth factors, chemokines or other regulatory molecules (Wagers, 2012). The basal lamina directly contacting MuSCs or epidermal stem cells plays a main role during tissue muscle and skin regeneration as they release retained factors after ECM disruption (Choi et al., 2015; Thomas et al., 2015). In the brain, discrete functional aggregates of heparan sulfate proteoglycans and laminin termed fractones are deposited around the neurogenic niches and bind to growth factors with heparin-binding motifs such as FGF-2, heparin-binding epidermal growth factor (HB-EGF) or leukaemia inhibiting factor (LIF) and cytokines such as interleukins (IL), interferons (IFN) or tumour necrosis factor (TNF) controlling their activity on the SCs (Mercier, 2016). More specifically,

expression of the laminin receptor alpha6beta1 integrin allows brain SCs to interact with the basal lamina of irrigating blood vessels and this interaction modulates their activity (Shen et al., 2008).

Finally, different physical parameters such as matrix rigidity, temperature or oxygen tension also influence the stem cell response to the microenvironment (Wagers, 2012). In particular, the oxygen availability greatly influences the adult SC biology (Kimura et al., 2015). O_2 partial pressure varies along the different tissues and it ranges from less than 1% up to 8-9%. It is worth noting that several SC reside in relative hypoxic microdomains such as at the hematopoietic, the mesenchymal or the neural stem cell niche. Interestingly, hypoxia has been related to quiescence maintenance trough the stabilization of the hypoxia inducible factor-1 alpha (HIF-1α) which translocates to the nucleus and regulates the expression of genes related to oxygen homeostasis, glucose metabolism, proliferation or the expression of growth factors such as VEGF or erythropoietin (EPO) (Mohyeldin et al., 2010).

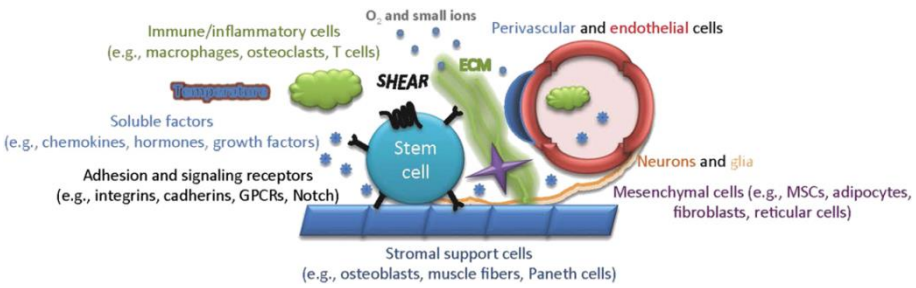

Figure 4. The SC niche. SCs reside in specialized niches composed of both cellular and acellular components that, in general, are common to the vast majority of SC compartments, despite some tissue-specific variations. Cell-cell interactions with mesenchymal, vascular, neuronal, glial or inflammatory cells and soluble factors secreted by these cells, interaction with the ECM and physical parameters as oxygen tension are known regulators of SC behaviour. Adapted from Wagers et al. 2012.

At the organismal level, the crucial role of innervation, i. e. sympathetic innervation to the bone marrow or nerve terminals within neurogenic niches, and systemic circulation, as revealed by parabiosis experiments, in regulating SC niche homeostasis and regeneration in different tissues has strongly emerged in the recent years and has added a new level of complexity to the understanding of niche biology (Conboy and Rando, 2012; del Toro and Mendez-Ferrer, 2013).

2. Subependymal neural stem cells (NSCs) and adult neurogenesis

Nowadays, it is well established that, in the adult vertebrate brain, new neurons are continuously produced throughout adult lifespan (Bond et al., 2015). In adult mammals, neurogenesis mainly occurs in two germinal zones: the sub-granular zone (SGZ) of the dentate gyrus in the hippocampus and the sub-ependymal zone (SEZ; also known as ventricular-subventricular zone or V-SVZ) adjacent to the lateral ventricles. These brain regions harbour discrete populations of neural stem cells (NSCs) which are maintained undifferentiated while they generate new differentiated progeny (Bond et al., 2015). Like in other systems, the discovery of adult neurogenesis (Altman and Das, 1965) and the identification of the responsible tissue-specific SCs (Doetsch et al., 1999a; Seri et al., 2001) led to a shift in our understanding of neural plasticity and opened new perspectives based on the use of this previously denied potential for brain repair upon injury or neurodegeneration. To this goal, the study and knowledge of the NSC biology and regulation may provide the essential tools for an eventual manipulation of endogenous NSCs.

2.1. Adult subependymal NSCs have an embryonic origin

The adult central nervous system (CNS) is derived from the embryonic neuroectoderm, a pseudo-stratified neuroepithelium in the dorsal surface of the developing embryo that invaginates during neurulation to form the neural tube.

The neuroepithelial cells of the neural tube are the embryonic primary precursors of the CNS and proliferate dividing symmetrically to expand the neural tube until the ventricular zone (VZ) is formed. These primary precursors eventually transform into radial glial cells (RGCs) which divide both symmetrically and asymmetrically to generate two RGCs or one RGC and a neuroblast which migrates radially away from the VZ to the expanding neural parenchyma, respectively. Asymmetric division becomes more prominent following the onset of neurogenesis. RGCs have a long basal cytoplasmic process contacting the pial surface which is used by the newborn neurons as guiding scaffolds to migrate up to marginal zones where they differentiate and connect with other neurons (Bjornsson et al., 2015; Kriegstein and Alvarez-Buylla, 2009). At mid-gestation, RGCs can also divide asymmetrically to give rise to intermediate progenitor cells which also contribute to neuron generation. These intermediate progenitors accumulate above the VZ forming a new germinal layer, the sub-ventricular zone (SVZ) which acts as a second germinal zone (Bjornsson et al., 2015). At the end of foetal development, RGCs switch to produce glial and ependymal cells (Figure 5). Thus, foetal RGCs are responsible for the generation of the majority of neurons and of glial and ependymal cells of the adult CNS (Anthony et al., 2004; Malatesta et al., 2000; Miyata et al., 2001; Noctor et al., 2001; Spassky et al., 2005).

After birth, the remaining RGCs in the VZ differentiate either into ependymal cells, that will line the lateral ventricles, or into glial cells, including NSCs that retain many of the RGC features and populate the two adult neurogenic niches (Merkle et al., 2004; Tramontin et al., 2003). Additionally, different recent studies have also demonstrated that during intermediate embryonic stages (E13.5-E15.5), RGCs can eventually derive into NSCs that remain relatively quiescent until adulthood when they can be re-activated (Fuentealba et al., 2015; Furutachi et al., 2015).

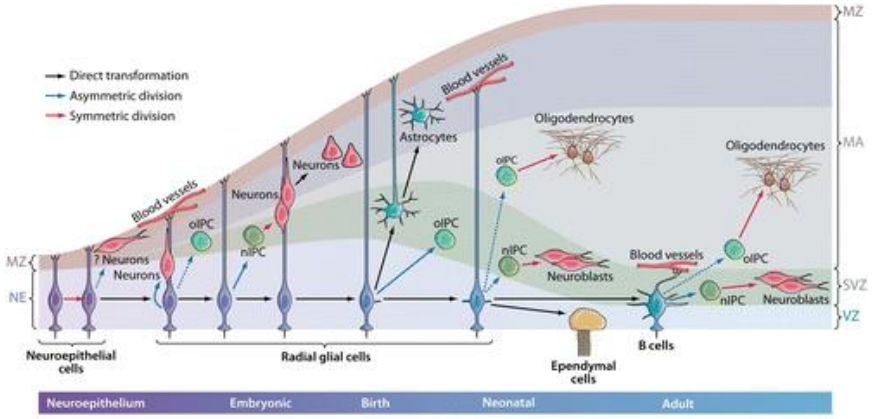

Figure 5. Adult NSCs are lineage-related to embryonic radial glial cells. During development, radial glial cells (RGCs) in the ventricular zone (VZ) first generate neurons and intermediate progenitors (IPCs) and then glial and ependymal cells. Additionally, from mid-gestation to postnatal stages, some RGCs give rise to NSCs that will remain quiescent in specific locations of the brain until postnatal/adults ages. Adapted from Kriegstein et al. 2009.

2.2. The SEZ neurogenic niche: neurogenesis and gliogenesis

The SEZ is a very active neurogenic niche and the largest germinal zone in the adult brain, properties that have promoted its thorough characterization during the last decades. Furthermore, the early establishment of "neurosphere" cultures from this region for molecular and biochemical studies have converted the SEZ into an attractive niche to study NSC regulation. Subependymal NSCs and their progeny are distributed along the entire extent of the lateral ventricle walls, embedded between the ependymal cell layer that coat the ventricular space and the striatum. These residing tissue-specific SCs are responsible of the production of new OB neurons along life. This process follows a hierarchical progression where multipotent NSCs, initially identified as type B1 cells, when activated give rise to TAPs or type C cells which divide a few more times before becoming migrating neuroblasts or type A cells (Doetsch et al., 1999a; Doetsch et al., 1997).

This neurogenic niche continuously generates large numbers of neuroblasts which migrate from the SEZ through the rostral migratory stream (RMS) to the

olfactory bulb (OB). New-born neuroblasts are organized in chains surrounded by a layer of astrocytes and migrate tangentially along this 'gliotubes' to the OB (Doetsch and Alvarez-Buylla, 1996; Lalli, 2014). Here, the arriving immature neuroblasts continue migrating radially to the granule (GCL) and the glomerular (GL) cell layers until they are differentiated and integrated as mature interneurons (Doetsch and Alvarez-Buylla, 1996). SEZ neurogenesis provide different subtypes of interneurons that integrate in the OB contributing to OB function and the neural plasticity of olfactory information processing (Chaker et al., 2016; Livneh et al., 2014; Lledo and Valley, 2016) (Figure 6).

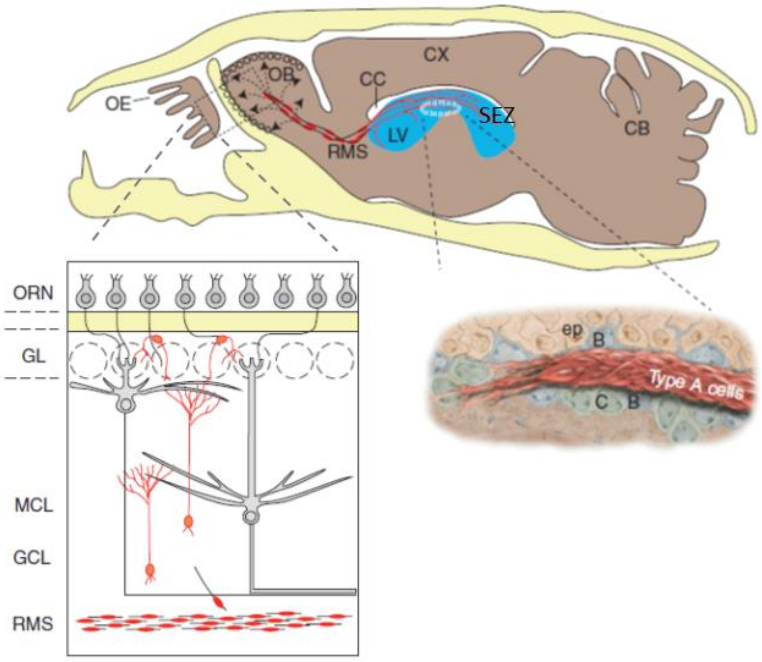

Figure 6. Adult OB neurogenesis from the mouse SEZ. (A) New-born neuroblasts or type A cells produced in the SEZ in the walls of the lateral ventricle (LV) migrate through the rostral migratory stream (RMS) surrounded by astroglial cells to the olfactory bulb (OB). Here, neuroblasts migrate radially and differentiate into mature neurons that integrate in the granular (GCL) and glomerular layers (GL). Adapted from Lim et al. 2016.

Additionally, the SEZ also contributes, although to a lesser extent, to the production of either new niche astrocytes that migrate to the RMS and the corpus callosum (CC), and oligodendrocytes that mainly contribute to the CC re-myelination (Menn et al., 2006; Sohn et al., 2015). Although SEZ gliogenesis is not as productive as neurogenesis under homeostatic conditions, the generation of new oligodendrocytes and astrocytes increases after injury which migrate to the lesioned site and play an active role in tissue repair (Benner et al., 2013; Nait-Oumesmar et al., 1999; Picard-Riera et al., 2002).

2.3. The subependymal NSC lineage

Type B1 NSCs are glial cells that show ultrastructural and molecular features of other brain astrocytes such as the expression of the markers glial fibrillary acidic protein (GFAP), glutamate aspartate transporter (GLAST) and brain lipid-binding protein (BLBP) (Doetsch, 2003; Doetsch et al., 1999a). However, unlike non-neurogenic niche astrocytes which show a branched morphology, B1 cells display a more radial shape (Doetsch et al., 1997) and retain an apical-basal polarity similar to embryonic RGCs contacting the cerebrospinal fluid (CSF) that fills the ventricles through an apical process that ends in a single primary cilium. This primary cilium intercalates among multiciliated ependymal cells organized in structures displaying a pinwheel pattern (Mirzadeh et al., 2008). Type B1 cells also have long basal processes that run radially or tangentially to the ventricular surface for long distances to contact the basal lamina of capillaries of the extensive planar plexus of blood vessels that irrigate this area through specialized cell endings (Shen et al., 2008; Tavazoie et al., 2008) (Figure 7).

It has been long demonstrated that type B1 astrocytes are relative quiescent cells that behave as NSCs under homeostasis and regeneration. The administration of antimitotic drugs revealed the presence of quiescent B1 cells that survive the treatment and completely regenerate the SEZ afterwards (Doetsch et al., 1999b). Additionally, cell-lineage genetic tracing of GFAP cells demonstrated their ability to

generate TAPs and neuroblasts that migrate to the OB (Doetsch et al., 1999a). Furthermore, type B1 cells are also able to form multipotent self-renewing neurospheres *in vitro* that can be maintained and expanded for many passages thus fulfilling *in vivo* and *in vitro* hallmarks of SCs (Doetsch et al., 1999a).

From there, several lineage-tracing strategies have been used to identify the NSC pool studying the potentiality of different marker expressing-cells to behave as NSCs and generate progeny. Inducible Cre drivers such as *Gfap* (Mich et al., 2014), *Glast* (Calzolari et al., 2015; Mich et al., 2014), *Nestin* (Chaker et al., 2015; Imayoshi et al., 2008) and *Gli1* (Ahn and Joyner, 2005; Mich et al., 2014) has demonstrated the ability of this cells to behave as multipotent NSCs generating either OB neurons and astrocytes and oligodendrocytes. Additionally, other lineage-tracing reporters such as *Dlx1* (Mich et al., 2014), *Ascl1* (Kim et al., 2011; Kim et al., 2007; Mich et al., 2014), *Sox1* (Venere et al., 2012), *Sox2* (Kang and Hebert, 2012), *Fgfr3* (Young et al., 2010), *Tlx* (Liu et al., 2008), *Musashi* (Takeda et al., 2013), *Id1* (Nam and Benezra, 2009) or *Hes5* (Giachino et al., 2014) expressing-cells has also showed the ability of this cells to generate new OB neurons but not oligodendrocytes or astrocytes. However, whether a single tripotent NSC exists or, alternatively, there are separated neurogenic and gliogenic compartments is still unclear.

Once activated, type B1 NSCs cells can undergo asymmetric division to self-renew and generate type C cells (Ortega et al., 2013a; Ortega et al., 2013b) which behave as TAP cells dividing symmetrically approximately three times before becoming type A cells, which remain proliferative for one or two more rounds (Ponti et al., 2013). Type C cells start a process of commitment losing the astroglial features of NSCs such as the expression of GFAP or GLAST. Instead, type C cells are characterized by the expression of the transcription factor achaete-scoute homologue 1 (ASCL1) or the ependymal growth factor receptor (EGFR) (Doetsch et al., 2002a). Type A cells, in contrast, are distinguished by the expression of the

neuronal isoform of tubulin β-III-tubulin, doublecourtin (DCX), and polysialylated neural-cell-adhesion molecule (PSA-NCAM) (Doetsch et al., 1997).

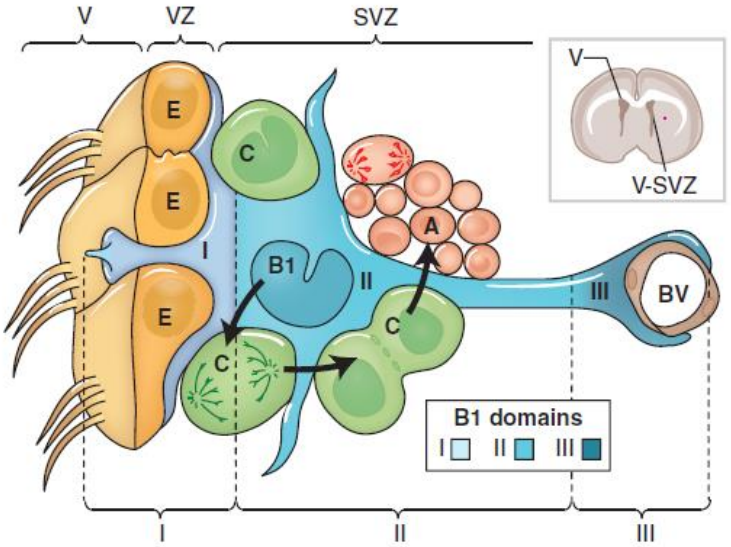

Figure 7. Cell composition and cytoarchitecture of the SEZ. Type B1 NSCs displaying a radial morphology present (I) an apical domain, (II) an intermediate domain and (III) a basal domain. The apical domain ends in a primary single cilium that contacts the lateral ventricle through the ependymal cell layer. Type B1 cells are activated to generate proliferating type C cells and migrating type A cells which are in close contact with the cell body of NSCs in the intermediate domain. The basal domain corresponds to long specialized processes that contact with blood vessels. Adapted from Lim et al. 2016.

Embryonic RGCs, which are highly proliferative, exit the cell cycle during mid-gestation to become NSCs that remain quiescent until they are activated in the adulthood for the generation of OB neurons (Fuentealba et al., 2015; Furutachi et al., 2015). This return to quiescence is an essential event for the establishment and maintenance of the adult NSCs (Furutachi et al., 2013). In the adulthood, unlike other tissues such as the muscle or the liver where almost all SCs remain quiescent under homeostatic conditions, adult NSCs can be found at multiple stages of activation (Codega et al., 2014; Llorens-Bobadilla et al., 2015; Mich et al., 2014). During the earlier characterization of B cells at the ultraestructural level it was

already observed that two types of B cells coexisted lining the ventricles: type B1 cells have light cytoplasm, contact the ventricle and show null replication activity, and type B2 cells with darker cytoplasm, are closer to blood vessels and replicate the DNA content incorporating traceable nucleoside analogues (Doetsch et al., 1997). This description soon suggested the existence of at least two different proliferative states. More recently, it has been shown that a subset of GFAP+ and Glast+ astrocytes expressing EGFR are sensitive to antimitotic drugs such as cytosine β-D-arabinofuranoside (Ara-C) or temozolomide (TMZ) indicating that this subset of NSCs is actively dividing. In contrast, a pool of EGFR- NSCs remain quiescent, survive the treatments, and retain the ability to restore the production of new OB neurons through the regeneration of the entire lineage (Codega et al., 2014; Mich et al., 2014; Pastrana et al., 2009). It is now clear that both pool of cells, quiescent and active NSCs (qNSCs and aNSCs), participate in tissue homeostasis; however, whether they represent two states of the same cell or different SC populations that can interconvert is still unknown.

Due to all the features shared between neurogenic and non-neurogenic astrocytes like the expression of the same glial markers such as GFAP or GLAST, the identification and isolation of *bona fide* NSCs has been a challenging task. Moreover, the existence of a pool of NSCs that remain quiescent from embryonic stages and along adulthood (Codega et al., 2014; Fuentealba et al., 2015; Furutachi et al., 2015; Llorens-Bobadilla et al., 2015; Mich et al., 2014) has called into question nucleoside retaining methods as ways to unequivocally label quiescent cells as some of them may never become labelled. Slow-cycling cells such as those label-retaining cells (LRCs) that incorporate and retain nucleoside analogues may only be attributed to a previously activated population and thus, cannot be generally used to distinguish between quiescent dormant neurogenic astrocytes and niche astrocytes.

Unfortunately, so far there is no single marker that unequivocally identifies each pool of NSCs like there is in other systems such as the case with Lgr5 and Bmi1 in the intestinal epithelium (Tian et al., 2011) or Pax7 in the skeletal muscle (Rodgers et al., 2014). However, several different strategies based in fluorescence activated cell sorting (FACS) have been used to successfully isolate SEZ cells that display functional *in vivo* and *in vitro* properties of aNSCs and qNSCs (Codega et al., 2014; Daynac et al., 2013; Giachino et al., 2014; Khatri et al., 2014; Llorens-Bobadilla et al., 2015; Mich et al., 2014). Interestingly, EGFR expression is used in all cases to differentiate between a quiescent and an activated state. Nevertheless, they differ in the marker combinations used to distinguish between qNSCs and other niche astrocytes including CD133 and *GFAP*::GFP reporter mice (Codega et al., 2014) or GLAST (Llorens-Bobadilla et al., 2015), LeX (Daynac et al., 2013), PlexinB2 and GLAST (Mich et al., 2014) or the *Hes5*::GFP reporter mice and BLBP (Giachino et al., 2014). Additionally, the expression of CD24 has also been used to discard immature neuroblasts (Codega et al., 2014; Daynac et al., 2013; Llorens-Bobadilla et al., 2015; Mich et al., 2014).

Isolation of NSC pools displaying different activation states has allowed a deeper characterization of each of them. Transcriptome analysis of both populations has revealed that qNSCs and aNSCs are molecularly heterogeneous (Codega et al., 2014). qNSCs show enrichment in gene categories of cell-cell adhesion, extracellular-matrix-response and anchorage-dependent niche signals, but also of cell communication, signalling receptors, transmembrane transporters and ion channels, a combination that reflects their active regulation and communication with the microenvironment. In contrast, aNSC transcriptome is more related with cell-cycle and DNA repair gene categories (Codega et al., 2014). Furthermore, qNSCs and aNSCs also differ in the expression of metabolism-related genes displaying the quiescent pool a preference in glycolysis and fatty acid metabolism whereas aNSCs up-regulate oxidative phosphorylation genes (Codega

et al., 2014). Additionally, and accordingly with their active state, aNSCs also display higher translational rates than qNSCs (Llorens-Bobadilla et al., 2015).

Following this line, a recent work has further refined the transition of NSCs from quiescence to activation to eventually become immature neuroblasts (Llorens-Bobadilla et al., 2015). Taking advantage of the novel single-cell RNA-seq technologies, the authors described a more detailed sequence of molecular changes that take place between qNSCs, aNSCs, TAPs and neuroblasts which has revealed the existence of different quiescent and active states. Clustering of individual NSC transcriptomes by principal component analysis revealed the existence of four different cell populations which, placed in a pseudo-time line of 'differentiation', suggested a gradual transition from a 'dormant' state (qNSC1) that is 'primed' (qNSC2) before actively dividing states (non-mitotic aNSC1 and mitotic aNSC2). It is worth noting that a similar progression has been observed in a parallel cell-single transcriptome analysis of SGZ NSCs (Shin et al., 2015). The molecular hallmarks of each state also suggested that NSC activation and early lineage progression is organized as a continuum of successive molecular events. For example, dormant qNSC1 showed the highest levels of glial markers while aNSCs have already started a down-regulation of the glial gene expression programme. Instead, aNSCs up-regulate the expression of lineage-specific transcription factors such as Ascl1. Interestingly, the qNSC2 pool displayed intermediate features between dormant and active cells such as the activation of the protein synthesis machinery (Llorens-Bobadilla et al., 2015) (Figure 8). It is worth noting that the existence of a 'primed' quiescent state that is set-up for activation vastly resembles to the G_{alert} state observed in MuSCs (Rodgers et al., 2014). In agreement with this, the qNSC2 pool increases upon ischaemic brain injury suggesting that qNSCs detect injury signals which may regulate their transition to a primed state for a subsequent activation. However, it has not been explored whether this is a reversible state or which are the molecular mechanisms or the effectors that regulate priming and activation of qNSCs.

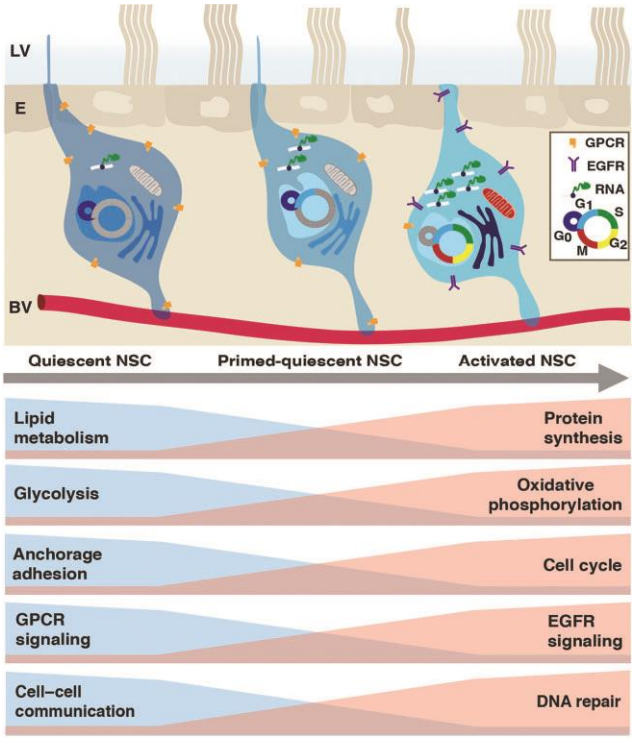

Figure 8. NSC states are molecularly heterogeneous. qNSC transcriptome is enriched in genes related with lipid metabolism and glycolysis, cell adhesion, G protein-coupled receptor (GPCR) and membrane receptors for cell-to-cell communication. Before activation, qNSC adopt a primed state that up-regulates translational machinery. Upon activation, NSCs suffer profound molecular changes particularly up-regulating genes involved in oxidative phosphorylation metabolism, cell-cycle regulation, EGFR signalling, and DNA repair. Adapted from Chacker et al. 2016.

Another source of heterogeneity that is currently under debate is whether individual NSCs differ in their long-term self-renewal potential. Lineage-tracing using Ascl1 or Dlx1 inducible Cre-drivers, which are supposed to label only active NSCs and TAP cell progeny, show a declined production of new offspring in less than one month. Nevertheless, *Glast* or *Gfap* expressing cells, which label qNSCs as well, displayed a sustained neurogenesis to the OB even 2 months after induction (Mich et al., 2014). However, lineage tracing of nestin+ cells, which are known to be already activated NSC, allowed the detection of new OB neurons even more than one year after Cre induction (Chaker et al., 2015; Imayoshi et al., 2008). Additionally, Hes5, Fgfr3 or Gli1+ NSCs also display long-term neurogenic potential although these markers do not appear to label a specific proliferative state (Ahn and Joyner,

2005; Giachino et al., 2014; Young et al., 2010). These data suggest that qNSCs may present a more sustained self-renewal potential while aNSCs seem to have a more limited self-renewal potential. Furthermore, these results also question whether aNSCs are capable of returning to quiescence thus maintaining a long-term self-renewal potential. Recent clonal analysis of single NSCs either using the confetti reporter mice (Calzolari et al., 2015) or embryonic retroviral library bar-coding (Fuentealba et al., 2015) and inducible Cre under the Glast promoter support this idea as the majority of individual NSCs, once activated, produced the expansion of neurogenic progeny for a limited number of rounds before becoming exhausted. Nevertheless, it is worth noting that a few clones contained both OB neurons and SEZ NSCs after long periods indicating that at least some activated NSCs may revert to a quiescent state keeping a long-term self-renewal potential. Although this is still under debate, it is currently clear that NSCs are dynamically, molecularly and functionally heterogeneous.

2.4. Subependymal NSC *in vitro* culture: the neurosphere assay

Several tissue-specific SCs were initially isolated and characterized by culturing tissue dissociates under conditions that promote their selective expansion. Initial work by Reynolds and Weiss led to the establishment of defined culture conditions that allowed the isolation and expansion of individual cells from young adult (2-month old) mouse periventricular tissue under non-adhesive conditions. These cells were initially maintained in a serum-free medium containing EGF to induce their proliferation. Under these culture conditions most of the cells died during the first days in culture, but a small population of cells began to divide and formed floating aggregates of cells with immunocytochemical features of neuroepithelial cells, called primary "neurospheres" (Reynolds and Weiss, 1992). Subsequent mechanical dissociation and subculture of these neurospheres allowed propagation of the cultures, revealing the self-renewal capacity of some of the cells. Additionally, when cultured onto an adhesive substrate in the presence of

serum, they could produce both astrocytes and neurons. This provided the first *in vitro* evidence that multipotential SCs were present in the adult mammalian brain and a method to expand large numbers of postnatal NSCs (Reynolds and Weiss, 1992).

Since these early experiments, the neurosphere culture has evolved into a powerful tool that enables the study of NSC proliferation, self-renewal and developmental potential under highly controlled environmental conditions (Belenguer et al., 2016). Once primary neurospheres are obtained from the SEZ tissue, they can be expanded for extended periods of time by dissociating them after 4-7 days and seeding individual cells under the same conditions. Either primary or secondary cultures can be assayed for the neurosphere assay (NSA), the gold standard of the NSC studies *in vitro* which allows the study of the clonogenic capacity and self-renewal of NSCs. Additionally, NSCs cultures can be challenged for differentiation to study the process itself and quantify the different populations of differentiated progeny or to assess the multipotency of individual clones. It is worth noting that the establishment of *in vitro* cultures allows to characterize NSCs from a molecular and biochemical point of view that otherwise could not be fulfilled (Belenguer et al., 2016) (Figure 9). Although the neurosphere assay approach only grants an operational definition of a stem cell, the culture of NSCs has notably increased our knowledge on how these cells are regulated, for example by signals from their microenvironment or niches (Porlan et al., 2013b).

However, this type of culture is not exempt of limitations. The most important one is that neurosphere cultures contain a heterogeneous population of cells as NSCs coexist with their progeny (different types of more committed progenitors and even differentiated cells). Stem cells unavoidably produce cell progeny *in vitro* and some of the highly proliferative committed progenitors or TAP cells appear also capable of forming neurospheres, albeit only for a few passages (Doetsch et al., 2002a; Reynolds and Rietze, 2005). Indeed, only a fraction of the total cells in

the culture behave as *bona fide* NSCs and, therefore, the assays need to carefully address their specific properties. In addition, qNSCs only extremely rarely form neurospheres while the strong mitogenic stimulation of culture conditions promote the selective expansion of aNSCs or TAPs (Codega et al., 2014; Mich et al., 2014). Therefore, the neurosphere assay in the current culture conditions better reflects the potential of aNSC and TAPs (Belenguer et al., 2016; Pastrana et al., 2011). However, the development and application of new NSC culture protocols to isolated populations of qNSCs and aNSCs appears as a promising strategy to further understand the fundamental properties and behaviour of the different types of NSCs.

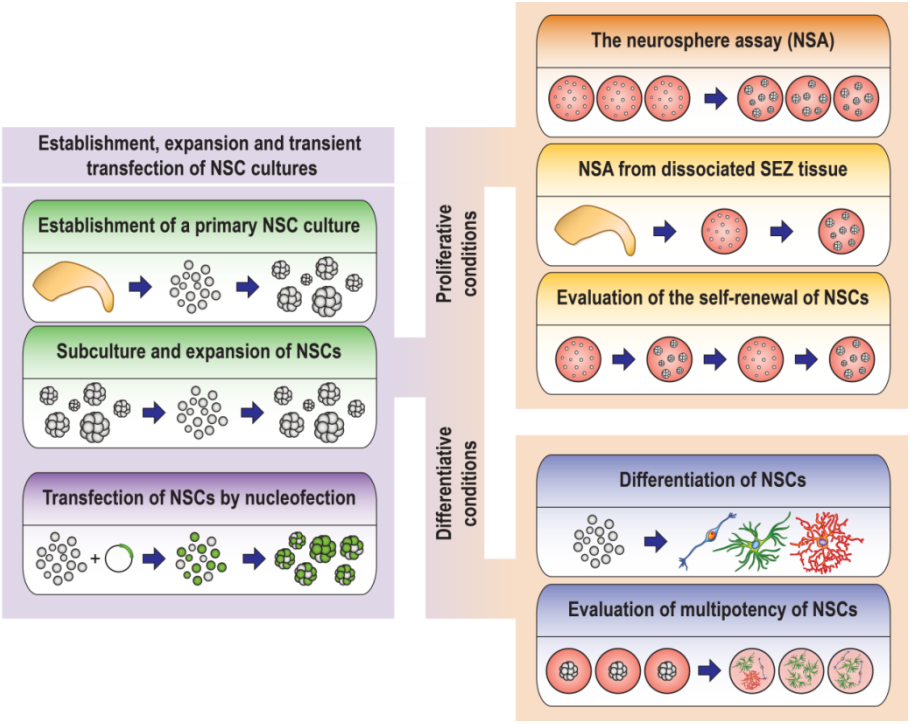

Figure 9. Subependymal NSCs *in vitro* culture is a powerful tool that enables the study of NSC proliferation, self-renewal, differentiation and molecular features. SEZ NSCs can be cultured in a serum-free medium containing EGF and FGF where they are stimulated to proliferate and generate heterogeneous clones called neurospheres. After the establishment of a primary NSC culture, NSCs can be maintained and expanded for several passages. Interestingly, the *in vitro* culture allows the NSCs to be transfected (i.e. by nucleofection) for molecular characterization. Under these proliferative conditions, NSCs can be challenged in a neurosphere assay (NSA), the

gold standard *in vitro* approach, which allows the evaluation of the NSC clonogenic capacity, either from primary or secondary cultures. Additionally, performing a sequential NSA by disaggregating initial clones and sub-culturing them again allows the evaluation of NSC self-renewal. Finally, after mitogen retrieval, NSCs are differentiated into neurons, astrocytes and oligodendrocytes in serum-containing media allowing the study of differentiated progeny and the clonal analysis of NSC potential.

3. The regulation of adult subependymal NSCs

A proper cell turnover during homeostasis or a functional tissue repair upon injury is the consequence of a finely regulated balance between quiescence and activation, self-renewal, proliferation, cell fate and differentiation of SCs. Current increasingly knowledge in the adult neurogenic niches is revealing the active participation of multiple players, either cell intrinsic determinants or signals from the extrinsic niche.

3.1. Intrinsic regulators of adult subependymal NSCs

Regulation of NSC gene expression by transcription factors (TF) is a crucial mechanism that regulates adult NSCs (Hsieh, 2012). For instance, the transcription factor SRY (sex determining region Y)-box 2 (Sox2) is expressed in multiple SEZ cell types including NSCs (Ellis et al., 2004) and its deletion results in NSC depletion and impaired neurogenesis (Ferri et al., 2004). Achaete-scoute homologue 1 (Ascl1) is expressed in aNSC and TAPs and target cell-cycle regulators promoting an active state and blocking a re-entry into quiescence (Urban et al., 2016). Moreover, Ascl1 is required for both neuronal and oligodendroglial lineages (Parras et al., 2004). Olig2 is also expressed in some NSCs and TAPs and appears to repress the neuronal lineage to promote oligodendrogenesis (Marshall et al., 2005; Menn et al., 2006). Interestingly, the recent data obtained from the single-cell RNA-seq has identified different TF that may be related to quiescence maintenance such as Sox9, Id2 or Id3, while Egr1, Fos, Sox4, Sox11 or Ascl1 are associated with an active state (Llorens-Bobadilla et al., 2015).

Regional heterogeneity is emerging as a key component of SEZ SC identity and cell fate. Fate mapping experiments have revealed that the diversity of OB interneurons subtypes or the production of astrocytes and oligodendrocytes is regionally specified and this is also correlated with a regional expression of specific TF. Thus, the observed different lineages may actually be intrinsically defined by the combinations of lineage transcription factors that, in addition, seem to be already defined during embryonic stages (Chaker et al., 2016; Llorens-Bobadilla and Martin-Villalba, 2016).

NSC maintenance and neurogenesis also depends on the tightly regulated cell cycle progression which is controlled by multiple regulators including cyclins, cyclin-dependent kinases (CDK), CDK inhibitors or TF. For instance, up-regulation of CKIs p16 and p19 impairs NSC self-renewal (Molofsky et al., 2003; Molofsky et al., 2006). Instead, CKI p27 has been related to TAP regulation and prevention of premature differentiation (Doetsch et al., 2002b). Furthermore, other regulators such as p21 has been implicated in NSC cell-cycle regulation preventing qNSCs release but also with non-cell autonomous functions preventing a premature differentiation through the inhibition of bone morphogenetic protein 2 (BMP2) over-expression (Kippin et al., 2005b; Porlan et al., 2013a). Moreover, p21 also displays a direct regulation of SOX2 expression eventually modulating NSC self-renewal (Marques-Torrejon et al., 2013).

Additional controls of NSC behaviour come from the regulation of gene expression by heritable epigenetic modifications. DNA methylation through DNA methyl transferase 3A (DNMT3A) or histone modification mediated by BMI1, a component of the poly-comb repressive complex 1 (PRC1), are good examples of this novel component of NSC regulation as they regulate the expression of key neurogenic genes that participate in NSC maintenance (Mich et al., 2014; Molofsky et al., 2003; Wu et al., 2010).

Recent studies have revealed changes in energetic demands during different stem cell behaviours. Activation of qNSCs is accompanied by down-regulation of glycolytic metabolism and up-regulation of mitochondrial oxidation in both SEZ and SGZ (Llorens-Bobadilla et al., 2015; Shin et al., 2015). These evidences suggest that a glycolytic metabolism may be important for maintaining NSC self-renewal and multipotency while oxidative phosphorylation is needed to fulfil the higher energetic demands that sustain proliferating states. In fact, it has been shown that NSCs have a stronger dependency on glycolytic metabolism than neurons and lower requirements for oxidative metabolism (Candelario et al., 2013). Additionally, lipid metabolism, mitochondrial metabolism and protection to the associated generation of reactive oxygen species (ROS) are also emerging as potential regulators of NSC activity (Knobloch and Jessberger, 2017).

3.2. Niche-dependent regulation of adult subependymal NSCs

The SEZ is a specialized microenvironment containing a variety of cells types which actively participate in the global decision making of NSCs. Moreover, this neurogenic niche presents a remarkable cellular architecture which allows the interaction with local cells and the surrounding ECM while receiving soluble factors from different sources, either locally or systemically produced. On their apical side, NSCs contact the CSF that fills the ventricles and continuously flows beaten by multiciliated ependymal cells (Mirzadeh et al., 2008). On their basal side, NSCs contact with an extensive vascular plexus that runs parallel to the SEZ (Shen et al., 2008; Tavazoie et al., 2008). Additionally, NSCs receive external signals from neural innervation and from the immune system through residing microglia (Bjornsson et al., 2015) (Figure 10).

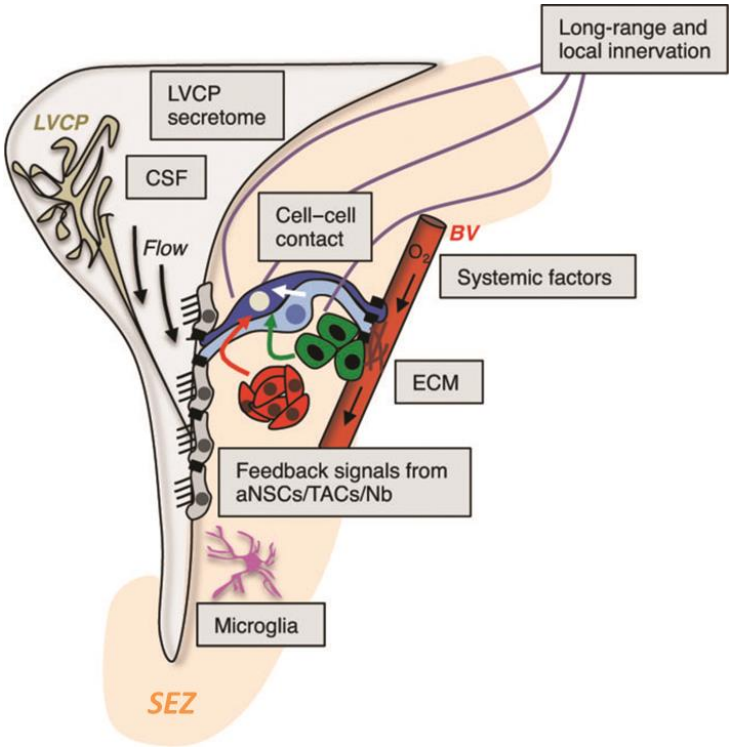

Figure 10. Multiple signals produced by SEZ niche components regulate adult subependymal NSCs. The SEZ is a specialized microenvironment containing a variety of cell types and non-cellular components with remarkable tissue-specific features: NSCs interact through adhesion molecules and signalling receptors with different support cells including astrocytes and ependymal cells, with differentiated progeny as well as with the surrounding ECM. On their apical side, NSCs contact the cerebrospinal fluid (CSF) of lateral ventricle, whereas they contact with the vasculature on their basal side from where NSCs receive different soluble and angiocrine factors. Additionally, NSCs receive external signals from neural innervation and from the immune system. Finally, gradients of non-cellular components as O_2 and small ions also participate in the global regulation of NSCs.

Ependymal cells are connected through gap junctions forming a simple epithelium that delimitates the SEZ niche from the ventricle. They form a specialized layer with elaborated adherens junctions that express several channel proteins, conferring a permissive interchange between the CSF and the interstitial fluid. They also express numerous molecules that regulate adult neurogenesis and NSCs including Noggin, a BMP antagonist, and PEDF (Colak et al., 2008; Lim et al., 2000; Ramirez-Castillejo et al., 2006). Cell-cell interactions between ependymal

cells and NSCs through N-cadherin have been also implicated in the maintenance of NSC quiescence and the cleavage of these connections through the matrix metallopeptidase MT5-MMP is required for proper activation of NSCs (Porlan et al., 2014). Likewise, NSC apical end-feet express high levels of the adhesion and signalling molecule vascular cell adhesion molecule-1 (VCAM1) for interaction with ependymal cells which is required for pinwheel organization and quiescence (Kokovay et al., 2012). Cell-cell interactions with derived progeny are also relevant, acting as negative feedback signals to prevent NSC exhaustion. Membrane-bound notch-ligand Dll1 is expressed in aNSCs and TAPs and send pro-dormancy signals to qNSCs, which express the receptor Notch2 (Kawaguchi et al., 2013; Llorens-Bobadilla et al., 2015). Mature astrocytes secrete delta-like homologue 1 (DLK1) that binds to the membrane-bound isoform present in NSCs to regulate self-renewal (Ferron et al., 2011).

The motile cilia present in ependymal cells actively beat the CSF which contains multiple factors secreted by the choroid plexus (ChP), a thin highly vascularized epithelium floating attached to the lateral ventricle cavity. It participates both in brain homeostasis (Redzic et al., 2005) and in neurogenic regulation through the secretion of signalling factors (Lun et al., 2015). For instance, the CSF provides migratory cues that guide neuroblasts to reach the RMS (Sawamoto et al., 2006). A recent global transcriptome analysis of the ChP has revealed the expression of multiple growth factors and signalling molecules with previously known effects on NSCs and neurogenesis, including neurotrophin 3 (NT3) (Delgado et al., 2014), insulin growth factor 2 (IGF2) (Ziegler et al., 2012) or FGF2 (Zheng et al., 2004) and novel candidates such as BMP5 or IGF1 (Silva-Vargas et al., 2016).

The intimate connection between NSCs and the parallel vascular plexus strongly suggests that NSCs reside in a vascular niche which provides important extrinsic signals (Shen et al., 2008; Tavazoie et al., 2008). Moreover, NSCs contact

the blood vessels at specialized sites with a relatively permissive blood-brain barrier (BBB) due to the lack of astrocyte end-feet (Tavazoie et al., 2008). Therefore NSCs receive both local extrinsic signals from the endothelial cells, known as angiocrine factors (Rafii et al., 2016), and distant produced factors from the blood stream including hormones, cytokines, metabolites and gases that can cross the BBB. Endothelial cells produce a variety of described NSC regulating molecules such as VEGF and PEDF which participate in NSC self-renewal (Ramirez-Castillejo et al., 2006; Shen et al., 2004), NT3 involved in quiescence maintenance (Delgado et al., 2014), or the chemokine stromal cell-derived factor 1 (SDF1) that regulates survival and migration of the NSC lineage (Kokovay et al., 2010). Additionally, direct cell-cell contact between NSCs and endothelial cells has also been demonstrated to promote quiescence (Ottone et al., 2014).

NSCs express receptors and respond to a variety of neurotransmitters (Berg et al., 2013). For instance, neuroblasts produce and release gamma-aminobutyric acid (GABA) to promote NSC quiescence thus auto-regulating the neuroblast demand (Liu et al., 2005a). The SEZ is also innervated by a variety of mature neurons including dopaminergic, serotonergic, cholinergic or nitric oxide (NO) neurons. Serotonin and acetylcholine increase NSC proliferation (Paez-Gonzalez et al., 2014; Tong et al., 2014) whereas studies of NO and dopamine suggest dual actions on NSC and progenitor proliferation (Hoglinger et al., 2004; Kippin et al., 2005a; Romero-Grimaldi et al., 2008). In addition, supraependymal 5HT serotoninergic axons originating from the raphe nucleus directly interact with NSCs to increase their proliferation via 5HT2C (Tong et al., 2014).

NSCs are located in a relatively hypoxic environment and this low oxygen tension has been suggested to facilitate stemness and prevent NSC differentiation (Mohyeldin et al., 2010). Although NSCs are in contact with blood vessels, the cell body of the qNSC resides closer to the ependymal cell layer, far from regions with higher gas renewal, what suggests that hypoxia may be related to a quiescent

state. Additionally, a less dependency on oxidative phosphorylation of qNSCs further supports this idea (Candelario et al., 2013; Llorens-Bobadilla et al., 2015). Hypoxia is known to regulate gene expression through the transcriptional factor HIF-1α, which has been recently implicated in NSC maintenance and SEZ vascular stability (Li et al., 2014).

4. Regulation of adult NSCs by the innate immune system

4.1. The role of inflammation in regeneration

Living organisms are constantly exposed to a variety of internal and external stimuli and some of them can be classified as danger signals that either represent a direct consequence of tissue damage (like the release of proteins and metabolites normally sequestered within cells, hypoxia, mechanical or chemical traumas, among others) or indicate the presence of harmful agents that may threaten tissue and even organism integrity (like invading microbes of viral and bacterial origin). When such signals are detected, a complex response is set in motion that is aimed at eliminating the danger signals and eventually restoring tissue and organism homeostasis. This response is generically referred to as inflammation, which represents a fundamental part of the innate immune system and its overall blueprint has been determined early in the evolution of metazoans, as indicated by the presence of a typical inflammatory response to wounds in invertebrates (Aurora and Olson, 2014). Inflammatory responses appear both essential for homeostasis and potentially dangerous. Activation of the immune system and its response to injury has evolved in vertebrates in the direction of promoting wound sealing and scarring to protect the damaged tissue of adult homeothermic individuals from pathogen invasion in a very rapid and efficient way. The down-side effect of this refined adaptive immune response is the loss of epimorphic

regeneration that is characteristic of cold-blooded organisms (Aurora and Olson, 2014).

Despite the loss of extensive regenerative capacity, adult mammalian tissues contain resident SCs that support cell turnover and production of new cells under physiological conditions. Inflammation has been shown to act on several SC niches, but the observation of changes in tissue turnover that could reflect both detrimental and beneficial effects has left the precise role of inflammation in tissue maintenance and regeneration as controversial and generated an area of intense investigation (Kizil et al., 2012a; Kizil et al., 2015; Kyritsis et al., 2014).

The initial phase of inflammation recruits the participation of resident immune cells, such as macrophages outside the CNS and microglial cells in the brain, which then secrete pro-inflammatory cytokines that initiate a cascade of molecular events. Acute inflammation is followed by active resolution by anti-inflammatory molecules. Within this complex temporal progression, the response of cells, including SC, to the changing landscape of cytokines is an intense research field which includes the study of the specific cross-talk between inflammation and stem cells (Kizil et al., 2015). Failed resolution results in chronic inflammation which is considered as hazardous to tissues, as reflected in its involvement in the onset and progression of many diseases.

4.2. Microglia, neuroinflammation and neurogenesis

Microglia are the resident macrophages and serve as primary immune effector cells of the CNS. These cells have a foetal hematopoietic origin and are derived from a specific type of myeloid progenitors that infiltrate the brain through blood vessels between E8.5 and E9.5 and hence are observed in the neuroepithelium of rodents before the onset of foetal neurogenesis. Moreover, their numbers increase throughout embryogenesis and postnatal stages through division within the CNS (Ginhoux et al., 2010). They have a multitude of functions, ranging from

phagocytosis to neuroprotection and immune surveillance during infection and injury. In the adult brain, microglia in the resting state continuously survey the local environment, with their dynamic processes interacting with a number of cell types, including astrocytes, neurons, and endothelial cells (Nimmerjahn et al., 2005). Microglial cells engage an innate immune reaction to various forms of pathogenesis and insults (Aguzzi et al., 2013).

Effects of microglia in CNS homeostasis and reaction to injury depend largely on their balanced secretion of pro-inflammatory and anti-inflammatory cytokines and chemokines. They are also emerging as a fundamental component of the neurogenic niches both in homeostasis and upon injury through cytokine secretion and phagocytosis and debris clearance (Borsini et al., 2015; Sato, 2015; Sierra et al., 2010). As such, recent studies have shown that adult neurogenesis is modulated by inflammatory cytokines in response to an activated immune system. Interestingly, microglia is a conspicuous component of the SEZ and RMS and, compared to other microglial cells, SEZ microglia comprise a morphologically and antigenically distinct cell subtype characterized by an activated phenotype, low expression of purinoceptors and lack of ATP-elicitable chemotaxis (Goings et al., 2006; Ribeiro Xavier et al., 2015).

Immune cell activation is among the first responses detected in a tissue upon injury and a peripheral inflammatory response is transduced to the brain through different mechanisms, including cytokine passage through the BBB by saturable transport systems or peripheral cytokine-induced self-stimulated release of pro-inflammatory molecules from CNS cell sources like microglia or endothelial cells (Banks and Erickson, 2010). Cytokines are low molecular-weight (8 to 40 kDa) glycoproteins secreted by various cell types, such some leukocytes, endothelial cells and resident macrophages like microglia, in response to infection, noxious stimuli that induce an immune response, inflammation, and trauma. Some cytokines act to make disease worse whereas others serve to reduce inflammation

and promote healing. Pro-inflammatory cytokines, such as IL-1β and IL-6, TNF-α, also known as cachectin, or IFN-γ are produced predominantly by activated macrophages and microglia and are involved in the up-regulation of inflammatory reactions. The anti-inflammatory cytokines are a series of immunoregulatory molecules that control the pro-inflammatory cytokine response. Major anti-inflammatory cytokines include IL-4, IL-10, IL-11, and IL-13. LIF, IFN-α, IL-6, and TGF-β can act as either anti-inflammatory or pro-inflammatory cytokines. Among all the anti-inflammatory cytokines, IL-10 is a cytokine with potent anti-inflammatory properties, repressing the expression of inflammatory cytokines such as TNF-α, IL-6 and IL-1 by activated macrophages and microglia (Zhang and An, 2007).

Experimental evidence has accumulated in the last decade indicating that inflammation can play a negative role in mammalian neurogenesis (Carpentier and Palmer, 2009; Gonzalez-Perez et al., 2010; Kizil et al., 2015; Montgomery and Bowers, 2012). Maternal inflammation induced by viral infection results in reduced ventricular proliferation in the foetal brain (Stolp et al., 2011). Intracerebral injection of the bacterial cell wall component lipopolysaccharide (LPS), which is a potent activator of the innate immune system, in adult mice causes microglial activation and suppression of neurogenesis in the SGZ (Ekdahl et al., 2003). Injecting LPS peripherally leads to a similar effect that can be antagonized by administration of the non-steroidal anti-inflammatory drug (NSAID) indomethacin (Monje et al., 2003; Wolf et al., 2009). Reduction in the production of new neurons in a NSAID-sensitive way has also been found in the *dentate gyrus* of rodents under chronic neuroinflammatory conditions such as irradiation, experimental epilepsy, experimental autoimmune encephalomyelitis, and induced inflammatory bowel disease (Ekdahl et al., 2003; Monje et al., 2003; Pluchino et al., 2008; Zonis et al., 2015). These reports demonstrated clear negative effects of neuroinflammation on neuroblast generation and viability, as well as on neuronal physiology (Jakubs et al., 2008).

All the previously mentioned results have contributed to the generalized assumption that inflammation negatively regulates neuroregenerative potential. However, there are evidences that support a potentially beneficial role of inflammation in neurogenesis. Firstly, peripheral blood leukocytes and resident microglia can enhance the rate of production and/or survival of newly-generated neurons (Butovsky et al., 2006; Deierborg et al., 2010; London et al., 2013; Schwartz, 2010; Schwartz et al., 2009; Schwartz and Shechter, 2010). Secondly, in contrast to mammals, non-mammalian vertebrates exhibit a great capacity to regenerate lost tissue. The adult zebrafish harbours NSCs that are capable of regenerating brain tissue after a traumatic injury through the activation of injury-induced molecular programs and inflammation-related signalling (Kyritsis et al., 2012). Fish adult NSCs share many characteristics with their mammalian counterparts, like their position at the ventricular surface and radial glial features (Adolf et al., 2006). It can, therefore, be hypothesized that adult NSCs in the mammalian brain could respond positively to certain inflammatory signals, a reaction that would be obscured by the more dramatic detrimental effects of inflammatory cytokines on neurogenesis. Added to the controversy over evidences indicating both positive and negative effects of inflammation and inflammatory cytokines (Borsini et al., 2015) in the process of adult neurogenesis, effects on mammalian NSCs have not been directly evaluated.

4.3. Tumour necrosis factor alpha (TNF-α) and progranulin (PGRN): characteristics and signalling

The TNF ligand superfamily member pro-inflammatory cytokine TNF-α was initially characterized as a molecule that could induce tumour regression through the induction of cell death (Carswell et al., 1975). TNF-α mainly produced by immune cells is prototypically involved in the innate immune response and apoptosis, but it is a multifunctional protein expressed in many other cell types with a broad range of activities in different systems and can exert different actions

depending on which receptor is activated (Aggarwal et al., 2012; Montgomery and Bowers, 2012). TNF-α is generally synthetized as a type II transmembrane protein precursor (tmTNF-α or pro-TNF-α) which is proteolytically cleaved at the cell surface by the matrix metalloprotease TNFα converting enzyme (TACE, also known as ADAM17) to release the soluble 17 kDa sTNF-α homotrimer. Both forms are biologically active and can interact with two single-pass transmembrane glycoprotein receptors, TNF-receptor 1 (TNFR1; also known as p55 or TNFRSF1A) and TNFR2 (also known as p75 or TNFRSF1B). TNFR1 is expressed by most cells, whereas TNFR2 expression is apparently restricted to cells of the hematopoietic system, including microglial and endothelial cells, and certain CNS cells. TNFα interaction with the TNFR1 generally triggers apoptosis and cytotoxicity whereas engagement of the TNFR2 is usually associated with cell protection and proliferation (Faustman and Davis, 2013; MacEwan, 2002; Montgomery and Bowers, 2012). TNFR2 agonism has been experimentally shown to be associated with pancreatic regeneration, cardioprotection, remyelination, survival of some neuron subtypes, and SC proliferation (reviewed in Faustman and Davis, 2013). Effects of TNFα in both the induction or the inhibition of neurogenesis *in vitro* have been reported (Bernardino et al., 2008; Keohane et al., 2010; Liu et al., 2005b). Some studies have focused on neural progenitor proliferation and have shown different, difficult to reconcile, results. Effects in promoting apoptosis, in lowering or increasing proliferation have been reported for different types of progenitors, both foetal and adult, in different rodent species (Ben-Hur et al., 2003; Bernardino et al., 2008; Keohane et al., 2010; Monje et al., 2003; Widera et al., 2006a; Wong et al., 2004). These data suggest that the effects of this molecule are complex maybe through the engagement of the two distinctive TNFRs.

TNFR2 can be activated also by progranulin (PGRN), also known as granulin–epithelin precursor (GEP), proepithelin (PEPI), acrogranin, and GP88/PC-cell derived growth factor (PCDGF), a secreted glycoprotein of around 600 amino acids bearing 7.5 copies of the unique highly conserved 12-cysteine-rich granulin (GRN) repeat

(Bateman and Bennett, 2009; De Muynck and Van Damme, 2011). Found in most eukaryotes, PGRN is one of the most ancient extracellular regulatory proteins. Although the original name emphasizes its presence in cells of the innate immune system, such as granulocytes, PGRN is a multifunctional protein expressed by different cell types. PGRN is abundant in epithelia with a high rate of cell turnover, such as the intestinal crypts or the epidermis suggesting potential actions on proliferation of stem cells and progenitors (Daniel et al., 2000). Its expression in fibroblasts and endothelial cells increases notably after injury and favours the proliferation and migration of these cells at the injury site (He et al., 2003).

In the adult CNS, PGRN is present in neurons and microglia (Petkau et al., 2010). Inactivating mutations in the human *GRN* gene give rise to frontotemporal lobar degeneration with ubiquitinated TDP-43-positive inclusions (FTLD-TDP), a neurodegenerative disorder characterized by a prominent atrophy of the frontal and temporal lobes of the brain resulting in severe cognitive and memory impairments and profound personality changes (McKhann et al., 2001). Variant alleles of GRN resulting in reduced expression of the gene have also been reported in cases of Alzheimer's disease (Brouwers et al., 2008). Homozygous GRN mutations result in adult onset neuronal ceroid lipofuscinosis, a lysosomal storage disease characterized by accumulation of lipofuscin that manifest with progressive loss of vision, retinal dystrophy, cerebellar ataxia, and seizures (Smith et al., 2012).These data together with experimental *in vitro* evidence (Van Damme et al., 2008) indicate that PGRN is involved in the survival of mature neurons.

Interestingly, PGRN expression increases dramatically when microglia becomes activated by injury (Petkau et al., 2010; Philips et al., 2010). After secretion, the full-length protein can be proteolytically cleaved in seven granulin peptides (GRN A-G) and a one-half granulin-containing paragranulin by metalloproteinases such as matrix metalloproteinase-9 (MMP-9), MMP-14 and a disintegrin and metalloproteinase with thrombospondin type 1 motif 7 (ADAMTS-

7), and the neutrophil-secreted serine proteases elastase and proteinase 3 (De Muynck and Van Damme, 2011). Interestingly, both PGRN and its constituent GRNs exhibit biological activity; PGRN is generally anti-inflammatory whereas proteolytically released GRNs promote inflammation. Full-length PGRN acts as an anti-inflammatory molecule and antagonizes the effects of TNFα by acting as a ligand of the TNFR2 (Kessenbrock et al., 2008; Zhu et al., 2002).

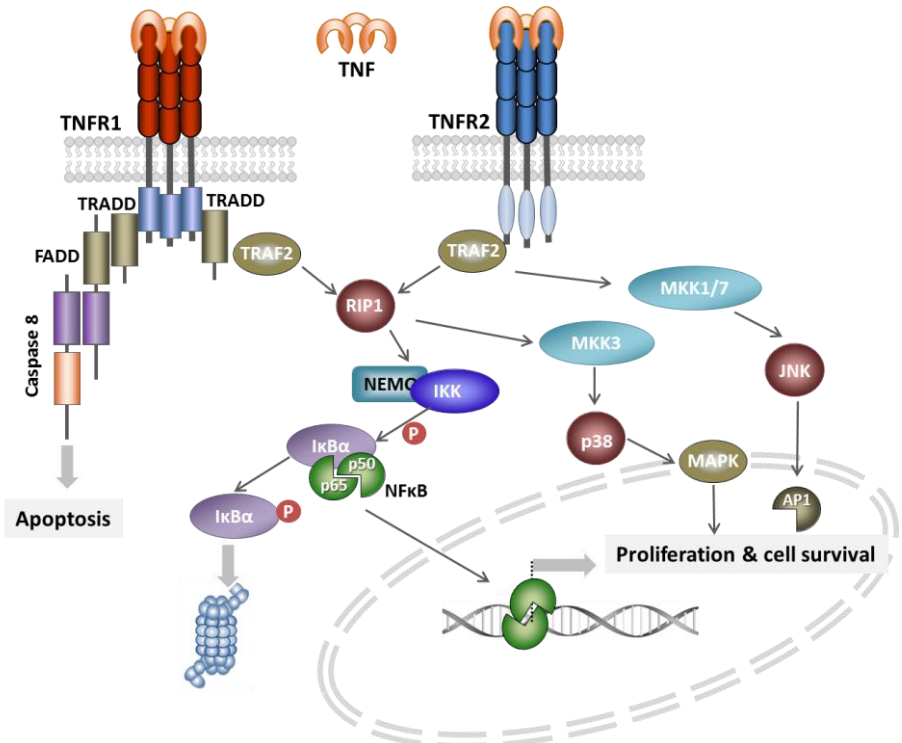

Figure 11. TNFR1 and TNFR2-mediated signalling of TNF-α. The binding of TNF-α induces the trimerization of TNFR1 and TNFR2. TNFR1 activation leads to the formation of different signalling complexes in which the receptor interacts, through the adaptor protein TRADD, with procaspase 8, triggering the apoptotic process, or TRAF2 and RIP1 to activate NF-κB, p38 or JNK pathways. TRAF2 also interacts directly with TNFR2 upon activation. This complex triggers signals leading to the activation of the transcriptional factor AP-1 through the activation of MKK3, MKK1/7 and JNK. Additionally, Rip1 activates the IKK complex that leads to several ubiquitin modifications needed for the correct activation of the transcriptional factor NF-κB implicated in the activation of proliferation and cell survival genes.

TNF receptors lack catalytic activity, but their cytoplasmic domains can, upon ligand engagement, induce the assembly of adaptor proteins that mediate the intracellular responses. TNFR1, but not TNFR2 has a death domain that allows the association of the TNF receptor-associated death domain (TRADD) and subsequent recruitment of Fas-associated death domain (FADD), DED caspases, and induction of apoptosis. In addition to caspase activation through TNFR1, cytoplasmic association of TNF receptor-associated factor 2 (TRAF2) and cellular inhibitors of apoptosis (cIAP 1 and 2) to TNF-R1-bound TRADD or to TNF-R2 directly, results in the activation of receptor interacting protein (RIP) and induction of downstream nuclear factor kappa B (NFκB), or in the activation of mitogen-activated protein kinases (MAPK) or stress-activated protein kinases (SAPKs) JNK and p38 (Cabal-Hierro and Lazo, 2012; Escos et al., 2016; Gaestel, 2006; Wajant et al., 2003) (Figure 11).

Initially discovered in the immune system where NF-kB-regulated gene expression is essential for the processes of inflammation and host defense, NF-kB comprises a group of dimeric transcription factors which have demonstrated to play a major role in various aspects of brain function. NF-kB transcription factors are expressed throughout the brain in both in neurons and glial cells and are present in neurogenic areas, suggesting potential roles in NSC behavior (Aggarwal, 2000; Sethi et al., 2008). NF-kB controls the expression of numerous genes involved in cell division, apoptosis, and inflammation (Chen and Green, 2004), but has never been implicated in stem cell self-renewal. Before stimulation, the family of transcription factors Rel/ NF-kB is retained in the cytoplasm in a latent form by association with inhibitor proteins of the inhibitor kB (IkB) family, with the most common neuronal species being the p50–p65 heterodimer and the p50–p50 homodimer. Of the five mammalian proteins of the Rel/NF-kB family (NF-kB 1/p50, p105, NF-kB 2/p49/52, p100, RelA/p65, RelB and c-Rel), only p65 (RelA) is expressed by B cells of the adult SEZ (Denis-Donini et al., 2005). The canonical mechanism of NF-kB activation involves phosphorylation of the inhibitory IkB subunit by the IkB

kinase complex (IKK) leading to its ubiquitination and subsequent proteasomal degradation, thereby releasing the active NF-kB factor dimmer. Free Rel/NF-kB then moves to the nucleus where it activates transcription of target genes (Widera et al., 2006a; Widera et al., 2006b).

The binding of TNF-α to cell surface receptors engages other signal transduction pathways, including three groups of mitogen-activated protein kinases (MAPK): extracellular-signal-regulated kinases (ERKs); and the stress-activated protein kinases (SAPK) c-Jun N-terminal (JNK) and p38 kinases (Bogoyevitch et al., 2010; Sabio and Davis, 2014). TNF-induced activation of the JNK and p38 pathways occurs through a non-apoptotic TRAF2-dependent pathway. MAP kinase pathways share a common structure formed by three sequentially acting protein kinases, generally including a MAP kinase kinase (MAP2K or MKK) and a MKK kinase (MAP3K or MKKK) (Sabio and Davis, 2014). JNK and p38 pathways are engaged by similar MAP3K isoforms, but diverge during the activation of MAP2K isoforms that selectively activate them. The JNK family includes three members (JNK1, JNK2, and JNK3) and four members of the p38 MAP kinase family have been identified (p38α, p38β, p38γ, and p38δ) (Gaestel, 2006; Sabio and Davis, 2014). The different JNK isoforms are activated by dual phosphorylation (Lee et al., 1997; Wajant et al., 2003; Yeh et al., 1997). JNK is activated by the MAP2K isoforms MKK4 and MKK7. MKK4 and MKK7 preferentially phosphorylate JNK on tyrosine and threonine, respectively and efficient dual phosphorylation therefore requires collaborative actions of both kinases. Indeed, compound MKK4/7-deficiency prevents TNFα-stimulated JNK activation (Tournier et al., 2001; Wajant et al., 2003). Upon activation, JNKs translocate into the nucleus and phosphorylate, thereby enhancing, the activity of transcription factors c-Jun, AP-1 or ATF2 (Chang and Karin, 2001; Shaulian and Karin, 2002). TNF not only robustly activates the JNK-inducing MAP kinase cascade, but also the p38-MAPK signalling cascade (Gaestel, 2015). The p38 MAP kinases can be activated by MKK3, MKK4, and MKK6 *in vitro*, but p38 MAP kinase activation *in vivo* is primarily

mediated by MKK3 and MKK6 (Brancho et al., 2003). The activation of p38 MAP kinases (by MKK3 and MKK6) and JNK (by MKK4 and MKK7) is induced by members of the MAP3K protein kinase family. Roles for ASK1, MEKK, MLK, TAK1, and TPL2 isoforms of MAP3K in the TNFα response have been reported. The relative importance of these pathways appears to be cell type-dependent and context-specific. Mechanisms that account for the selective involvement of these MAP3K isoforms in TNFα signalling have not been completely defined (Sabio and Davis, 2014).

Objectives

Tissue-specific SCs appear co-exist in two states of activation in most adult niches, but the transitions between these states as well as their regulation remain largely unknown. Moreover, some adult SCs appear to respond to remote injuries in ways that are not fully understood. This work proposes the hypothesis that adult NSCs react to inflammatory signals triggered in the periphery by modifying their activation state within the stem cell quiescence cycle.

The specific objectives proposed to test this hypothesis are:

1.- Development of a cell cytometry-based protocol for the prospective identification and analysis of adult subependymal NSCs and their progeny.

2.- Characterization of the quiescent cell cycle of adult subependymal NSCs during regeneration and in response to inflammation.

3.- Analysis of the effects of the inflammatory mediators TNF-α and progranulin and their common receptor TNFR2 on NSCs.

Material and methods

1. Experimental animals

1.1. Mice handling

All animals used along this thesis were acquired from Charles River Laboratories and then were breed and housed at the local animal housing facility (University of Valencia, Burjassot) according to the European Union 86/609/EEC and Spanish RD-1201/2005 guidelines and under official veterinary supervision. All experimental procedures with animals were approved by the corresponding local ethics committee.

When performance of highly invasive techniques was inevitable, mice were prior deeply anesthetized by intraperitoneal (i.p) injection of a mixture of medetomidine (0.5-1 mg *per* gram of body weight) and ketamine (50-75 mg *per* gram of body weight) diluted in saline solution (0.09% NaCl).

1.2. Mice strains

All experiments were done using adult mice of 2 to 4 months of age in all cases. The following mouse strains were used along this thesis:

- C57Bl6 (WT): wild-type strain used as a source of biological samples along the different *in vivo* or *in vitro* experiments. These mice were also used as a control reference to compare with genetically modified mice strains.

- B6;129S-*Tnfrsf1a*^{tm1Imx}/J (R1KO): null mutant mice lacking *Tnfrsf1a* (TNFR1) gene expression. The mice colony was kept in homozygosis.

- B6;129S-*Tnfrsf1b*^{tm1Imx}/J (R2KO): null mutant mice lacking *Tnfrsf1b* (TNFR2) gene expression. The mice colony was kept either in homozygosis or in heterozygosis and inter-crossed to generate homozygous mice.

- B6;129S-*Tnfrsf1a*^{tm1Imx} *Tnfrsf1b*^{tm1Imx}/J (DKO): double null mutant mice lacking both *Tnfrsf1a* and *Tnfrsf1b* gene expression. The mice colony was kept in homozygosis.

1.3. Genotyping

The genotype of the different genetically modified mice was determined by end-point Polimerase Chain Reaction (PCR) of genomic DNA extracted from tail samples. Tail tissue was lysed and processed for gDNA extraction using the Maxwell® 16 Mouse Tail DNA Purification Kit (Promega, cat no. AS1120) and a Maxwell® 16 instrument (Promega, cat no. AS2000). The presence of mutant or wild-type alleles was determined using 2 µl of gDNA and specific primers designed to amplify fragments of different length (see Table 1). PCR was performed with GoTaq® G2 Flexi DNA Polymerase (Promega, cat no. M7801). The PCR products were resolved by electrophoresis in a 2.5% agarose gel in TAE buffer (Tris, glacial acetic acid, 1 mM EDTA).

Gene	Primer sequence	amplicon	allele	T_a (°C)	Nr cycles
Tnfrsf1a	JAX834 GGATTGTCACGGTGCCGTTGAAG	120 bp	WT	64TD58	12 + 23
	JAX835 TGACAAGGACACGGTGTGTGG				
	JAX836 TGCTGATGGGGATACATCCAT	155 bp	KO		
	JAX837 CCGGTGGATGTGGAATGTGTG				
Tnfrsf1b	JAX838 AGAGCTCCAGGCACAAGGGC	275 bp	WT	69	35
	JAX839 AACGGGCCAGACCTCGGGT				
	JAX837 CCGGTGGATGTGGAATGTGTG	160 bp	KO		
	JAX838 AGAGCTCCAGGCACAAGGGC				

Table 1. Genotyping primers and PCR amplification conditions. 64TD58 indicates a touch-down PCR protocol where annealing temperature (T_a) starts at 64°C and decreases to 58°C during the first 12 cycles at a rate of 0.5°C per cycle. The remaining 23 cycles are perfomed at 58°C.

2. In vivo methods

2.1. Drug administration

Different drugs were administered for *in vivo* experiments:

- Lipopolysaccharide (LPS) (from E. Coli O111:B4, Sigma, cat no. L2630) was reconstituted at 1 mg/ml in saline solution and intraperitoneally injected at a single dose of 5 mg/kg.

- Temozolomide (TMZ) (Sigma, cat no. T2577) was reconstituted at 10 mg/ml in 25% DMSO saline solution and heated at 65°C until it was dissolved. Room temperature (RT) TMZ was intraperitoneally administered at 100 mg/kg/day for 3 consecutive days.

2.2. *In vivo* labelling of proliferating SEZ cells by thymidine analogues administration

Mitotically active cells that reside in the SEZ differ in their proliferative state and cell cycle kinetics, a property that has been extensively used to distinguish slow-cycling NSCs from highly proliferative TAPs and neuroblasts. In order to evaluate the proliferative state of NSCs, mice first received a regimen of seven i.p. injections (one every 2 h) with 10 mg/ml 5-Chloro-2'-deoxyuridine (CldU; Sigma, cat no. C6891) in saline solution (0.09% NaCl) dispensing a final dose of 50 mg of thymidine analogues per Kg. After 28 days, highly proliferative cells are expected to have diluted the incorporated CldU into their progeny, while slow-cycling cells, mainly active NSCs, are expected to retain the label defining this population as LRC (Porlan et al., 2014). Finally, to score all the proliferating cells, a single i.p. pulse of 10 mg/mL 5-Iodo-2'-deoxyuridine (IdU; Sigma, cat no. I7125) diluted in saline solution with 40% dimethyl sulfoxide was administered i.p. 1 h prior of sacrifice.

2.3. Perfusion and histology

In order to preserve brain structures and cell integrity for the subsequent histological analysis, mice were transcardially perfused with 27.5 mL of saline solution followed by 82.5-110 mL of 4% paraformaldehyde (PFA) in 0.1M Phosphate Buffer Saline (PBS) at a flow rate of 5.5 mL/min. Then, brains were extracted and post-fixed in 4% PFA during another hour at RT. After washing the tissue with abundant PBS, brains were included in warm 2% agar solution and cooled until solidification. Serially collected coronal sections of 30 µm of thickness were obtained in a Leica VT1000 vibratome and kept in PBS-0.05% azide at 4ºC until the analysis.

2.4. Immunohistochemistry (IHC)

Prior to specific antigen detection with primary antibodies, potential unspecific binding sites were neutralized incubating the tissue slices in blocking solution (5% Foetal Bovine Serum (FBS), 1% Glycine, 1% Bovine Serum Albumin (BSA), 0.1-0.2% Triton^{TM} X-100 (TX-100) and 0.05% azide in 0.1M phosphate buffer (PB)) for 1 h at room temperature. Next, samples were incubated with primary antibodies diluted in blocking solution (see Annex 1) at 4ºC for 24 h. After 3 washes with 0.1M PB, primary antibodies were detected with fluorescent-labelled secondary antibodies (see Annex 1) diluted in blocking buffer and incubated for 1 h at RT. Finally, cell nuclei were stained with 4',6-diamidine-2'-phenylindole dihydrochloride (DAPI; 1 mg/mL in distilled water) during 5 min. Labelled tissue was extended over glass microscope slides and mounted with FluoromountG (Electron Microscopy Sciences, cat. no. 17984) medium.

For detection of thymidine analogues, an initial step of chromatin denaturalization was required so the tissue was previously incubated in 2N HCl for 20 min at 37ºC. Then acid pH was neutralized with 0.1 M sodium borate buffer pH8.5 and before the blocking step, tissue was extendedly washed with 0.1 M PB.

2.5. SEZ cell counting

For the counting of the GFAP/Ki67/EGFR population, immunostained slide series containing the anterior horn of lateral ventricles were photographed in an Olympus FluoView FV10i confocal laser scanning microscope equipped with 405, 458, 488 and 633 nm lasers and images were processed using FV10-ASW 2.1 viewer software. Cell populations were manually counted and data was obtained as a percentage of positive cells relative to a subpopulation or total cells (DAPI count) in the lateral ventricle wall.

$CldU^+$, IdU^+ and $CldU/IdU^+$ cells laying the ventricle were manually counted in two entire series of tissue (10-11 slices) under a fluorescence microscope (NIKON eclipse Ni) and the number of total cells of each type in the SEZ was estimated applying the Cavalieri method, which takes into account the number of cells counted, the number of tissue slices counted, the number of total tissue series and the slice thickness.

2.6. SEZ dissection

Adult mice were sacrificed by cervical dislocation. Figure 12 illustrates the step-by-step procedure of SEZ dissection. The brain was removed (Figure 12a) and placed in a plate with ice-cold PBS (Biowest, cat no. X0515) where we discarded the olfactory bulbs and cerebellum to obtain a 4-5 mm thick slice that contains the lateral ventricles (Figure 12b). Both hemispheres were then separated for fine dissection (Figure 12c). First, the tissue was opened following the corpus callosum line (Figure 12d) separating the hippocampus, septum and diencephalon from the cortex and exposing the SEZ (Figure 12e). Next, the SEZ area was delimited by removing the surrounding tissue using as reference the white matter tracts (corpus callosum dorsal and anterior capsule/stria terminalis ventral to the SEZ) (Figures 12f-i). Finally, the SEZ block was finely cut under the surface of the ventricle wall to

obtain a tissue slice as thin as possible, separating the SEZ from the subjacent striatal parenchyma (Figures 12j-l).

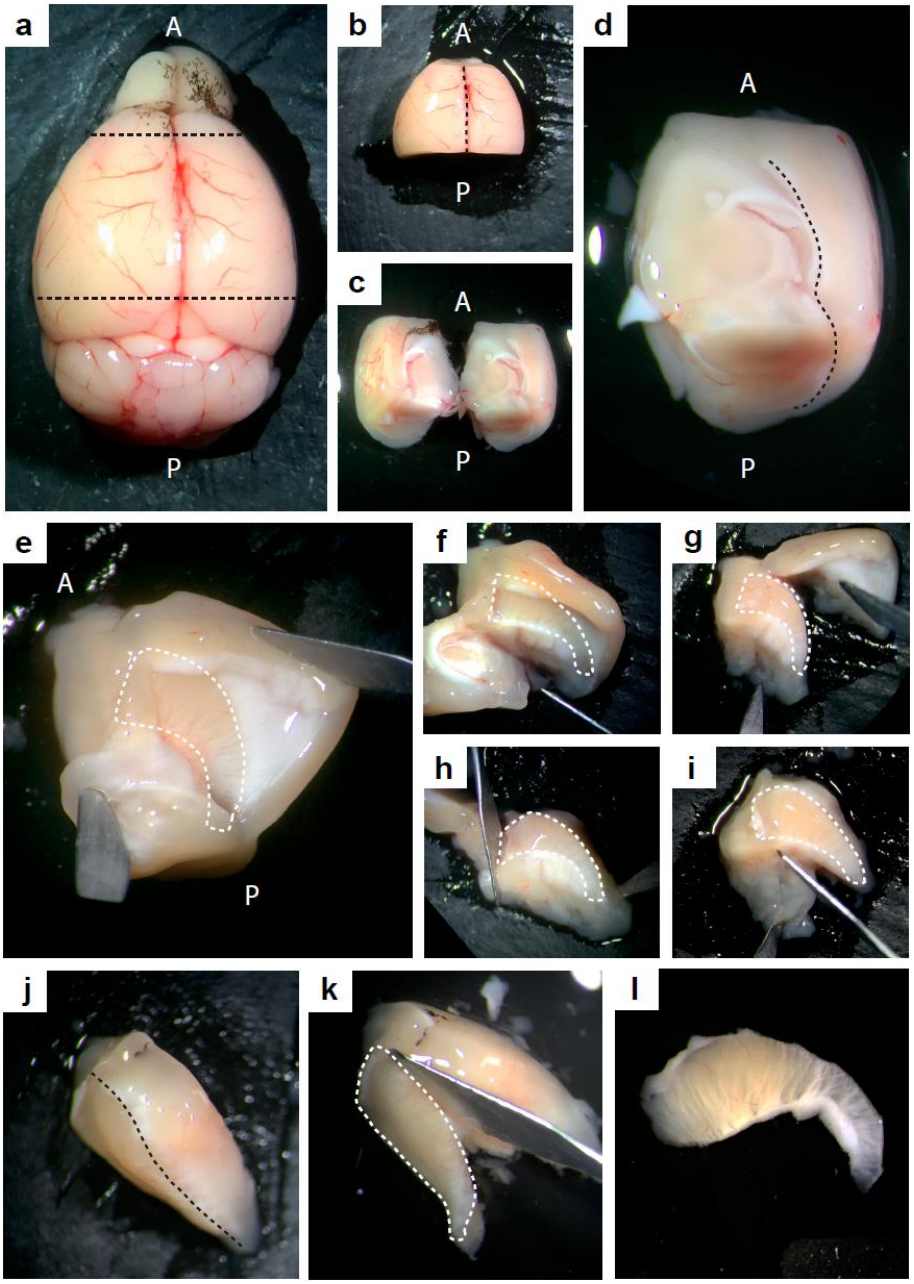

Figure 12. Dissection of the SEZ with detailed pictures of the step-by-step process. The whole dissection procedure is thoroughly described in the text, with references to each picture (a–l).

Black dashed lines mark where to cut while white dashed lines plot the shape of the SEZ. A: anterior region, P: posterior region.

2.7. SEZ wholemount preparations and analysis of migrating neuroblasts

Migrating neuroblast chains were directly analysed in the intact SEZ as whole-mount preparations. After dissection, fresh tissue was fixed and permeated in PFA 4% with 0.5% Tx-100 at 4°C. The next day, the tissue was washed three times with 0.5% Tx-100 PBS and incubated for 1 h in blocking buffer (0.5% Tx-100, 10% FBS in PBS). Primary antibodies (see Annex 1) were added to fresh blocking buffer and SEZ samples were incubated at 4°C for 2 days. After washing three times with 0.1% Tx-100 PBS, fluorescent-labelled secondary antibodies were incubated in blocking buffer at 4°C. The following day, the tissue was washed and incubated with 1 µg/ml DAPI in 0.1% Tx-100 for 10 minutes. Finally, wholemount preparations were mounted in abundant FluorMount-GT medium. The whole SEZ area was photographed in a Fluoview FV10iW confocal microscope (Olympus) and the SEZ area occupied by DCX^+ chains was quantified using the image J analysis software.

2.8. SEZ dissociation, flow cytometry analysis and MACS® separation

In order to preserve antigen integrity and reduce the presence of debris or dead cells, the preparation of SEZ samples was optimized for flow cytometry analysis or cell sorting. After dissection, both SEZs from each mice were minced and enzymatically digested at 37°C for 20 min with 1 ml of enzymatic mix (Hanks balanced salt solution (HBSS) without Calcium and Magnesium, 10 mM HEPES, 0.4 mM EDTA and 1:10 Trypsin/EDTA (GIBCO-BRL, cat no. 25200-056)). Digestion was quenched with 3 ml of 100 µg/ml trypsin inhibitor (Sigma, cat no. T6522) diluted in washing medium (0.6% Glucose, 0.1% $NaHCO_3$, 5 mM HEPES, 2 mM L-glutamine, 0.4% BSA, 1X Antibiotic/Antimicotic in DMEM/F-12) and the digested pieces were centrifuged at 15 xg for 5 min. After removing the medium, remaining tissue was mechanically dissociated in 2 ml of washing medium with 10 µg/ml DNase I (Roche,

cat no. 000000004716728001) pipetting up and down 10 times through a fire-polished glass Pasteur pipette. Cell suspension was diluted with 3 ml of washing medium and then it was filtered through a 40 µm nylon filter. After washing the filter with extra 5 ml of washing medium, cells were pelleted (300 xg, 10 min) and incubated with 100 µl of Dead cell removal microbeads (Miltenyi, cat no. 130-090-101) at RT for 15 min. Magnetically labelled cells were then diluted in 0.5 ml of binding buffer (Miltenyi, cat no. 130-090-101) and passed through a previously equilibrated MS column (Milteny, cat no. 130-042-201) on an OctoMACS® magnetic separator (Miltenyi, cat no. 130-042-109). The columns were washed 4 times with binding buffer and all the eluted fractions were collected together. Finally, the eluted living fraction was pelleted (300 xg, 10 min), resuspended in 100 µl blocking buffer (HBSS without Calcium and Magnesium, 10 mM HEPES, 2 mM EDTA, 0.1% Glucose, 0.5% BSA) and incubated with the specific primary antibodies and reagents (see Table 2) at 4°C for 30 min. After washing with 1 ml of blocking buffer, labelled samples were centrifuged (300 xg, 10 min at 4°C) and resuspended in 0.5 ml of blocking buffer. Cells were analysed using a LSR-Fortessa cytometer (Becton Dickinson) with 350, 488, 561 and 640 nm lasers.

Antibody/ Reagent	Working concentration	Provider	Cat no.
CD45-BUV395	1:200	BD	565967
O4-Biotin	1:30	Miltenyi	130-095-895
CD31-BUV395	1:100	BD	740239
Ter119-BUV395	1:200	BD	563827
Streptavidin-Alexa350	1:200	Molecular Probes	s11249
Dapi 50 µg/ml	1:500	Sigma	D9542
EGF-Alexa488	1:300	Molecular Probes	E13345
Mitotracker® Orange CM-H_2TMRos	1:2000	Molecular Probes	M7511
CD24-PerCP-Cy5.5	1:300	BD	562360
GLAST-APC	1:20	Miltenyi	130-095-814
PSA-NCAM-APC	1:50	Miltenyi	130-093-273

CD9-Vio770	1:20	Miltenyi	130-102-384
CD45-Biotin	1:100	BD	553077
O4-Biotin	1:20	BD	130-095-895
CD31-Biotin	1:100	BD	558737
Ter119-Biotin	1:100	BD	553672
CD24-Biotin	1:100	Miltenyi	553260

Table 2. Fluorescent and biotin-labelled antibodies and reagents used in the flow-cytometry and MACS® sorting strategies.

For cell MACS® isolation of Lin- cells, SEZ samples were dissociated and filtered as mentioned above. Then, samples were incubated at 4°C for 30 minutes in 100 µl of blocking buffer with biotinylated antibodies against CD45, CD31, Ter119, CD24 and O4 (see Table 2). Cells were washed with 3 ml of blocking buffer and centrifuged at 300 xg for 10 min. The resultant pellet was resuspended in 70 µl of blocking buffer and incubated with 30 µl of anti-biotin microbeads (Miltenyi) at 4°C for 15 min. Excess of beads were washed with 3 ml of blocking buffer and, after pelleting the cells (300 xg, 10 minutes), magnetically labelled samples were resuspended in 0.5 ml of blocking buffer and loaded into a previously equilibrated MS column held in an OctoMACS® separator magnet. The eluted fraction was collected and the column was washed 3 times with 0.5 ml of blocking buffer. Finally, the column was removed from the magnet and the retained fraction eluted in 1 ml of blocking buffer by gently pushing with a plunger. Both fractions were centrifuged at 300 xg for 10 min and the pellet was incubated in 100 µl of Dead cell removal microbeads for 15 min at RT. Finally, using the OctoMACS® separator, the living fraction was collected as previously described. The eluted cells were pelleted (300 xg, 10 min) and resuspended in neurosphere growing medium for cell culture or in blocking buffer for flow cytometry analysis.

3. *In vitro* cell culture methods

3.1. Cell culture media

3.1.1. NSCs

Reagent	Working conc.	Stock conc./ storage T	Provider	Cat. no.
DMEM/F12 (1:1) with L-Glutamine	1x	1x (4 °C)	Gibco, BRL	11320-074
D(+)-Glucose	0.6 %	30% (-20 °C)	Panreac	141341
$NaHCO_3$	0.1 %	7.5% (4 °C)	Biowest	L0680-500
HEPES	5 mM	1M (4 °C)	Biowest	L0180-100
L-Glutamine	2 mM	200nM (-20 °C)	Gibco, BRL	25030-081
Antibiotic/Antimycotic	1x	100x (-20 °C)	Gibco, BRL	15240-062
"Hormone mix"	1x	10x (-20 °C)	Homemade (**Table 4**)	
Heparin sodium salt	0.7 U/ml	350U/ml (4 °C)	Sigma	H3149
Bovine Serum Albumin (BSA)	4 mg/ml	powder (4 °C)	Sigma	B4287

Table 3. Preparation of "control medium". DMEM/F12 (Dulbecco's Modified Eagle Medium / Ham's F12 Nutrient Mixture)

Reagent	Working conc.	Stock conc./ storage T	Provider	Cat. no.
DMEM/F12 (1:1) with L-Glutamine	1x	1x (4 °C)	Gibco, BRL	11320-074
D(+)-Glucose	0.6 %	30 % (-20 °C)	Panreac	141341
$NaHCO_3$	0.1 %	7.5 % (4 °C)	Biowest	L0680-500
HEPES	5 mM	1 M (4 °C)	Biowest	L0180-100

Apo-Transferrin	0.8 mg/ml	Powder	Sigma	T2252
Bovine insulin	500 nM	5 µM in 0.01N HCl	Sigma	I6634
Putrescine	0.1 mg/ml	1 mg/ml	Sigma	P7505
Progesterone	0.2 nM	2 mM in 95% EtOH	Sigma	P6149
Sodium Selenite	0.3µM	3 mM	Sigma	S9133

Table 4. Preparation of 10x "hormone mix"

Reagent	Working conc.	Stock conc./ storage T	Provider	Cat. no.
Control medium		As described in **Table 3**		
EGF	20 ng/ml	4 µg/ml (-20 °C)	Gibco, BRL	53003-018
bFGF	10 ng/ml	25 µg/ml (-20 °C)	Sigma	F0291

Table 5. Preparation of "complete medium"

3.1.2. N13 cell line

Reagent	Working conc.	Stock conc./ storage T[a]	Provider	Cat. no.
RPMI	1x	1x (4 °C)	Gibco, BRL	21875-091
FBS	10%	100% (-20 °C)	Biowest	S181B-500
L-Glutamine	2 mM	200nM (-20 °C)	Gibco, BRL	25030-081
Penicillin/Streptomycin	1x	100x (-20 °C)	Gibco, BRL	L0018-100

Table 6. Preparation of N13 culture medium

3.2. Reagents and drugs

Along the different experimental procedures, a variety of treatments were added to the NSC cultures: recombinant mouse TNF-α (R&D, cat no. 410-MT-010) was reconstituted at 10 µg/ml in sterile PBS with 0.1% BSA and used at concentrations from 0.1 to 20 ng/ml. TNF-α was added at 10 ng/ml unless otherwise is stated. Recombinant mouse PGRN (R&D, cat no. 2557-PG) was reconstituted at 250 µg/ml in sterile PBS and used between 10 and 500 ng/ml. The final concentration of PGRN used was 100 ng/ml unless otherwise is stated. TNFR1 was specifically activated with 1 µg/ml of an anti-TNFR1 antibody (R&D, cat. no. AF-425-PB) with described agonistic properties (Tesz et al., 2007). TNFR2 was stimulated with 5 µg/ml of an agonistic anti-TNFR2 antibody (Hycult biotech, cat. no. HM1011)(Marchetti et al., 2004). P38 inhibitor SB203580 (Sigma, cat. no. S8307) was added 30 minutes before other treatments and used at a final concentration of 1 µM.

3.3. Establishment of primary NSC culture and estimation of the number of SEZ neurosphere-forming cells

For general purposes, adult NSC cultures from the SEZ were obtained from 2 to 4 month-old mice. Both SEZs from each mice were minced together and enzymatically digested in 1 ml of a previously activated (30 minutes at 37°C) enzymatic solution (12 U/ml of papain (Worthington Biochemical Corporation, cat. no. LS003120), 0.2 mg/ml L-cysteine hydrochloride (Sigma, cat. no. C8277) and 0.2 mg/ml EDTA (Sigma, cat. no. E6511) in EBSS (Earle´s Balanced Salt Solution, Gibco™, cat. no. 24010-043). After an incubation of 30 min in a thermostatic bath at 37°C, digestion was stopped by diluting papain with 3 ml of control medium (see Table 3 and Table 4). The pieces were centrifuged at 100 x*g* for 2 min and after removing the supernatant, the tissue was mechanically dissociated in 1 ml of control medium pipetting up and down through a p1000 micropipette tip. Then the homogenate was washed in 10 ml of control medium and centrifuged at 200 x*g* for 10 min.

Finally, the pellet was re-suspended and plated in complete medium (see Table 5). For standard primary culture establishment, we distributed cells obtained from 2 SEZs (one brain) into 8 wells of a p48-well plate containing a final volume of 0.5 ml. SEZ homogenates were incubated at 37ºC in a 5% CO_2 humidified incubator for 7-10 days. During this time differentiated cells will die while NSCs and some progenitors will start to proliferate and to form neurospheres (Figure 13a).

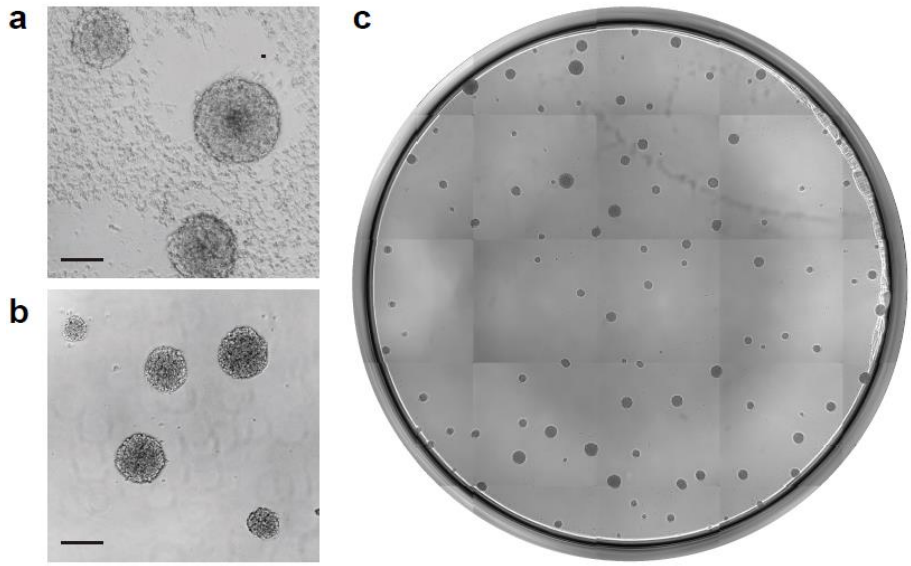

Figure 13. Culture and expansion of adult NSCs. (a) Bright-field pictures of primary neurospheres. (b) Bright-field pictures of 5 days in vitro (5 DIV) secondary spheres. (c) 2-D composition of a whole 96-well with clonal neurospheres derived from a neurosphere assay (NSA). Scale bars: 100 mm in a, b.

In experiments where the number of SEZ-derived primary neurospheres was compared, the cell density of the re-suspended homogenate was previously determined using a propidium iodide-based automatic cell counter ADAM (Digital Bio). 20.000 cells were plated *per* 48 well and 5-7 days after incubating at 37ºC in a 5% CO_2 humidified incubator, the number of neourospheres was manually counted

on an inverted microscope with phase contrast optics. The total number of primary neurospheres *per* SEZ was estimated using the formula **(N/C) x S** where:

- **N:** is the average number of neurospheres *per* well.
- **C:** is the number of viable cells seeded *per* well.
- **S:** is the total number of viable cells *per* SEZ.

3.4. Subculture and bulk expansion of established NSC cultures

Once primary neurospheres are obtained from the SEZ tissue, they can be expanded for extended periods of time by dissociating them after 4-7 days and seeding individual cells under the same conditions.

Grown neurospheres were transferred to a 15 ml conical tube and centrifuged 5 min at 100-130 xg depending on the overall neurosphere size. Pelleted cells were dissociated with 200 µl of Accutase® solution (Sigma, cat. no. A6964). After 10 min at RT, Accutase® was diluted with 800 µl of control medium and neurospheres were mechanically dissociated by thoroughly pipetting 10-15 times with a p1000 micropipette. After washing the cell suspension in 8-10 ml with control medium, individual cells were centrifuged 10 min at 200 xg. The resultant pellet was re-suspended in complete medium to estimate the concentration of viable cells using the automatic ADAM cell counter system.

For culture passage and bulk expansion, 10.000-viable cells/cm^2 were seeded on fresh pre-warmed complete medium and incubated at 37°C in a 5% CO_2 humidified incubator. After 5-7 days, new neurospheres were ready for subculturing (Figure 13b).

3.5. The neurosphere formation assay (NSA)

Proliferation and self-renewal of NSCs was assessed evaluating the ability of individual cells to generate new neurospheres. After obtaining a single cell suspension as mentioned above, cells were plated at pseudo-clonal density (5

cel/µl) seeding 1000 cells in 200 µl of complete medium *per* 96 well. When different treatments were evaluated, cells were prepared at twice the concentration required (10 cel/ µl) to plate cells in 100 µl of complete medium and mix them with the same volume of double concentrated treatment diluted in complete medium as well. After 5-6 days at 37ºC in a 5% CO_2 humidified incubator, neurospheres were manually counted on an inverted microscope under phase contrast optics. For diameter assessment, neurospheres were photographed in an INCELL Analyzer 2000 (General Electric) (Figure 13c) and sphere diameter was measured by image analysis using the Image J software.

An increase in self-renewal might not lead to higher number of neurospheres in a NSA, but obtained neurospheres would be enriched in NSCs. Consequently, if these neurospheres are dissociated and submitted to a second round of NSA, more secondary neurospheres will be scored revealing the phenotype. In parallel, from the same original cell suspension, NSC were plated in 24-well plates by seeding 25,000 in 1 ml of NSC complete medium per well. The different treatments were added to each well maintaining the final volume of 1 ml. After 5 days at 37ºC in a 5% CO_2 humidified incubator neurospheres were collected from the 24-well plates and dissociated with 40 µl of Accutase® solution as previously described. Accutase® was diluted with 160 µl of complete medium and after obtaining a single cell suspension and estimating the number of viable cells, a second round of NSA assay was set up as mentioned above.

3.6. Activated microglia conditioned medium and immunodepletion of TNF-α

N13 microglia cells were grown in their specific culture medium (see Table 6) at 37ºC in a 5% CO_2 humidified incubator and passed every 2-3 days with Trypsin/EDTA (T/E) (Gibco-BRL, cat no. 25200-056). For NSC medium conditioning, 400.000 cells were plated in a 6-well plate and the next day the cells were stimulated to a pro-inflammatory M0 state with 250 ng/ml LPS. After 3 h, the growth medium containing LPS was removed and the cells were washed twice

with abundant PBS. Next, 3 ml of NSC control medium without BSA were conditioned for 24 h. Finally, the conditioned media was collected and filtered through a 0.45 µm pore-size filter.

The conditioned media was incubated with 2.5 µg/ml of anti-TNF-α antibody (Abcam, cat no. ab1793) or with a non-related antibody (anti-Nestin antibody, Abcam, cat no. ab6142) at the same concentration overnight at 4ºC in constant agitation. The next day, 40 µl of previously washed Dynabeads® Protein G (Life technologies, cat no. 10003D,) were added to the medium for an additional incubation of 1 h at 4ºC in constant agitation. Finally, Dynabeads® were magnetically removed from the media using a DYNAL® magnet (Invitrogen). The resultant conditioned media was diluted 1:4 in fresh NSC complete medium for treatment of NSC cultures in a neurosphere assay.

3.7. Cell viability assessment by MTS assay

Viability of NSCs in the presence of TNF-α was measured by MTS determination using the CellTiter 96® Aqueous Non-radioactive Cell Proliferation Assay (Promega, cat. No G5421). 5000 cells were plated in a 96-well with 100 µl of complete medium and incubated at different time points with a MTS/PMS working solution (20:1) at 37ºC in a 5% CO_2 humidified incubator. Absorbance at 490nm of each well was measured after 1 h in a Victor®3 Multilabel Plate Reader (PerkinElmer). Each experimental point was done by triplicate and the cell viability was calculated with the formula **(t_x A_{490} – blank A_{490}/ t_o A_{490} – blank A_{490}) x 100** where:

- **t_x A_{490}:** is the average absorbance at 490nm of each time point.
- **t_o A_{490}:** is the average absorbance at 490nm of the initial time point.
- **blank A_{490}:** is the average absorbance at 490nm of the complete medium without cells.

3.8. Cell cycle analysis

Single cells were plated in complete medium at a density of 10.000 cells/cm^2 and, after 24 h at 37ºC in a 5% CO_2 humidified incubator, cells were pelleted and dissociated in 50 µl of Accutase® solution. After 10 min, 200 µl of DNA PREP LPR reagent (Beckman Coulter, cat. no. 6607055) were directly added to permeate and fix the cells during 5 min. Finally, cells were stained with 250 µl of 100 µg/ml propidium iodide and 20 ng/ml of RNaseA. After 45 min at 37ºC, the DNA content was assessed in a FACSVerse (BD) flow cytometer.

3.9. Immunocytochemistry

In general, prior to antigen detection with specific antibodies, cells were attached and fixed for antigen preservation. Therefore, the day before, glass coverslips were incubated with Matrigel® (Corning®, cat. no. 354230) diluted 1:100 in control medium at 37ºC in a 5% CO_2 humidified incubator. The next day, before attaching cells, Matrigel-coated coverslips were washed twice with sterile dH_2O. Cells were plated on 48-well plates with coated coverslips and were incubated for 20 min to allow cell attachment. Next, cells were fixed in 1% PFA at 37ºC for 15 min and washed 3 times with PBS.

Before immunolabelling, unspecific binding of antibodies was minimized incubating the cells in blocking buffer (10% FBS, 1% Glycine, 0.1 M PBS) for 30 min. After that, samples were incubated with specific primary antibodies (see Annex 1) diluted in blocking buffer overnight at 4ºC. Primary antibodies were washed three times with PBS before incubating the cells with the corresponding fluorescent-labelled secondary antibodies (see Annex 1) diluted in blocking buffer for 1 h at RT. Finally, cells were washed with PBS and incubated with 1 µg/ml DAPI for 5 minutes before mounting the coverslips in microscope slides with Fluorsave™ Reagent (Millipore, cat. no. 345789).

3.10. Cell-pair assay for mode of division assessment

Symmetry of cell division was evaluated in recently-divided cells. Single cells were plated in complete medium at very low density (4.000 cel/cm^2) to minimize the aggregation of individual cells and were incubated at 37ºC in a 5% CO_2 humidified incubator. After 24 h, cells were gently dispensed in Matrigel®-coated coverslips for fixation and detection of EGFR expression by immunocytochemistry. At least 100 cell-pairs per condition were manually counted under a fluorescence microscope (NIKON eclipse Ni) to obtain the percentage of each type of division.

3.11. Evaluation of multipotency of NSC cultures

Pre-treated NSC cultures were dissociated and plated at a density of 25,000 cells in a 60 mm dish with 4 ml of complete medium to obtain isolated clones. Neurospheres were ready for clonal differentiation after 7 days at 37ºC in a 5% CO_2 humidified incubator. The day before picking clones, 96-well plates were coated with Matrigel® diluted 1:100 in control medium. The next day, Matrigel®-coated plates were washed twice with sterile dH_2O and filled with 100 µl of control medium. Individual clones were picked under a dissecting microscope in a horizontal laminar flow cabinet using a p20 micropipette and were transferred to the Matrigel®-coated wells (1 neurosphere/well). The plates were placed in the incubator for at least for 2 h to let neurospheres attach to the matrix. Empty wells and those containing more than one clone were discarded for subsequent differentiation. Once neurospheres were completely attached to the matrix, control medium was carefully aspirated and replaced with 200 µl of differentiation medium I (NSC control medium supplemented with 10 ng/ml of bFGF). After the initial 2 days of incubation, the differentiation medium I was replaced by the differentiation medium II (NSC control medium supplemented with 2% FBS). Differentiated clones were ready for immunocytochemistry analysis of the presence of the three different lineages after 5 days. Each clone was analysed in a fluorescent inverted microscope and classified as unipotent (A, if only astrocytes

could be found), bipotent (AO/AN, if, besides astrocytes, there were neurons or oligodendrocytes in the well) or tripotent (AON, if all three lineages were observed).

3.12. Evaluation of cell proliferation dynamics by dilution of fluorescent tracers

SEZ homogenates were obtained as previously described except for mechanical dissociation of tissue pieces after papain digestion that was done in 1 mL of 10 mM HEPES and HBSS to avoid BSA-sequestering of the membrane-permeant fluorescent tracers. Then, 2 µg/ml of Cell Trace Far Red DDAO-SE (Thermo Fischer, cat. no. C34553) was directly added for incubation at 37ºC for 7 minutes. After that, cells were washed with control medium and centrifuged at 200 xg for 10 min. Finally the loaded pellet was seeded in NSC complete medium. After 10 days, when primary neurospheres had arose and the fluorescent tracer had heterogeneously diluted between the progeny, a second round of cell tracer loading was performed using the Cell trace Oregon Green 488 Carboxy-DFFDA-SE (Thermo Fischer, cat. no. C34555). Primary neurospheres were dissociated as described above and single cells were washed with 10 mM HEPES and HBSS and then were loaded with the second cell tracer in the same conditions. Double-loaded cells were finally plated in complete medium for a second round of proliferation to assess the proliferation dynamics of the label retaining cells. After 3 days at 37ºC in a 5% CO_2 humidified incubator, secondary neurospheres were dissociated and the fluorescence intensity of each cell tracer was measured in a FACS Fortessa flow cytometer (BD).

3.13. Transduction of NSC by Nucleofection®

Transient introduction of exogenous DNA for expression of the 5x κB luciferase-based reporter (5x κB-luc) was done by Nucleofection®, a method that combines electroporation with cell-type specific reagents developed by Amaxa. In general, a total number of 1.5 x 10^6 cells were used for transduction. Cells were

pelleted at 200 xg for 10 min and 5 µl of a mix containing the different plasmids were directly added to the cell pellet: 0.5 µg of 5x κB-luc was mixed with 0.05 µg of pRenilla endogenous control vector, 3 µg of pcDNA3.1 as adjuvant and 0.5 µg of pGFPmax (Lonza) reporter plasmid to monitor the transfection efficiency. The pellet was then resuspended in 95 µl of Nucleofection Solution from the Mouse Neural Stem Cell Nucleofector® Kit (Lonza, cat. no. VPG-1004) and placed in a Nucleofector® cuvette. The cells were electroporated in a Nucleofector® 2b device using the A-031 nucleofection program. Electroporated cells were gently collected with warm complete medium, seeded in a P100 cell culture plate containing 8 ml of complete medium and incubated for 24 h at 37ºC in a 5% CO_2 humidified incubator before using the cells for reporter expression under the different treatments.

3.14. Mitochondrial activity staining

After obtaining a single cell suspension as described above, cells were incubated with MitoTracker™ Orange CM-H_2TMRos diluted 1:2000 in 0.5 ml of blocking buffer for 30 min on ice. Then stained cells were washed with 1 ml of blocking buffer, centrifuged at 200 xg 10 min and resuspended in 0.5 ml of blocking buffer for flow cytometry analysis.

4. Molecular methods

4.1. RNA extraction, retro-transcription and real-time PCR

SEZ RNA samples were obtained using the Maxwell® 16 LEV simplyRNA Tissue Kit (Promega, cat. no. AS1280) following the instructions provided by the manufacturer. The RNA obtained was then quantified using the Qubit® RNA HS Assay Kit (Thermo Fischer, cat. no. Q32852) in a Qubit Fluorometer (Thermo Fischer).

In general, a total amount of 0.5 – 1 µg of RNA was retrotranscripted to cDNA using the PrimeScript™ RT-PCR Kit (Clontech, cat. no. RR014B) according to the manufacturer instructions.

Gene expression analysis was assessed by real-time PCR using 5-10 ng of cDNA, specific Taqman probes (Applied Biosystems) (see Table 7) and the Premix Ex Taq™ (Probe qPCR) Kit (Clontech, cat. no. RR390A). Real-time PCR was performed in a Step One Plus real-time PCR device (Applied Biosystems). The expression level of each gene was obtained by relative quantification (2e-ΔΔCt) using constitutive expression of *Gapdh* and *18S* genes as housekeeping endogenous controls.

Gene	Taqman probe reference	Gene	Taqman probe reference
18S	Hs99999901_s1	***Grn***	Mm00433848_m1
Aif1	Mm00479862_g1	***Hes1***	Mm00468601_m1
Ascl1	Mm04207567_g1	***Hes5***	Mm00439311_g1
Ccnd1	Mm00432359_m1	***Id1***	Mm00775963_g1
Pecam1	Mm01242584_m1	***Ifng***	Mm01168134_m1
Ptprc	Mm01293577_m1	***Il1b***	Mm00434228_m1
Cdkn1a	Mm04205640_g1	***Il6***	Mm00446190_m1
Cspg4	Mm00507257_m1	***Nes***	Mm00450205_m1
Dcx	Mm00438400_m1	***Nr2e1***	Mm00455855_m1
Egfr	Mm01187858_m1	***Olig2***	Mm01210556_m1
Fabp7	Mm00445227_m1	***Prom1***	Mm00477115_m1
Fgfr1	Mm00438923_m1	***S100b***	Mm00485897_m1
Fgfr2	Mm00438941_m1	***Slc1a3***	Mm00600697_m1
Fgfr3	Mm00433294_m1	***Sox2***	Mm03053810_s1
Gapdh	Mm99999915_g1	***Tnf***	Mm00443258_m1
Gfap	Mm01253033_m1	***Tubb3***	Mm00727586_s1

Table 7. List of Taqman probes used

4.2. Protein extraction, electrophoretic separation, transference and immunodetection by Western Blot

Cells or SEZ samples were lysed in cold RIPA buffer (NaCl 150 mM, 0.5 % sodium deoxycholate, 50 mM Tris-HCl pH 8.0, 1% Tx-100 and 1% SDS) supplemented with Complete® protease inhibitor cocktail (Roche, cat. no. 11836153001) and placed on ice for 30 min. Then the lysates were homogenized with sequential passing through a 23G and then a 20G needle. Finally, protein samples were centrifuged at 12000 xg for 10 min at 4ºC and the supernatant was transferred to a new Eppendorf tube.

The concentration of each sample was determined using the Pierce® BCA Protein Assay Kit (Thermo Fisher, cat. no. 23227) following the instruction of the manufacturer. BSA was used to stablish a standard curve and A_{560} was measured in a Victor®3 Multilabel Plate Reader.

Direct conditioned media or 20-80 µg of cell lysates were mixed with 4X sample buffer (Glicerol 20%, 10% SDS, 10% β-mercaptoethanol, 40 µg/ml Bromo phenol blue and 250 mM Tris-HCl 1M pH6.8,) and boiled at 95ºC for 10 min.

Samples were loaded in 10% poly-acrylamide gels and proteins were resolved by sodium dodecyl sulphate polyacrylamide gel electrophoresis (SDS-PAGE) at 20 mA/gel in an electrophoresis running buffer (25 mM Tris-base, 192 mM glycine and 1% SDS). Proteins were transferred to PVDF membranes using the Trans-Blot Turbo Transfer Pack (Bio-Rad, cat. no. 1704157) and the Trans-Blot Turbo transfer device (Bio-Rad).

The membrane was washed in TBS-T buffer (0.1 M Tris-HCl pH 7.5, 0.9% NaCl and 0.05% Tween®-20 (Sigma, cat. no P9416)) and incubated for 1h with blocking buffer (5% skimmed milk in Tris buffer) to minimize unspecific binding. Primary antibodies (see Annex 1) were diluted in blocking buffer and the membrane was incubated overnight at 4ºC or 1h at RT in continuous agitation. Next, after washing

the membrane with TBS-T several times, HRP-labelled secondary antibodies (see Annex 1) were added in blocking buffer and were incubated at RT for 1 h. Finally, after washing the membrane with TBS-T, proteins were revealed with Western Lightning® Plus-ECL (Perkin-Elmer, cat. no. NEL103001EA) and chemoluminescence was captured in an Alliance Mini HD9 (Uvitec) image capture system.

4.3. Luciferase activity detection

Transduced cells were collected and centrifuged at 200 xg for 10 min. The pellet was lysed in 50 µl of Passive Lysis Buffer (Promega, cat no. E1941) and homogenised by vortexing 10 min. Firefly luciferase (reporter-dependent) and Renilla luciferase (constitutively expressed) activity were determined in 10 µl of cell lysate with the Dual-Luciferase® Reporter Assay System (Promega, cat. no E1960) and luminescence was measured in a Victor®3 Multilabel Plate Reader.

4.4. Multiplex analysis of the phophorilated state of cell signalling mediators

Cells were collected, centrifuged and lysed in MILLIPLEX MAP Lysis buffer (Millipore, cat no. 43-040). Cell lysates were homogenized by vortexing 10 min at 4ºC and stored at -80ºC until they were processed by Neuron Biolabs S.L.U (Granada, Spain). The phosphorylated state and the total amount of CREB, JNK, NF-κB, p38, AKT, p70S6K and STAT3 was measured with the MILLIPLEX® MAP 9-plex Multi-Pathway Magnetic Bead Signaling kit Phosphoprotein (Millipore, cat no.: 48-680MAG) and the MILLIPLEX® MAP 9-plex Multi-Pathway Magnetic Bead Signaling kit Total (Millipore, cat no.: 48-681MAG) kits respectively following the instructions of the manufacturer. The same amount of protein in each experimental group was loaded per well (2.7-3.3 µg) and each condition was measured in two experimental replicates. The detection of phosphoproteins and total proteins was performed in a MAGPIX® luminex MAP® system coupled with two lasers. The phosphoprotein levels were normalized by the total amount of each protein and relativized to the untreated condition.

5. Statistical analysis

Significance differences between experimental groups were assessed using the unpaired or paired two-tailed Student t-test or one-way ANOVA with Bonferroni correction when appropriate using the GraphPad PRISM® 5 software. Relative values were transformed using the formula arcsen(square root (value)) and percentages were transformed using arcsen(square root (value/100)) before statistical analysis. Significance lower than p=0.05 were considered as significant differences in all cases. All data is expressed as mean ± standard error of the mean (sem) and the number of experiments carried out with independent cultures or animals (n) is specified in each figure. When data are represented, * refers to p< 0.05, ** to p< 0.01 and *** to p< 0.001.

6. Annex 1

Primary Antibody	Host	Provider	Cat. No	Application	Dilution
BrdU (CldU detection)	Rat	Abcam	ab6326	IHC	1:800
BrdU (IdU detection)	Mouse	BD	347580	IHC	1:500
Cleaved-Caspase 3	Rabbit	Cell Signalling	9661	ICC	1:100
Phospho-P38	Rabbit	Cell Signalling	9211	WB	1:1000
P38	Rabbit	Cell Signalling	9212	WB	1:1000
DCX	Goat	Santa Cruz	sc-8066	Wholemount	1:150
EGFR	Rabbit	Cell Signalling	4267	ICC/IHC	1:100
GFAP	Chicken	Millipore	ab5541	ICC/IHC	1:800
Ki67	Rabbit	Abcam	ab15580	IHC	1:100
O4	Mouse	Homemade	-	ICC	1:300
TNF-alpha	Mouse	Abcam	ab1793	Western Blot	1:250
TNFR1	Goat	R&D	410-MT	Agonist	1:200
TNFR2	Rat	Hycult biotech	HM1011	Agonist	1:20
βIII-tubulin	Rabbit	Sigma	T2200	ICC	1:400
Secondary Antibody	**Host**	**Provider**	**Cat. No**	**Application**	**Dilution**
AlexaFluor®488 anti-mouse	Donkey	Life Technologies	A-21202	IHC	1:800
AlexaFluor®647 anti-chicken	Donkey	Jackson ImmunoResearch	703-605-155	ICC/IHC	1:800
Biotinylated anti-mouse	Horse	Vector Laboratories	BA-2000	ICC	1:1000
Cy™3 streptavidin	-	Jackson ImmunoResearch	016-160-084	ICC	1:2000
AlexaFluor® 488 anti-rabbit	Donkey	Jackson ImmunoResearch	711-547-003	ICC/IHC	1:800

HRP anti-mouse	Goat	Dako	P0447	WB	1:1000
HRP anti-rabbit	Goat	Santa Cruz Biotechnology	Sc-2004	WB	1:5000
Cy™3 anti-rat	Donkey	Jackson ImmunoResearch	712-165-153	IHC	1:800
AlexaFluor® 647 anti-goat	Donkey	Jackson ImmunoResearch	705-606-147	Wholemount	1:800
Cy™3 anti-rabbit	Donkey	Jackson ImmunoResearch	711-165-152	ICC/IHC	1:800

List of primary and secondary antibodies used along the different applications.

Results

1. Characterization of the quiescent cell cycle in adult subependymal NSCs

1.1. Prospective identification of subependymal NSCs and their progeny

Since their discovery, identification of *bona fide* adult NSCs has been a challenging task because single specific markers that could unequivocally identify the different SEZ populations have not been found and the SEZ astrocytic lineage which includes the NSC population/s shows morphological, molecular and functional heterogeneity (Morrens et al., 2012). To overcome these limitations, different genetic lineage-tracing strategies and/or immunohistochemical approaches combining retention of thymidine analogues with different astroglial or stem cell markers have been classically used in histological analyses to study NSCs and their progeny (Kuhn et al., 2016). Nevertheless, recent evidences demonstrating that adult stem cells coexist in different quiescent (dormant qNSC1 *vs*. alert qNSC2 or primed) (Llorens-Bobadilla et al., 2015; Rodgers et al., 2014) and active (aNSC) states (Codega et al., 2014; Daynac et al., 2016; Giachino et al., 2014; Llorens-Bobadilla et al., 2015; Mich et al., 2014), have revealed a new level of complexity rendering these classical approaches insufficient to finely resolve the different pieces of this tricky puzzle.

In the last few years several groups have assayed different strategies to label and isolate NSCs or their progeny by flow cytometry (Codega et al., 2014; Daynac et al., 2016; Giachino et al., 2014; Llorens-Bobadilla et al., 2015; Mich et al., 2014). These approaches are usually based on the combination of multiple markers, either using transgenic reporters and/or labelling with fluorescent antibodies against cell surface proteins to then analyse the marker profile of each individual SEZ cell. Despite having proved their relative accuracy, none of the protocols published so far ensures the detection of the complete population of NSCs and their different proliferative states. Furthermore, strategies that rely on the expression of reporter transgenes such as hGFAP::GFP or Hes5::GFP mouse strains (Codega et al., 2014; Giachino et al., 2014), cannot be directly applied to the study of NSCs in other

genetic backgrounds. For these reasons, we first decided to develop our own strategy to identify, not only NSC in different activation states, but also the resulting progeny, using published cell surface markers and including CD9, a marker identified in a transcriptomic analysis at the single cell level (Llorens-Bobadilla et al., 2015; Mich et al., 2014).

Taking into account the heterogeneity of the SEZ niche and the potentially overlapping expression of markers among different cell types, we opted for a two-step strategy in which non-neurogenic differentiated cell types (microglia and circulating lymphocytes, endothelial cells, erythrocytes, ependymal cells, and oligodendrocytes) are first excluded using well established cell markers (Table 9). Subsequently, cells are stratified into NSCs/astrocytes, TAPs and neuroblasts according to the expression of the glial marker GLAST, the activation marker EGFR and the progeny marker CD24. In contrast to some early reports, we discarded the use of Prominin1 as a true NSC marker as it has been shown that in the $GFAP^{+}$ $Prominin1^{-}$ fraction there are also cells that behave as NSCs *in vitro*, indicating that Promini1 labels only a subset of NSCs (Codega et al., 2014). Instead, we decided to include the expression of CD9 to fractionate the $GLAST^{+}$ population as it has been recently shown that this member of the tetraspanin family is highly expressed in neurogenic astrocytes when compared to parenchymal astrocytes (Llorens-Bobadilla et al., 2015). Table 9 summarizes the different markers used in this work and the cell types in which they are expressed.

Antigen	Cell type expression	Reference
CD45	Microglia, lymphocytes	Mich et al. 2014; Llorens-Bobadilla et al. 2015
CD31	Endothelial cells	Crouch et al. 2015
Ter119	Erythrocytes	Mich et al. 2014
O4	Oligodendrocytes	Mich et al. 2014; Llorens-Bobadilla et al. 2015
CD24	Ependymal cells, neuroblasts	Pastrana et al. 2009; Codega et al. 2014;

		Mich et al. 2014; Llorens-Bobadilla et al. 2015; Daynac et al. 2016
PSA-NCAM	Neuroblasts	Mich et al. 2014; Llorens-Bobadilla et al. 2015
GLAST	Astrocytes, oligodendrocytes, TAPs	Mich et al. 2014; Llorens-Bobadilla et al. 2015
CD9	Neurogenic astrocytes, microglia, oligodendrocytes	Llorens-Bobadilla et al. 2015
EGFR	aNSC, TAPs, neuroblasts	Pastrana et al. 2009; Codega et al. 2014; Mich et al. 2014; Llorens-Bobadilla et al. 2015; Daynac et al. 2016

Table 9. List of cell markers selected for cytometry analysis, their target population(s) and references of previous use as a cell marker.

In our procedure, SEZ cells are first gated by size and cellular complexity (forward scatter -FSC- *vs*. side scatter -SSC-, respectively) to discard cell debris, myelin, and most of the dead cells (Figure 14a). Ependymal cells or neurons are expected to be also excluded due to their size and complexity (Murayama et al., 2002). After eliminating cell aggregates, we select the populations of interest as $CD45^-/CD31^-/Ter119^-/O4^-$ alive cells (Figure 14b,c). Although CD24 is reportedly restricted to neuroblasts and ependymal cells (Pastrana et al., 2009) we found different levels of this marker among SEZ cells, ranging from complete negativity up to high expression levels. The highest CD24 expression co-distributed with PSA-NCAM expression, suggesting that neuroblasts can be indeed recognized by high CD24 (Figure 14d). Furthermore, we realized that EGFR first appears in $CD24^-$ cells and continues to be present as CD24 increases its expression until it disappears in the $CD24^{high}$ population (Figure 14e). We believe that this progression is compatible with a situation where $CD24^-$ NSCs, once activated ($EGFR^+$), start expressing very low levels of CD24 that increase during transition to TAPs ($CD24^{mid}/EGFR^+$) and become maximum in undifferentiated ($CD24^{high}/EGFR^+$) and migrating ($CD24^{high}EGFR^-$) neuroblasts. Because of the continuum of CD24 expression along the neurogenic lineage, we took into consideration different levels of this marker to gate $CD24^{-/low}$, $CD24^{mid}$, and $CD24^{high}$ fractions (Figure 14e). The $CD24^{high}$ fraction can be subsequently divided into $EGFR^-$ and $EGFR^+$ as well, corresponding

respectively to migrating and non-migrating neuroblasts (Figure 14e), while virtually all CD24^{mid} cells are compatible with TAPs, since all of them express EGFR (Figure 14e).

Subependymal NSC-derived neuroblasts migrate through the RMS up to the OB where they differentiate and integrate as functional mature neurons (Chaker et al., 2016). This last step is a direct reflection of NSC dynamics in the SEZ and therefore we decided to include the analysis of OB neuroblasts in our flow cytometry strategy as a read-out for the production of newly-generated neurons. Flow cytometry analysis of CD24 and PSA-NCAM revealed the presence of a CD45$^-$/CD31$^-$/Ter119$^-$/O4$^-$ subset of cells that highly co-expressed both markers and which represented around 25% of all OB cells (Figure 14f). This provided us with a method to also evaluate neurogenesis in the same animals in which we were analysing NSC dynamics by flow cytometry.

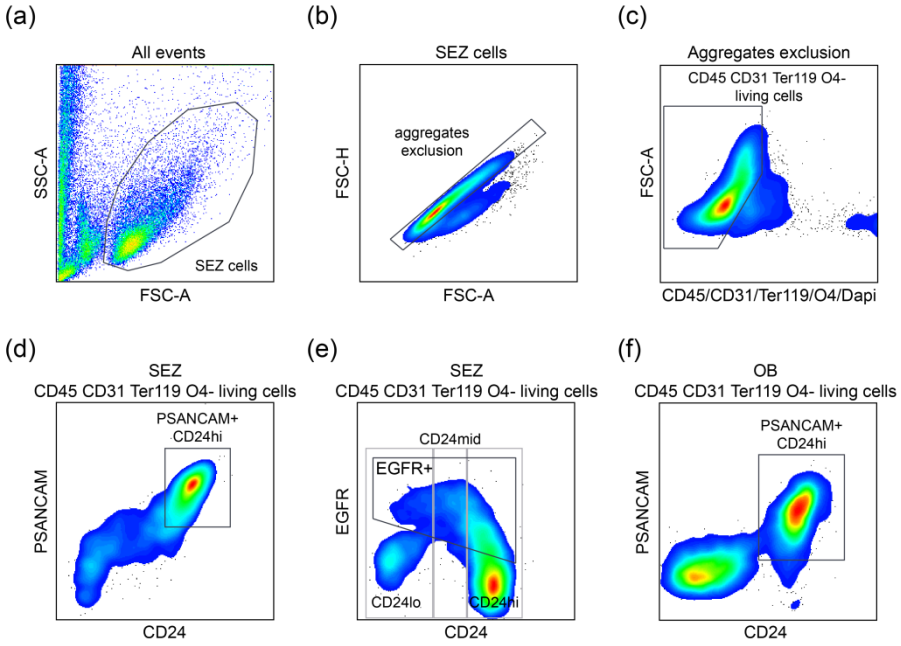

Figure 14. Prospective identification of NSC and their progeny from adult SEZ. (a-f) Representative FACS plots showing SEZ NSC-lineage gating strategy and OB neuroblast identification. **(a)** SEZ cells are selected by size (FSC) and cell complexity (SSC) and **(b)** after

excluding cell aggregates, **(c)** a negative selection is performed discarding cells positive for CD45, O4, CD31, Ter119 and Dapi (dead cells). **(d-f)** Then cells are gated based on their CD24 expression. **(d)** $CD24^{high}$ levels co-localize with PSA-$NCAM^{+}$ neuroblasts **(e)** whereas EGFR is expressed along the different CD24 levels which are used to define the gating for EGFR negative and positive neuroblasts ($CD24^{high}$), $EGFR^{+}$ TAPs ($CD24^{mid}$) and the NSCs containing pool ($CD24^{low}$). **(f)** After excluding CD45, O4, CD31, Ter119 positive cells and dead cells, OB neuroblasts are identified by co-localization of PSA-NCAM and CD24 high levels.

According to our surface marker strategy, the $CD45^{-}/CD31^{-}/Ter119^{-}/O4^{-}CD24^{-}$ fraction should be enriched in NSCs and, therefore, we decided to test for the enrichment in NSC markers and neurosphere forming capacity. To do so, we applied a gentle separation strategy based on a positive magnetic exclusion (MACS®) of all differentiated cell markers to obtain a negative fraction enriched in viable NSCs. SEZ homogenates were incubated with a mixture of biotinylated antibodies against CD45, CD31, Ter119, O4 and CD24 antigens and then the cells were labelled with anti-biotin magnetic microbeads. Labelled samples were passed through a column on a magnetic field and the eluted fraction was collected as the CD45/CD31/Ter11/O4/CD24 lineage-negative fraction or Lin^{-}. Additionally, the retained fraction was recovered and kept as the CD45/CD31/Ter11/O4/CD24 lineage-positive fraction or Lin^{+} (Figure 15a). Flow cytometry analysis of both fractions confirmed that Lin^{-} and Lin^{+} were greatly excluded (Figure 15b). $GLAST^{+}$ NSCs can be separated from $GLAST^{+}$ non-neurogenic astrocytes by their $CD9^{high}$ expression. Flow cytometry analysis of both fractions confirmed that the Lin^{-} portion was greatly enriched in $GLAST^{+}/CD9^{high}$ cells (as much as 60%). Almost half of them exhibited EFGR suggesting that this fraction would contain activated and quiescent NSCs (Figure 15c).

Furthermore, analysis of mRNA expression corroborated that the expression of NSC markers *Glast*, *Gfap* and *Egfr* was enriched in Lin^{-} samples, whereas microglia and lymphocyte markers *Iba1* and *Cd45*, the endothelial cell marker *Cd31*, the neuroblast marker *Dcx* and the ependymal cell and mature astrocyte-related *S100b* were expressed selectively by the Lin^{+} fraction (Figure 15d). Moreover, when

cultured in neurosphere medium supplemented with EGF and FGF for 7 DIV, neurosphere-forming capacity was enriched in Lin$^-$ cells when compared to unsorted or Lin$^+$ samples (Figure 15e). Together, this data demonstrated that after exclusion of CD45, CD31, Ter119, O4 and CD24 positive cells, the remaining negative fraction is clearly enriched in cells with NSC properties.

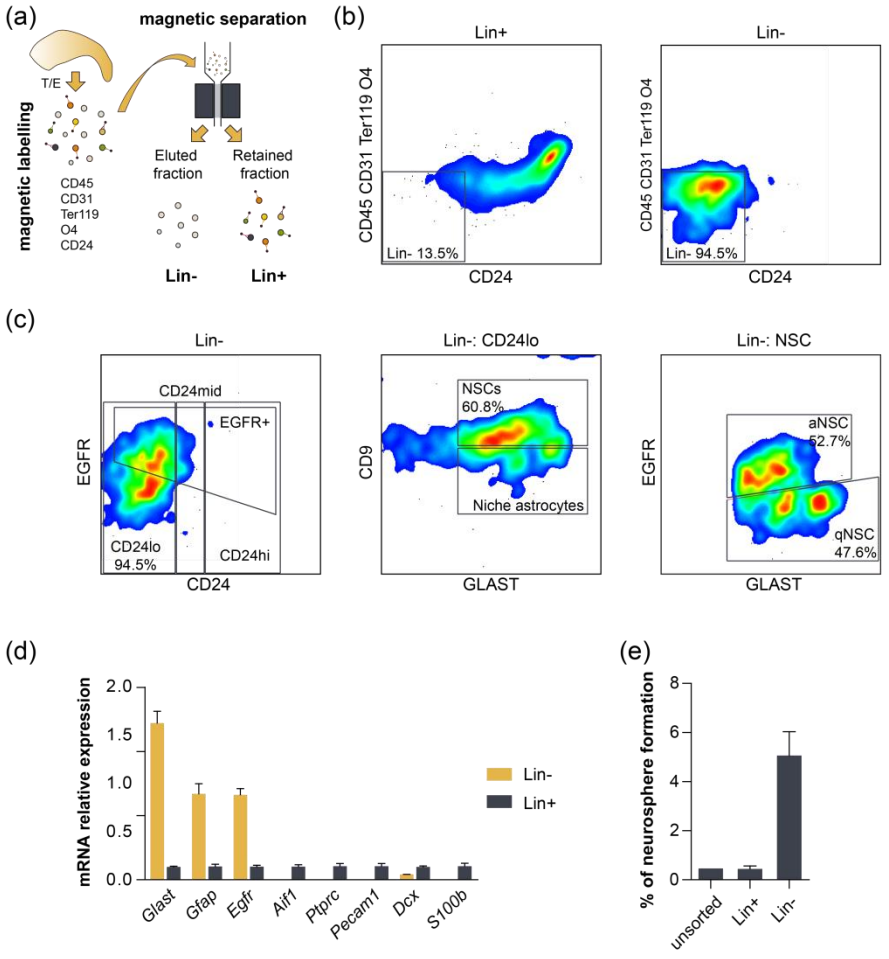

Figure 15. MACS®-sorted Lin- fraction (CD45/O4/CD31/Ter119/CD24$^-$) is enriched in cells with NSC features. (a) Schematic representation of the MACS® separation strategy. After SEZ dissociation, CD45, O4, CD31, Ter119 and CD24-positive (Lin$^+$) cells are magnetically labelled and separated from the Lin$^-$ fraction. **(b)** Representative plots showing the correct exclusion of markers in Lin$^+$ and Lin$^-$ cells and **(c)** the NSC gating of Lin$^-$ cells which are greatly enriched in cells with NSC

molecular features (CD24^{low} GLAST^{+} CD9^{high} +/- EGFR cells). **(d)** qRT-PCR gene expression analysis of NSC (*Glast*, *Gfap* and *Egfr*) and Lin^{+} (*Aif1* (Iba1), *Ptprc* (CD45), *Pecam1* (CD31), *Dcx* and *S100b*) related markers in RNA samples from Lin^{-} and Lin^{+} purified fractions (n=3). **(e)** The Lin^{-} fraction is enriched in neurosphere forming cells (n=3).

As previously described (Llorens-Bobadilla et al., 2015), the different NSC states can be classified by GLAST intensity and EGFR expression. After excluding non-neurogenic GLAST^{+} astrocytes from GLAST^{+} NSCs by CD9 levels (Figure 16a,b) the presence of the EGFR determines activation in subependymal NSCs and GLAST levels correlate with the two states previously characterized by transcriptomic analysis. In this way, inside the CD45^{-}/CD31^{-}/Ter119^{-}/O4^{-}/CD24$^{-/low}$/GLAST^{+}/CD9^{high}, qNSC1 are GLAST^{high}/EGFR^{-} cells, qNSC2 are GLAST^{low}/EGFR^{-} cells and aNSC are GLAST^{+}/EGFR^{+} cells (Figure 16c). Within the GLAST^{+}/CD9^{high} fraction, qNSC1 and qNSC2 cells represent around 30% each while the aNSC population represents up to 40%.

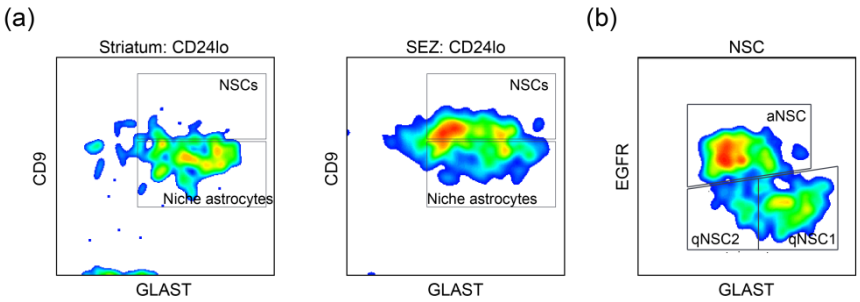

Figure 16. Identification of quiescent and activated NSC states. (a,b) Representative FACS plots showing SEZ NSC gating strategy. **(a)** The CD24^{lo} fraction contains GLAST^{+}CD9^{high} NSCs that are separated from GLAST^{+} CD9^{low} niche astrocytes and striatum astrocytes or other CD24^{lo}GLAST^{-} cells. **(b)** GLAST and EGFR expression define three NSC populations: qNSC1 (GLAST^{high} EGFR^{-}), qNSC2 (GLAST^{low} EGFR^{-}) and aNSC (GLAST^{low} EGFR^{+}).

Cell Type	Defining combination of markers	%
qNSC1	$Excl^-/CD24^{-/low}/GLAST^{high}/CD9^{high}/EGFR^-$	1.85 ± 0.28
qNSC2	$Excl^-/CD24^{-/low}/GLAST^{low}/CD9^{high}/EGFR^-$	1.05 ± 0.16
aNSC	$Excl^-/CD24^{-/low}/GLAST^+/CD9^{high}/EGFR^+$	2.30 ± 0.18
TAPs	$Excl^-/CD24^{mid}/EGFR^+$	4.77 ± 0.25
SEZ neuroblasts	$Excl^-/CD24^{high}/EGFR^+$	15.43 ± 0.50
Migrating neuroblasts	$Excl^-/CD24^{high}/EGFR^-$	51.55 ± 1.40

Table 10. Specific combination of markers that define the different SEZ populations and the percentage of representation of each population relative to the total number of cells in the SEZ. $Excl^- = CD45^-/CD31^-/Ter119^-/O4^-$.

Cell size and mitochondrial activity has been proposed to reflect different cell states and correlate positively with proliferation and cell cycle progression in cells, including some SCs (Knobloch and Jessberger, 2017; Llorens-Bobadilla et al., 2015; Rodgers et al., 2014). Therefore, we decided to evaluate whether we could correlate changes in cell size and/or mitochondrial activity within the different populations we had defined, by labelling SEZ homogenates with MitoTracker in combination with our marker panel. Additionally, we measured the mean cell size of each population using FSC parameter. Our analysis showed that both traits nicely correlate with the lineage progression being the lowest in quiescent NSCs and increasing progressively along the increasingly proliferating states (aNSC, TAPs, and $EGFR^+$ neuroblasts) (Figure 17a,b). Furthermore, we could even follow the progression up to non-proliferative $CD24^{high}/EGFR^-$ neuroblasts, which are expected to be less metabolically active, finding that they have lower FSC and MitoTracker level than $CD24^{high}/EGFR^+$ cells (Figure 17a,b). Of notice, qNSC2 presented a slightly bigger size than the dormant pool, a trait that has been previously reported for alerted MuSCs (Rodgers et al., 2014)(Figure 17b).

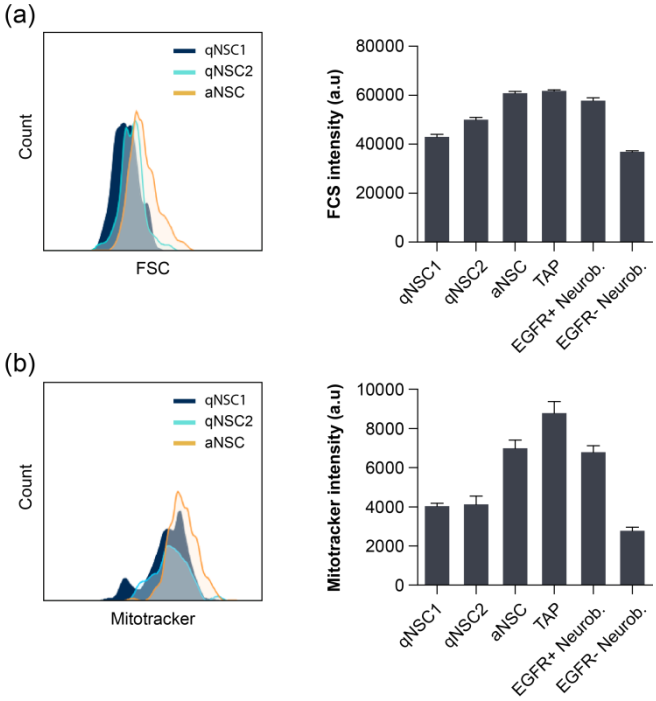

Figure 17. Proliferating cells exhibit increased cell size and high mitochondrial activity. (a) Representative histogram of the FSC intensity in qNSC1, qNSC2 and aNSCs and quantification of the mean FSC intensity in each cell type (n=5) reflecting that the proliferative populations (aNSCs, TAPs and EGFR$^+$ neuroblasts) display bigger cell size. **(b)** Representative histogram showing MitoTracker intensity in qNSC1, qNSC2 and aNSC and quantification of mean intensity in each cell type (n=3). Note that proliferating aNSCs, TAPs and EGFR$^+$ neuroblasts increase their mitochondrial activity until they become EGFR$^-$ neuroblasts.

1.2. qNSC2 or alerted NSCs represent an intermediate state between dormancy and activation

As a first validation of our cell classification strategy, we decided to interrogate our populations in a regeneration paradigm. Subependymal NSCs can completely regenerate the structure following near complete elimination of their proliferating cell progeny with a subacute treatment with anti-mitotic agents, such as Ara-C or TMZ, which kill the different proliferative SEZ cell types including aNSCs while sparing quiescent cells (Doetsch et al., 1999a; Mich et al., 2014; Pastrana et al., 2009). We performed some initial experiments with AraC infused intra-cortically

for 6 days using osmotic minipumps, but the surgery induced a very high brain microglial reaction in both saline and AraC-injected animals, as detected with antibodies to IBA-1 (data not shown). Because we wanted to evaluate effects of inflammation in subependymal NSCs, we decided to use the alternative anti-mitotic drug TMZ which is administered to the animals by intraperitoneal (i.p.) injection. It has been shown that 3 doses of TMZ during 3 days effectively eliminate the activated NSCs and neurosphere forming cells, forcing the remaining qNSCs to exit from dormancy, become activated, and regenerate the SEZ (Mich et al., 2014). TMZ or vehicle DMSO was intraperitoneally administered for 3 consecutive days and mice were sacrificed 3 days after the last injection. The effectiveness of the treatment was confirmed by scoring the number of primary neurospheres *in vitro* and quantifying neuroblast chains in whole-mounts of the lateral ventricle wall immunostained for neuroblast marker DCX (Figure 18b,c). Flow cytometry analysis of TMZ-treated SEZ tissue showed the almost complete abolition of the $CD24^{mid/high}$ cell fraction containing neuroblasts and TAPs (Figure 18d). Additionally, at the OB we could observe that the portion of cells co-expressing CD24 and PSA-NCAM (arriving immature neuroblasts) had also disappeared after the treatment (Figure 18f). Interestingly, the $CD24^{-/low}$ fraction was greatly enriched after the anti-mitotic treatment; moreover, the vast majority of them could be identified as quiescent NSCs whereas aNSC were almost completely absent (Figure 18e) in line with previous reports showing their sensitivity to anti-mitotic drugs (Doetsch et al., 1999a; Mich et al., 2014; Pastrana et al., 2009). This result supports the concept that the selected $CD45^{-}/CD31^{-}/Ter119^{-}/O4^{-}CD24^{-/low}/GLAST^{+}/CD9^{high}/EGFR^{-}$ cells are mainly quiescent and that the absence of EGFR distinguish them from the activated pool of NSCs.

To further confirm this idea, we tested the ability of the remaining quiescent NSCs to be activated and to replenish the TAP and neuroblast populations analysing the SEZ and OB of TMZ lesioned mice after 35 days. Although it has been described that cell replenishment is complete by 90 days, signs of regeneration can

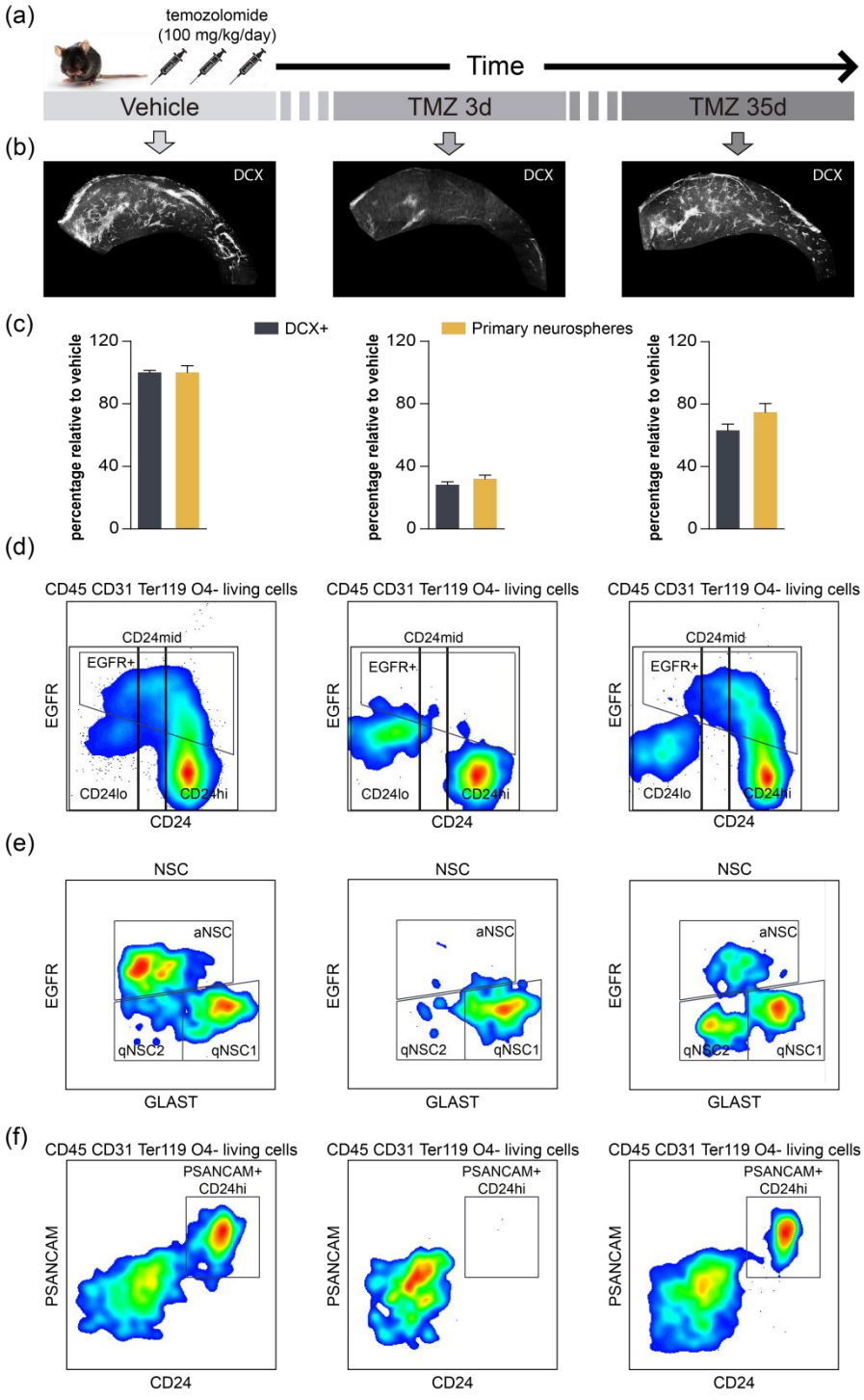

Figure 18. Proliferating but not quiescent predicted states are effectively targeted by

temozolomide administration and are partially restored 35 days after the lesion. (a) Schematic representation of experimental design. Mice were intraperitoneally injected with vehicle or TMZ (100 mg/kg/day) for 3 consecutive days and sacrificed 3 or 35 days later to analyse the initial and intermediate stages of SEZ regeneration. **(b)** Reconstruction of confocal images obtained from immunostained SEZ wholemount preparations showing the reduction of DCX^+ neuroblast chains 3 days after TMZ administration and their restoration after 35 days. **(c)** Quantification of primary neurospheres and DCX^+ neuroblast chains in vehicle (n=6), 3 days (n=3) and 35 days (n=4) after TMZ administration confirms that proliferating cells are efficiently eliminated and progressively restored. **(d)** Representative FACS plots of CD45/O4/CD31/Ter119-negative cells showing the reduction and re-apparition of $EGFR^+$ cells in the $CD24^{low}$ (NSCs), $CD24^{mid}$ (TAPs) and $CD24^{high}$ (neuroblasts) fractions after TMZ administration. **(e)** Representative plots of the NSC gating showing that aNSC are greatly affected by TMZ treatment whereas qNSC are resistant. Note that the aNSC pool re-appeared 35 days later. **(f)** Representative plots of OB neuroblast ($PSA\text{-}NCAM^+$ $CD24^{high}$) showing that TMZ supresses the migration of neuroblasts to the OB, migration that is restored after 35 days.

already be observed as early as 35 days (Mich et al., 2014). We confirmed the successful regeneration of the neurogenic niche as the number of SEZ-derived primary neurospheres and neuroblast migrating chains were restored to a significant extent after 35 days (Figure 18b,c). We could observe the reappearance of cells with increasing levels of CD24 which likely included TAPs and neuroblasts in analyses with flow cytometry after this period of regeneration (Figure 18d,e). Moreover, we could observe increased numbers of $CD24^{high}/PSANCAM^+$ cells in the OB confirming that the migration of neuroblasts to the OB was also restored (Figure 18f). Altogether, these results support the accuracy of gating strategy for the specific detection of SEZ NSCs in different proliferative states as well as their resulting committed progeny.

It has been proposed that activated NSCs should be able to self-renew and return to a quiescent state, since regeneration seems to be conservative and is not accompanied by a reduction in the qNSC pool (Mich et al., 2014). Nevertheless, it is not known whether the acquisition of an alerted qNSC2 phenotype is an obligated step between quiescent and activated states during this process. To gain insight into this possibility, we analysed the different proliferative states of NSCs at different time points after the treatment. Interestingly, among the qNSCs that were spared by the treatment most of the remaining ones were in a qNSC1 dormant state (Figure 19a,b). This observation suggested that pre-existing qNSC2

might have either been activated and died during the days of treatment, or returned to a q1 state. In any case, in this scenario, remaining qNSCs are expected to regenerate the missing populations and indeed, 35 days after the lesion, some of them were in an active state in line with the partial restoration of the TAP and neuroblast populations in the SEZ (figure 19b,c). Moreover, in agreement with previous reports, we could see that the total number of qNSCs remained roughly constant during the entire process (Figure 19b). However, compared with 3 days after treatment when most of them were qNSC1, at this moment of active regeneration, around 50% of qNSCs were again qNSC2 (Figure 19a). These data suggested that the alert state seems to be an intermediate step in the transition from deep quiescence to activation and that, even in a situation where dormant NSCs are forced to activate and divide, a parallel mechanism must exist that, coupled with self-renewal, ensures the maintenance of the quiescent pool, supporting the idea of the reversibility of the system.

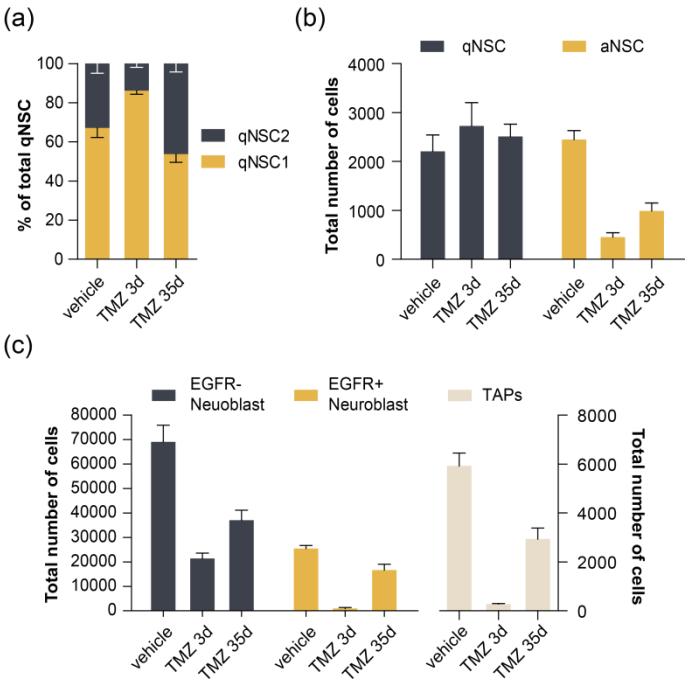

Figure 19. Dormant qNSCs are resistant to TMZ antimitotic treatment and transit through an intermediate alert state in order to activate and regenerate the niche. (a-c) Quantification by

flow cytometry of the different NSC states, TAPs and EGFR$^+$ and EGFR$^-$ neuroblasts during a TMZ-based regeneration paradigm. **(a)** 3 days after TMZ, most of the quiescent NSCs that remain in the SEZ are in a dormant qNSC1 state, but 35 days later, qNSC2 have re-appeared and the balance between both populations has returned to basal levels. **(b)** qNSCs remain roughly constant whereas TMZ administration drastically reduces the total number of aNSCs observed at 3 days, which are partially restored 35 later. (**c**) NSC progeny, i.e. TAPs, EGFR$^+$ and EGFR$^-$ neuroblasts, is greatly reduced 3 days after TMZ administration and is partially restored 35 days after. (vehicle n=6; TMZ 3d n=3; TMZ 35d n=3).

2. The effects of inflammation in the quiescent cell cycle of adult subependymal NSCs

2.1. LPS-induced systemic inflammation disrupts SEZ homeostasis and modulates NSC activity

One of the main objectives of this thesis was to assess the effects of inflammation on subependymal NSCs and neurogenesis. Thus, initially, in order to get a general picture of the SEZ response, we induced systemic inflammation with a well-established and extensively used procedure, consisting in the i.p. injection of LPS. Mice were injected with saline or 5 mg/kg of LPS and the SEZ was analysed at 1h, 24h, 3 days or 6 days after the administration. As a first approach to evaluate the effect of inflammation on SEZ homeostasis, we performed quantitative real time PCR (qRT-PCR) analysis of a set of genes selected as representative markers of the different populations on the SEZ neurogenic niche. Significant changes were observed at 24h after injection that were mainly characterized by a downregulation of most of the genes (*Sox2, Hes5, Fabp7, Cyclind1, S100β, Ascl1, Nr2e1, Nestin, Olig2, Cspg4, Egfr, Dcx, Hes1, Tubb3, Fgfr1 or Fgfr2*) (Figure 20a) indicating potentially negative effects of inflammation over most of the SEZ populations. However, we simultaneously found increased expression of some NSC-related genes (*Gfap, Prom1, Cdkn1a, Id1* or *Fgfr3*) suggesting that positive effects might have been specifically promoted in these cells (Figure 20a). Interestingly, during the days following the initial perturbation, expression profile of the evaluated genes returned to the initial pre-inflammation levels (Figure 20a). This analysis

corroborated that peripheral inflammatory signals can affect SEZ homeostasis and suggested a complex cellular response where detrimental effects might be coexisting transiently with a stimulation of the NSC pool.

In an attempt to further test this hypothesis, we scored the total number of cells acutely extracted from SEZ tissue at the same time points after LPS injection, finding a considerable reduction in cell yield that was most evident at 3 days and maintained even at 6 days after LPS treatment (Figure 20b). However, when these SEZ dissociates were seeded in neurosphere culture medium, we could see that the portion of SEZ cells capable of forming neurospheres was significantly enriched after 24h of LPS treatment, suggesting again that inflammation causes global detrimental effects on the SEZ niche and a positive response in NSCs (Figure 20c). To look specifically at this population, we injected wild-type mice with the nucleoside analogue CldU and waited 28 days to induce acute inflammation with LPS, so we could analyse its effects on subependymal activated label-retaining (LR) NSCs. After the treatment with LPS, animals were injected with a different analogue, IdU, which can be distinguished from CldU by specific antibodies (Moreno-Estelles et al., 2012), 1h before the sacrifice. According to the previous results, LPS-injected mice showed a significant reduction in total proliferating cells (IdU^+ cells) (Figure 20d). The number of $CldU^+$ LR-NSCs was unaffected indicating no changes in the survival of aNSCs that had incorporated the nucleoside 28 days before the treatment; but interestingly, the proportion of $CldU^+$ LR-NSCs that had re-entered the cell cycle and, hence, become IdU^+ cells increased after LPS administration (Figure 20e,f). Furthermore, 3 days after LPS induction, a moment when detrimental effects on total cell numbers were evident (Figure 20b), the proportion of $GFAP^+$ cells co-expressing the activation markers EGFR and Ki67 in the intact SEZ was also higher (Figure 20g). These results confirmed that peripheral inflammation, despite having an overall negative effect on the SEZ niche, promotes the activation of the NSC pool.

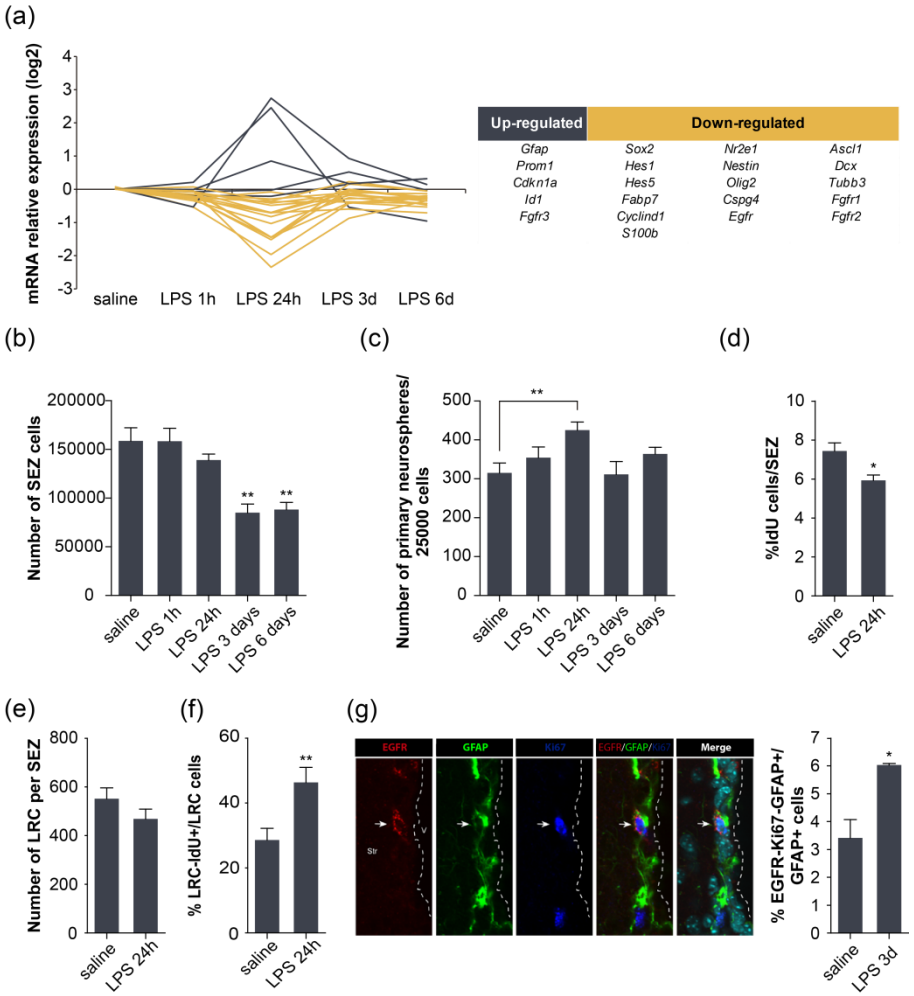

Figure 20. LPS-induced systemic inflammation causes global detrimental effects on SEZ populations but positively modulates NSC activity. (a) qRT-PCR detection of the expression levels of multiple genes expressed by different SEZ populations in the SEZ of LPS-injected mice at 1h, 24h, 3 days and 6 days relative to saline basal expression. Up-regulation of some NSCs-related genes and down-regulation of many others at 24h reflects a complex scenario that tends to return to homeostasis after 6 days (n=5). **(b)** Quantification of the total number of viable cells retrieved form the SEZ shows that LPS produces a long-term (3-6 days) detrimental effect (n=5). **(c)** The number of SEZ-derived primary neurospheres after LPS administration reveals an enrichment of neurosphere-forming cells at 24h (n=5). **(d)** The proportion of SEZ cells labelled after a single pulse of IdU 1h before sacrifice is reduced 24h after LPS administration (saline n=4; LPS n=3). **(e)** Quantification after 24h of saline or LPS injection of the LRC fraction labelled after 28 days of ClDU administration showing that the LRC pool is not negatively affected. **(f)** Analysis of LRC that are labelled after a single pulse of IdU 1h before sacrifice reveals that LPS induces the LRC fraction to re-enter cell-cycle (saline n=8; LPS n=6). **(g)** Confocal images of SEZ samples immunostained for GFAP, EGFR, Ki67 and Dapi and quantification of GFAP$^+$ cells co-expressing EGFR and Ki67 markers 3 days after LPS administration showing increased GFAP$^+$ cells displaying activated markers (n=3).

In order to evaluate effects of LPS in the different NSC populations the SEZs of naïve, saline or LPS-injected mice were dissociated 24h after the injection and prepared for flow cytometry. While naïve and saline groups showed similar proportion of activated NSCs, as expected, we found that qNSC/aNSC profile shifted towards activation in the LPS-injected mice (Figure 21a). Additionally, we could see that this increased activation led to a significant enrichment in TAPs and EGFR$^+$ neuroblasts but not in EGFR$^-$ neuroblasts (Figure 21b-d). These results corroborated that acute inflammation is promoting activation of both aNSCs, as indicated by the nucleoside incorporation experiments shown above, and qNSCs, as indicated by the flow cytometry analysis. The observation that this activation does not result in increased levels of EGFR$^-$ neuroblasts is in line with reportedly reduced neurogenesis observed after LPS treatment and suggests direct deleterious effects of inflammation in neuroblasts (Monje et al., 2003).

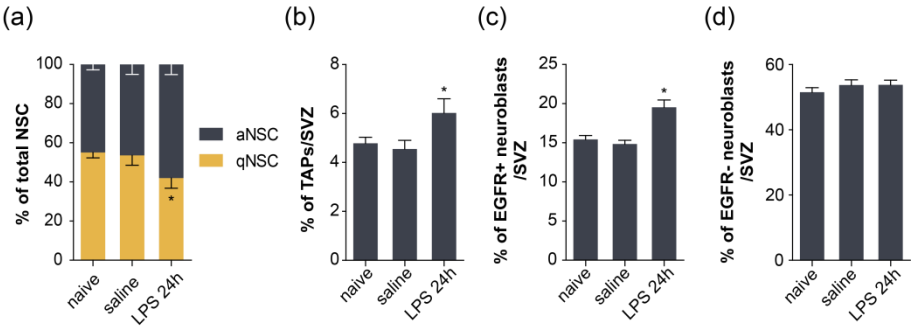

Figure 21. LPS-induced systemic inflammation activates NSCs and increases the production of TAPs and EGFR$^+$ neuroblasts. (a-d) Flow cytometry analysis of NSCs, TAPs and neuroblasts in naïve, saline and LPS groups. Quantification of each cell type 24h after LPS injection shows **(a)** a higher proportion of NSCs in activated state and **(b)** increased TAPs **(c)** and EGFR$^+$ neuroblasts but not **(d)** EGFR$^-$ neuroblasts in the SEZ (naive n=6; saline n=4; LPS 24h n=4).

We further stratified the NSC population in our LPS paradigm. Apart from the previously observed increase in activated NSCs, we found that the remaining quiescent pool contained more alert cells (qNSC2) at the expense of the qNSC1 population compared to the naïve basal situation (Figure 22a) suggesting that inflammation was indeed activating qNSC1 to promote a qNSC2 state.

2.2. A mild peripheral lesion drives quiescent NSCs into an alert state

In the course of the previous experiments, we found a surprising result. Although we did not find more activated aNSCs in saline-injected mice compared to the naïve non-injected animals (Figure 22b), this group showed exactly the same alert phenotype in the quiescent population than the LPS group (Figure 22a). Therefore, although unexpected, it seemed that acute inflammation targets the qNSC pool promoting its activation, but these quiescent cells can also respond to mild peripheral stimuli, such as an i.p. sterile saline injection, acquiring an alert state.

NSCs responding to the i.p. administration of saline solution generated an interesting scenario where qNSCs in the SEZ become alert but not activated, in contrast to LPS-induced inflammation where qNSCs are alerted and also activated. This suggested the interesting possibility that the intensity and/or type of peripheral remote signals could differentially regulate NSC dynamics in the SEZ. Despite the mentioned finding of the existence of a pool of qNSC displaying an alerted phenotype, little is known about the regulation of this process and its potential reversibility. To address this question, we analysed the alerted state of NSCs over time after a single i.p. injection of sterile saline. After the initial increase in qNSC2 24h post-injection, we observed a progressive regression of the q2NSC/qNSC1 ratio back to basal naïve levels during the following 3 to 6 days (Figure 22a). Interestingly, in contrast with LPS, peripheral injection-mediated response did not lead to an increase in the activated NSC pool (Figure 22b) suggesting that qNSC are not only able to acquire an alerted phenotype but also they retain the ability to revert to a dormant state.

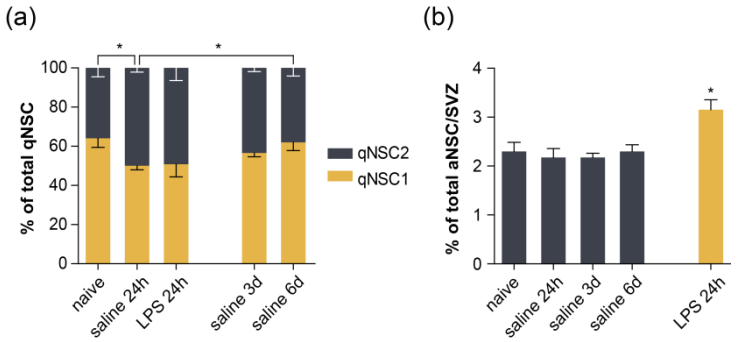

Figure 22. I.p. injection of sterile saline or LPS induces qNSCs to acquire a reversible alert state but only LPS drives qNSC into activation. (a,b) Flow cytometry analysis of qNSCs and aNSC in saline-injected mice at 24h, 3 days and 6 days compared to LPS-induced systemic inflammation at 24h. (**a**) Proportion of total qNSC in dormant or alert state showing a shift towards qNSC2 24h after LPS or saline injection which reverts to basal levels after 6 days. (**b**) LPS but not saline i.p. injection increases the proportion of aNSC in the SEZ. (naïve n=6; saline 24h n=4; saline 3d n=4; saline 6d n=4; LPS 24h n=4).

2.3. Common patterns of cytokine expression in the SEZ following peripheral intervention injections

LPS injection is a well-known model of systemic inflammation and it has been described that these peripheral signals can reach the CNS causing secondary neuroinflammation. Systemic administration of LPS causes a peripheral inflammatory cascade that is transduced to the brain via IL-1β from the cerebral vasculature and causes a strong up-regulation of central pro-inflammatory cytokine production by microglia (Godbout et al., 2005; Qin et al., 2007; Turrin et al., 2001). Accordingly, we found increased mRNA levels of several pro-inflammatory molecules in the SEZ tissue after LPS administration: TNF-α and IL-1β presented a fast induction (1h) that increased at 24h and remained upregulated even after 6 days (Figure 23a). Additionally, IL-6, PGRN and IFN-γ expression was also higher at 24h but were downregulated to normal levels after 3 days (Figure 23a).

We hypothesised that some of these molecules might be mediating the observed changes in NSC alert and activation, so we assessed their expression in the saline and TMZ injected animals. Almost identical to the LPS profile, 24h after

saline injection, we saw an induction of TNF-α, IL-1β, IL-6 and PGRN, but not IFN-γ, although at much lower intensity (Figure 23b). Moreover, in line with the cytometry results indicating a transitory response, all these cytokines returned to basal levels during the following 3 to 6 days (Figure 23b). Curiously, we could see that, during the initial hours of regeneration after the TMZ lesion, only TNF-α and PGRN mRNAs presented a transient up-regulation, while expression of IL-β, IL-6, or IFN-γ remained unaltered (Figure 23c).

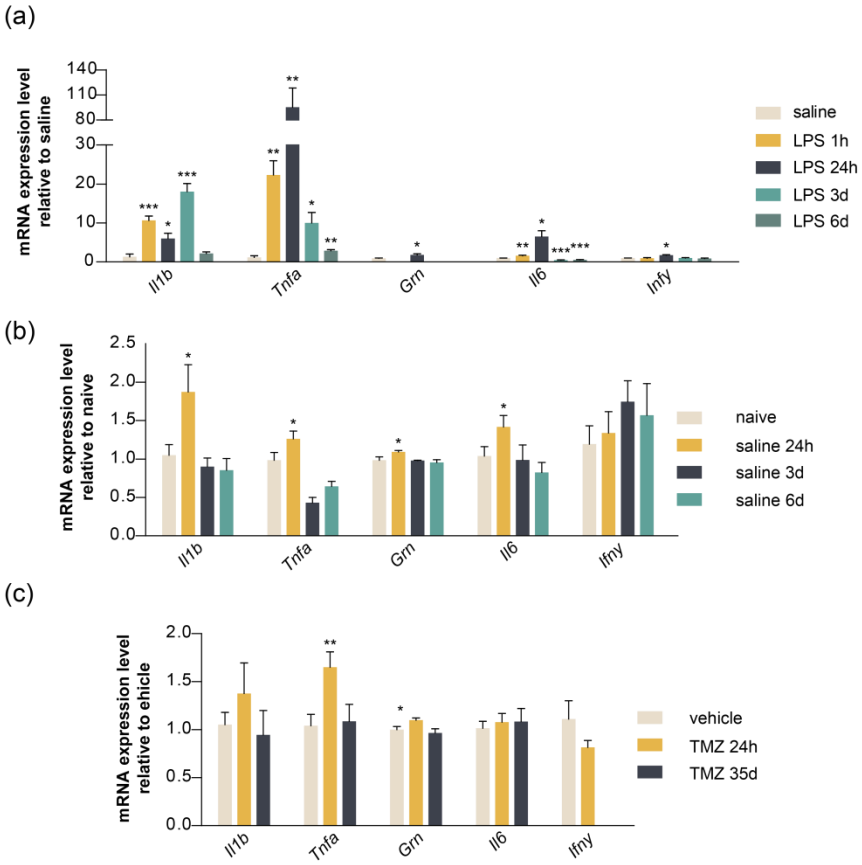

Figure 23. LPS, sterile saline and TMZ peripheral administration induce the expression of several cytokines with a common cytokine expression in the SEZ. (a-c) Gene expression levels of *Il1b, Tnfa, Grn, Il6 and Infy* detected by qRT-PCR in SEZ samples obtained from **(a)** saline (n=4) or LPS-injected mice at 1h, 24h, 3 days and 6 days (n=5), **(b)** naïve (n=8) or saline-injected mice at 24h (n=8), 3 days (n=4) and 6 days (n=4) and **(c)** vehicle (n=8) or TMZ-injected mice at 24h (n=8) and 35 days (n=4). Note that *Tnfa* and *Grn* are upregulated in all three situations 24h after i.p administration.

Taken together, these results indicated that, in response to different stimuli that have in common the conservative mobilization of the dormant NSC pool, either to become activated (TMZ and LPS injections) or just to acquire a transient alert phenotype (saline injection), inflammatory mediators TNF-α and PGRN are induced in the SEZ tissue and might, therefore, be act as niche factors regulating these processes.

3. Dual effects of TNF-α in adult subependymal NSCs

3.1. Mixed dose-dependent effects of TNF-α

In order to study the effects of TNF-α in NSCs in greater depth, we decided to take advantage of the neurosphere assay. Neurospheres contain a heterogeneous population of cells where a small fraction of NSCs coexist with their progeny (different types of more committed progenitors and even some differentiated cells). As a consequence, in order to address specific effects of a factor on the NSC population, neurosphere formation must be evaluated both in the presence of the tested molecule and in a sequential assay by disaggregating the treated neurospheres and sub-culturing them in the absence of the factor (Belenguer et al., 2016). NSCs were plated at very low density and treated with increasing concentrations of recombinant murine TNF-α. After 5 div, compared to untreated controls, cultures treated with the lowest concentration (0.1 ng/ml) formed more neurospheres, whereas increasing concentrations of TNF-α (10–20 ng/ml) led to a reduction in the number of neurospheres (Figure 24b). These results suggested that TNF-α modulates NSC proliferation and/or survival in a complex manner. Nevertheless, when dissociated and plated again in the absence of the factor, TNF-α pre-treated cells, at any concentration, consistently gave rise to a greater number of neurospheres (Figure 24c) suggesting that, besides its effects in proliferation/survival, TNF-α is specifically promoting the expansion of the population of neurosphere forming cells.

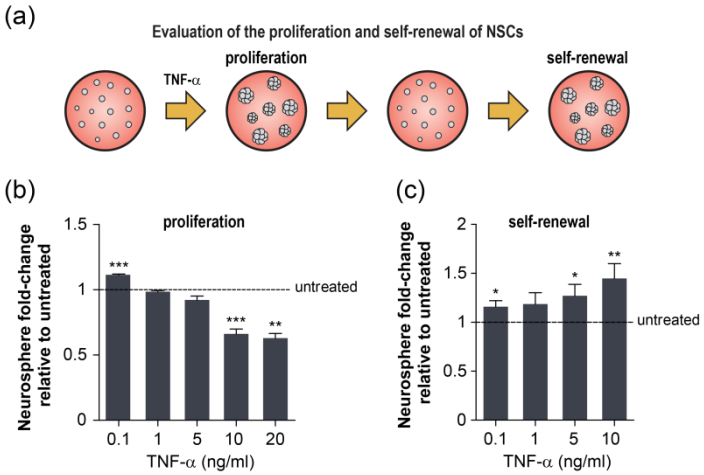

Figure 24. TNF-α treated NSC cultures display mixed effects in a dose dependent manner: a decrease in neurosphere formation is accompanied by an enhance expansion of the culture after the treatment. (a) Schematic representation of the experimental design. Neurosphere formation of single cells is evaluated first in the presence of TNF-α (proliferation) and in a sequential assay by disaggregating the treated neurospheres and sub-culturing them in the absence of the factor (self-renewal). **(b)** Quantification of the number of neurospheres formed in the presence of increasing doses of TNF-α. Compared to untreated control, TNF-α at 0.1 ng/ml stimulates neurosphere formation whereas doses higher than 10 ng/ml are detrimental (n=3-10) **(c)** Quantification of the number of neurospheres generated from dissociated pre-treated neurospheres relative to untreated neurospheres showing an increased expansion potential of TNF-α treated cultures (n=4-7).

Since concentrations of TNF-α higher than 10 ng/ml reduced the formation of neurospheres, we tried to address whether this was caused by a loss of cell viability and/or a cell-cycle arrest. After 24h in the presence of TNF-α at 10 ng/ml, we could see an increase in apoptosis as we scored more activated caspase-3 positive cells (Figure 25a). Accordingly, treated cells displayed reduced viability in an enzymatic MTS assay (Figure 25b). Additionally, when we analysed their DNA content, we found that this loss of cell viability was accompanied by impaired proliferation since we found fewer cells in S and G2/M phases of the cell cycle (Figure 25c). Taken all data together, we concluded that TNF-α at high concentrations exerts a negative effect on neurosphere formation by a combination of cell cycle arrest and induction of apoptosis.

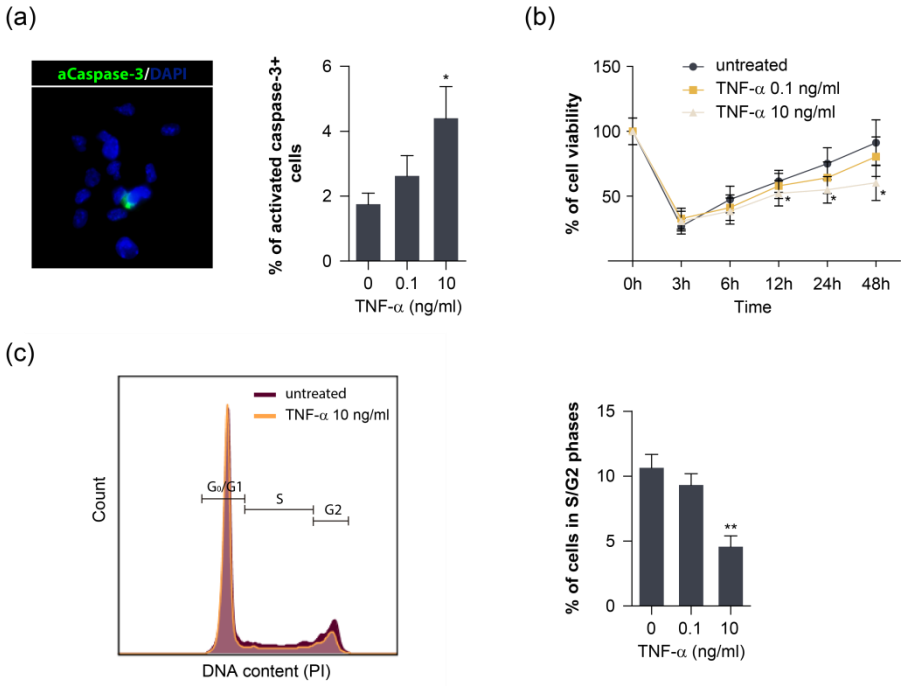

Figure 25. Negative effects of TNF-α on NSC proliferation are related to reduced cell viability and a cell cycle arrest. (a) Immunocytochemistry detection of activated caspase-3 (left) and the proportion of cells displaying aCaspase-3 respect to total cell nuclei (DAPI) in untreated or TNF-α-treated cells (right) (n=3) where it is observed that TNF-α at 10 ng/ml increases the number of aCaspase-3^{+} cells. **(b)** Cell viability assessment with MTS assay of untreated or TNF-α treated cultures at different time points referred to the initial plated cells (100%) reflects a progressive loss in cell viability in TNF-α-treated cultures (n=3). **(c)** Representative histogram showing the different cell cycle phases determined by cell DNA content in untreated or TNF-α-treated cultures (left). Quantification of cells in S and G2 cell cycle phases reveals a decreased proportion of cells those phases in the presence of 10 ng/ml of TNF-α (right) (n=3).

Although the increment in neurospheres seen in the presence of low levels of TNF-α pointed to a direct positive effect on NSC biology, the higher numbers of secondary neurospheres found after treatment might be the result of the neurosphere forming cells not being affected by negative effects of TNF-α and, therefore, being indirectly enriched in its presence. In order to clarify this, primary neurosphere cultures where grown in the continuous presence of 10 ng/ml of TNF-α during 4 serial passages. As expected, TNF-α reduced the number of cells

obtained in the first passage (P1). However, additional treatments of TNF-α during P2, P3 and P4 not only did not result deleterious, but also progressively generated cultures with greater expansion ability (Figure 26a). Additionally, after reaching passage 3, we evaluated the neurosphere forming potential of continuously treated or untreated control cells in the presence or absence of 10 ng/ml TNF-α. In line with our previous observation, a punctual treatment of naïve control cells yielded less neurospheres (Figure 26b). However, cells that had been grown continuously exposed to TNF-α, when assayed in the absence of the factor, formed more secondary neurospheres and even more intriguing, an additional treatment, instead of reducing their number, significantly promoted the formation of a higher number of neurospheres (Figure 26b). Interestingly, the size of the neurospheres after TNF-α treatment was reduced in both cases (Figure 26c) suggesting that negative effects on survival/proliferation were still present, although not in neurosphere-forming NSCs. Altogether, these results revealed that TNF-α negative and positive effects are separated phenomena and that the increased expansion of TNF-α-treated cells is rather due to an amplification of a specific pool of NSCs.

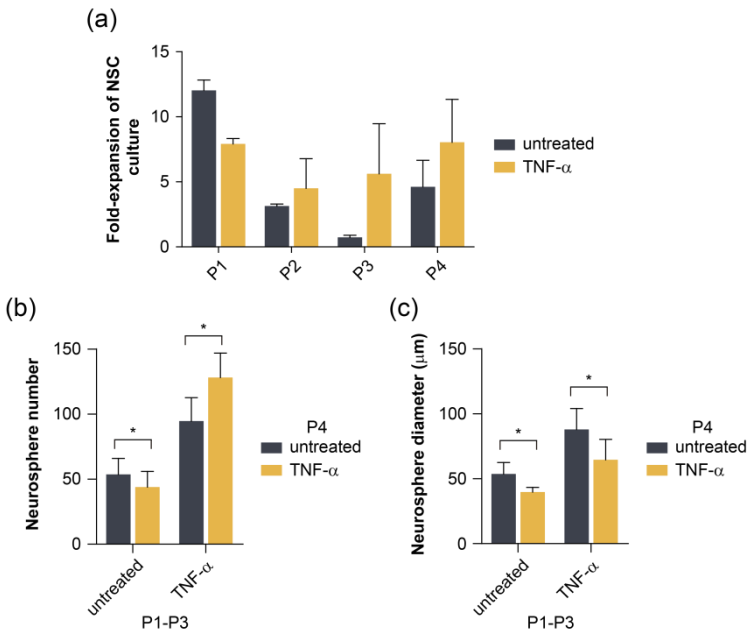

Figure 26. **Continuous exposure to TNF-α promotes the expansion of NSCs in neurosphere cultures. (a)** Evaluation of the number of cells obtained after each cell passage (P1 to P4) referred to the initial number of plated cells in each passage. NSC cultures continuously treated with 10 ng/ml of TNF-α show increased expansion potential after 3 serial passages. **(b)** Scoring of the number of neurospheres obtained from untreated, punctually treated or continuously treated cells during 4 serial passages with 10 ng/ml TNF-α reflects an exacerbation of neurosphere formation after a TNF-α reiterative treatment. **(c)** Representation of the mean neurosphere diameter in untreated or TNF-α treated cells reveals a reduction of neurosphere size when TNF-α is present. (n=3)

In order to test if TNF-α produced by microglia had the same effect as the recombinant one, we forced the acquisition of a pro-inflammatory state in the microglia cell line N13 by stimulation with LPS. Then we cultured activated microglia cells in neurosphere growth medium to obtain a medium conditioned by activated microglia (MCM) that could be added afterwards to NSCs. We observed that NSCs grown in the presence of MCM formed more neurospheres and that, when disaggregated and plated again in regular medium, MCM-treated cells continued to form more secondary neurospheres compared to MCM-untreated ones (Figure 27a,b). This result highlighted that activated microglia produce factors that increase not only NSC proliferation and/or survival, but also the expansion of the NSC pool through self-renewal.

Because activated microglia secrete several cytokines and modulators other than TNF-α, to test its specific contribution to this process we eliminated this cytokine from the MCM by immunoprecipitation with an excess of a TNF-α specific antibody (Figure 27c). NSCs cultured in the presence of immunodepleted medium or in medium immunoprecipitated with a non-related antibody of the same isotype as a control, still formed more neurospheres than those on regular medium (Figure 27d). This result revealed that microglia secreted factors, other than TNF-α, promote the proliferation and/or survival of NSCs *in vitro*. Nonetheless, when dissociated and submitted to a sequential neurosphere assay in regular medium, cells pre-treated with TNF-α immunodepleted medium did not show any increase in

their expansion capacity (Figure 27e), indicating that TNF-α specifically participates in NSC self-renewal, most likely increasing symmetrical divisions.

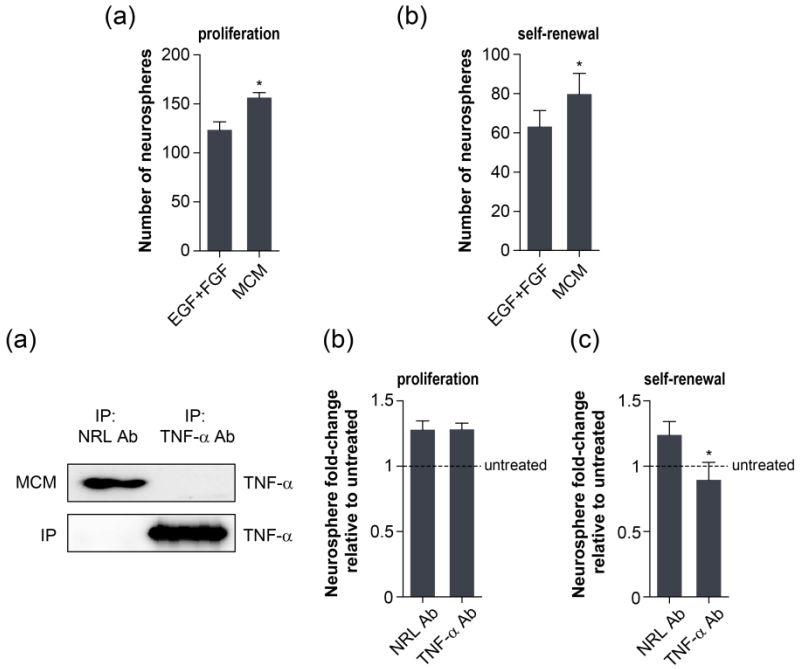

Figure 27. TNF-α secreted by activated microglia modulates neurosphere expansion *in vitro*. **(a)** LPS-activated microglia conditioned medium (MCM) stimulates neurosphere formation of NSC cultures. **(b)** Neurospheres formed in the presence of MSC, after dissociation and plating in fresh media, generate higher numbers of neurospheres (n=4). **(c)** A control Western blot showing the presence of TNF-α in MCM immuprecipitated with a non-related antibody (NRL Ab) and the complete immune-depletion of the cytokine with TNF-α specific antibodies (TNF-α Ab). (**d**) TNF-α immuno-depleted MCM stimulates neurosphere formation but **(e)** not the expansion of neurosphere forming cells (n=4).

3.2. TNF-α induces self-renewal of NSCs

To test whether TNF-α promoted an expansion of the NSC pool by increasing symmetrical divisions of neurosphere-forming cells, we plated individual NSCs at very low density and fixed them just 24h later in order to capture their first division. As NSCs grow in suspension forming clonal aggregates, recently divided cells remain attached to each other forming a 'cell-pair'. Symmetrical or asymmetrical divisions were scored by immunostaining cell-pairs to detect the expression of

EGFR, as it has been previously demonstrated to present a symmetrical or asymmetrical distribution in NSC cultures (Andreu-Agullo et al., 2009). As predicted, TNF-α treatment increased the probability of finding cell doublets with symmetrical distribution of EGFR in both cells, while reducing the proportion of asymmetric $EGFR^{hi}/EGFR^{lo}$ cell pairs (Figure 28a). This indicated that TNF-α is indeed expanding the NSC pool through symmetrical divisions.

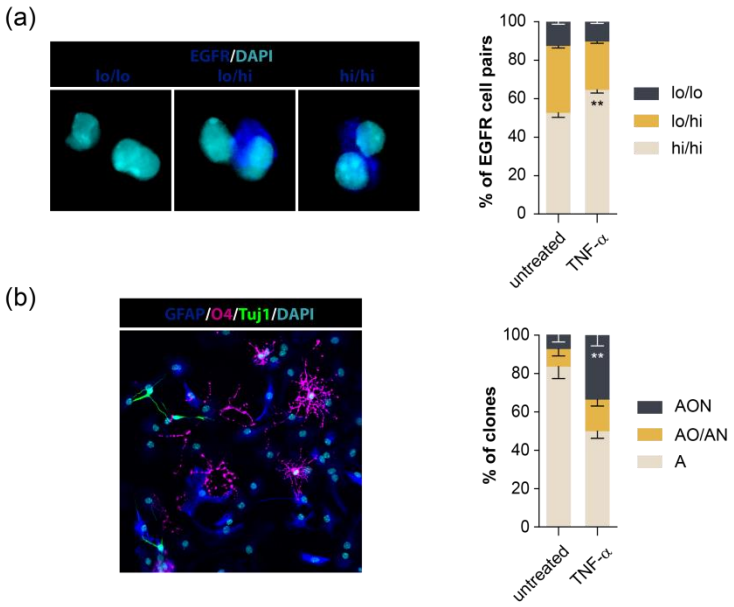

Figure 28. TNF-α modulates self-renewal of NSC *in vitro* promoting symmetrical divisions and expanding multipotent NSCs. (a) Images of EGFR immunocytochemistry showing symmetric $EGFR^{lo/lo}$ and $EGFR^{hi/hi}$ or asymmetric $EGFR^{lo/hi}$ cell pairs (left) and assessment of the proportion of each type in recently divided cells growing in presence or not of TNF-α (right) (n=3). **(b)** Immunocytochemistry of a single neurosphere clone differentiated into astrocytes ($GFAP^+$), oligodendrocytes ($O4^+$) and neurons ($Tuj1^+$) (left). The classification of each clone as unipotent (A), bipotent (AO/AN) or multipotent (AON) reveals an increased proportion in multipotent clones in TNF-α treated cultures (right) (n=6).

It has been previously mentioned that neurosphere cultures consist of a heterogeneous mixture of different populations where only true stem cells retain

the maximum potential (tripotency) while different progenitor cells will give rise to one (unipotency) or two at most (bipotency) cell types. Therefore, we sought to determine whether the augmented pool of NSCs induced by TNF-α retained its potential. Neurospheres formed in the presence of TNF-α were dissociated and the individual cells plated again at low density to allow them to generate new neurospheres; the latter were then individually transferred to matrigel-coated wells to start a differentiation protocol (Belenguer et al., 2016). After 7 days of differentiation, immunostaining with markers of the three neural lineages (GFAP for astrocytes -A-, Tuj1 for neurons -N-, and O4 for oligodendrocytes -O-) revealed that neurospheres from TNF-α-treated cultures were enriched in cells with full NSC potential (tripotent clones, AON) (Figure 28b), indicating that the observed expansion of neurospheres after TNF-α treatment is the consequence of an increase in self-renewing symmetric divisions of multipotent NSCs.

3.3. Differential effects TNF-α signalling are mediated by distinct receptors

We had found a combination of positive and negative effects of TNF-α on NSCs. It is well known that TNF-α is a multifunctional cytokine that can exert its functions binding to two different receptors, TNFR1 and TNFR2 (Cabal-Hierro and Lazo, 2012; MacEwan, 2002). In order to test whether the different effects of TNF-α on NSC behaviour were indeed mediated by different receptors, we established NSC cultures from wild-type (WT), single knockout for each receptor (R1KO and R2KO) and double knockout lacking both of them (DKO) mice, and treated them with low (0.1 ng/ml) or high (10 ng/ml) concentrations of TNF-α for 5 days to study neurosphere formation. Neither of the treatments had any influence on DKO cells (Figure 29b,c), confirming that the observed effects were mediated exclusively by these two receptors. However, when we analysed R1KO cells, instead of finding a dual effect depending on the concentration as it happens with WT cells, both concentrations of TNF-α promoted the formation of more neurospheres, either when present or in the next passage after treatment (Figure 29b,c). These data

supported our hypothesis that TNF-α negative effects on NSC cultures require an active TNFR1 and that, in its absence, TNF-α can only promote NCS expansion, presumably through TNFR2.

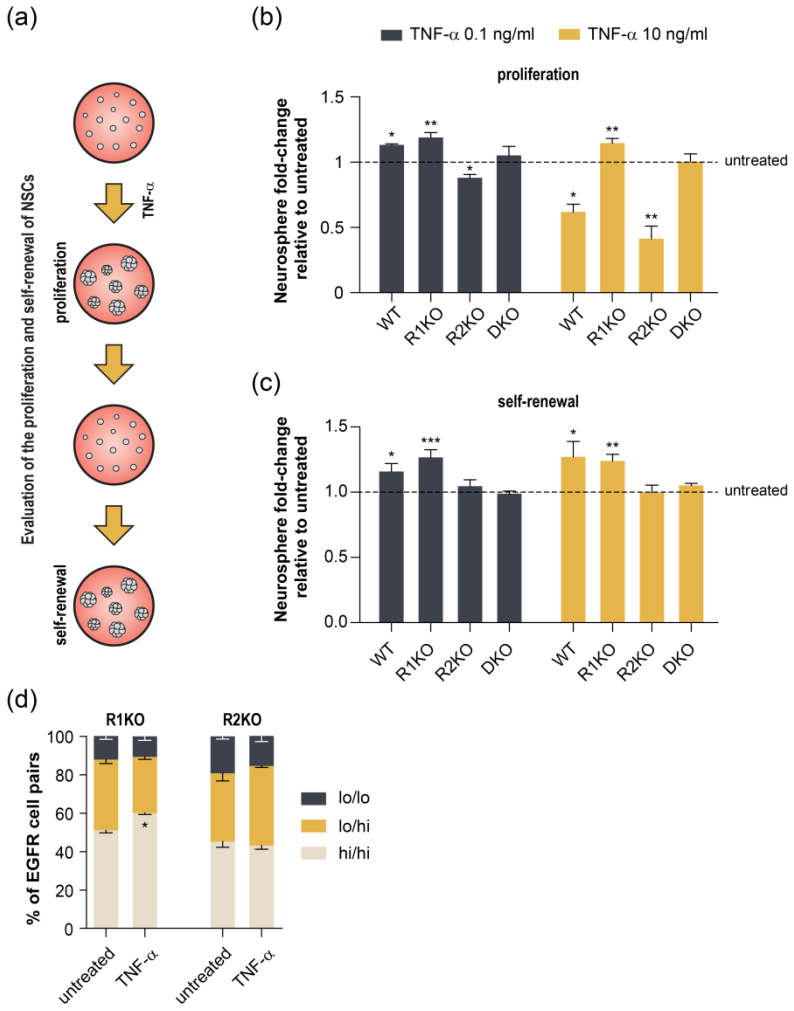

Figure 29. TNF-α signalling through TNFR1 is detrimental for neurosphere formation but its binding to TNFR2 expands the neurosphere-forming population *in vitro*. **(a)** Schematic representation of the experimental design. Neurosphere formation of WT, R1KO, R2KO or DKO cells is evaluated first in the presence of TNF-α (proliferation) and then in a sequential assay by disaggregating the treated neurospheres and sub-culturing them in the absence of the factor (self-renewal). **(b)** Number of neurospheres formed in presence of TNF-α and (**c**) sequential formation of neurospheres of untreated or TNF-α-treated cells relative to untreated cells in each genotype reflects the dual role of each receptor. (WT n=3; R1KO, R2KO and DKO n=4) (**d**) Proportion of symmetric or asymmetric cell pairs based in EGFR distribution scored in untreated or TNF-α treated R1KO and R2KO cells (n=3).

On the other hand, we observed that the elimination of TNFR2 abrogated all the positive effects on NSCs since R2KO cells formed less neurospheres than untreated controls in the presence of both concentrations of TNF-α, as well as failed to produce more neurospheres after passage (Figure 29b,c). This was further evidenced when we analysed the effect of TNF-α on cell-pairs of R1KO and R2KO cells. Expectedly, the only presence of TNFR2 in R1KO cells was sufficient to increase the number of symmetric EGFR+ cell divisions while the percentage of symmetric cell-pairs in TNF-α-treated R2KO cells was not affected (Figure 29d).

The experiments performed with knockout cells had evidenced the specific requirement of TNFR1 for negative and of TNFR2 for positive effects of TNF-α on NSCs, but we wanted to assess whether the sole activation of each receptor was sufficient to trigger the response, so we decided to treat cells with specific TNFR1 or TNFR2 agonistic antibodies. First, we cultured WT NSCs in the presence of R1-agonist or R2-agonist to test neurosphere formation. The reduced number of neurospheres observed in R1-agonist-treated cells confirmed that the specific activation of this receptor is responsible for the negative effects on NSC survival and proliferation (Figure 30a). However, in accordance with the previous data, the specific stimulation of TNFR2 resulted in an increased number of neurospheres with higher expansion potential (Figure 30a,b). Furthermore, the resultant neurospheres from an R2-agonist treatment, when challenged for differentiation, gave rise to a higher number of multipotent clones (Figure 30c).

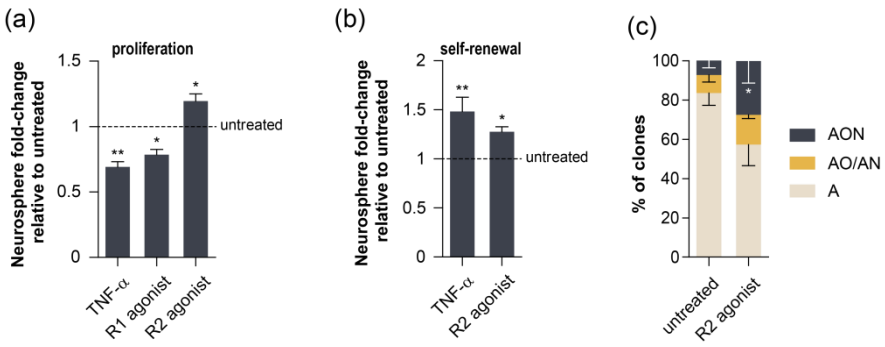

Figure 30. Specific activation of TNFR1 reproduces negative effects on neurosphere formation whereas specific TNFR2 signalling mediates symmetrical division of multipotent NSCs. (a) Number of neurospheres formed in the presence of TNF-α (n=4), R1 agonist (n=9) or R2 agonist (n=5) and **(b)** analysis of the neurosphere expansion potential of TNF-α (n=4) and R2 agonist (n=4) treated cells represented as fold-change relative to untreated controls. **(c)** Proportion of clones generated in the absence or presence of R2 agonist showing unipotent (A), bipotent (AO/AN) or multipotent (AON) differentiation capability (n=3).

Along with TNF-α, we had found PGRN up-regulated during our inflammation and regeneration experiments (Figure 31a-c). Interestingly, PGRN is a natural agonist of the TNFR2 and cannot activate TNFR1 (Wang et al., 2015), so we envisioned a scenario where activation of TNFR1 would lead to apoptosis and proliferation arrest, whereas signalling through TNFR2, in response to TNF-α and/or PGRN might promote symmetrical divisions and hence the expansion of the NSC pool in the culture. Treatment with PGRN (10-500 ng/ml) resulted in an increment of neurosphere formation of about 20% (Figure 31b). Additionally, when these treated neurospheres were passed and plated again in the absence of the factor, compared to untreated controls, PGRN-treated cultures yielded more secondary neurospheres (Figure 31c). These data indicated that PGRN mimics only the positive effects seen with TNF-α and seems to expand the population of NSCs *in vitro* without affecting the overall proliferation of the culture. Finally, we tested whether TNFR2 was also required by PGRN to exert its positive effect on NSCs. In line with the observations with TNF-α, presence of PGRN did not change the number of neurospheres formed by R2KO cells. Accordingly, the expansion of these cells was not affected after the treatment (Figure 31b,c).

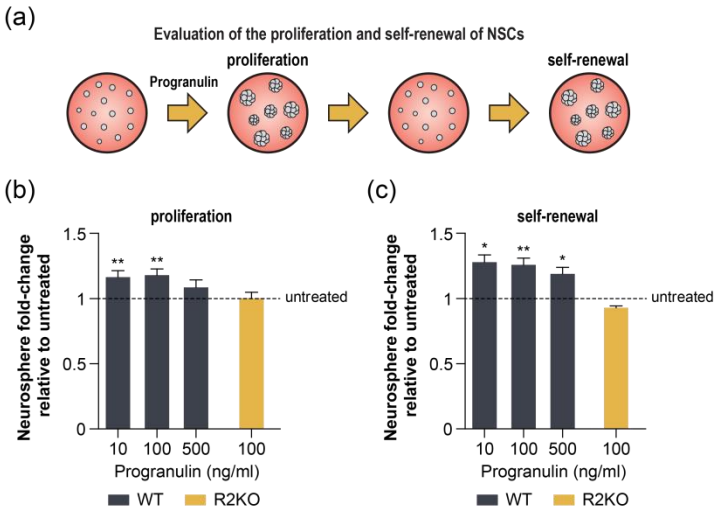

Figure 31. PGRN stimulates neurosphere formation and expands NSCs *in vitro* acting through TNFR2. (a) Schematic representation of the experimental design. Neurosphere formation of single cells is evaluated first in the presence of PGRN (proliferation) and then in a sequential assay by disaggregating the treated neurospheres and sub-culturing them in the absence of the factor (self-renewal). **(b,c)** Quantification of the number of neurospheres formed **(b)** in the presence or **(c)** after pre-treatment of increasing doses of PGRN compared to untreated WT (n=7) or R2KO (n=4) NSC cultures. PGRN stimulates neurospheres formation and their expansion potential in WT but not in R2KO cells.

3.4. TNFR2 signalling is mediated by the p38 MAP kinase

We next sought to explore the signal transduction pathway downstream of TNFR2 that could be mediating the observed effects. TNF-α receptors have been classically associated with different signalling pathways including NF-κB, p38, JNK, and the ceramide/sphingomyelinase signalling pathways (Cabal-Hierro and Lazo, 2012). Among them, NF-κB controls the expression of numerous genes involved in cell division, apoptosis, and inflammation. Therefore, we first tested whether TNF-α was able to induce the transcriptional activity of NF-κB through TNFR2 activation. WT, R1KO and R2KO NSCs were transfected with a luciferase reporter, bearing 5 in-tandem copies of the κB binding sequence, and cultured with TNF-α for 24h. As expected, TNF-α greatly activated the reporter expression in WT NSCs, but this induction was also observed in the absence of TNFR2 (R2KO cells) (Figure 32a). In contrast, the activation of the κB-luciferase reporter was completely abrogated

when cells lacking TNFR1 were treated with TNF-α. In agreement with these results, 5x κB-luc transfected WT cells treated with R1-agonist also showed higher reporter activity while R2-agonist failed to activate the reporter expression (Figure 32a). These results indicated that the NF-κB pathway is a downstream target of TNF-α but, in response to the binding to TNFR1 and not TNFR2.

In an attempt to identify possible signalling pathways downstream of TNFR2, once discarded the canonical transcriptional activation of NF-κB, we performed a multiplex assay based in the Luminex® technology. This technique allows the simultaneous analysis of the phosphorylation state of multiple downstream signalling mediators, in our case: CREB, JNK, NF-κB, p38, ERK, AKT, p70S6K and STAT3. We obtained cell lysates from untreated or TNFR2-stimulated NSCs after 1h in culture and quantified the ratio between active (phosphorylated) and total amount of each protein. Among all tested candidates, the p38 MAP kinase displayed a higher phosphorylated state after treatment with the R2-agonist suggesting that it is a downstream target of TNFR2 (Figure 32b). Accordingly, western blot analysis confirmed that cells treated with either TNF-α or TNFR2 agonist present higher levels of phosphorylated p38 (Figure 32c).

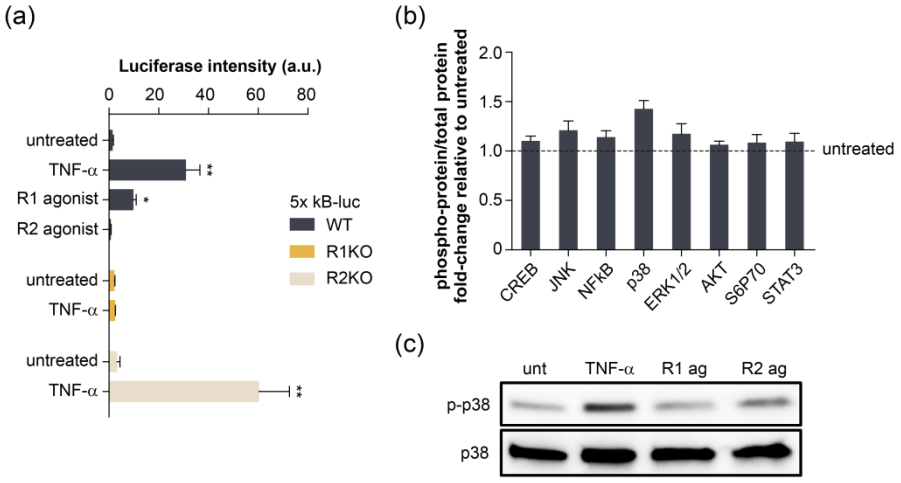

Figure 32. TNFR2 signalling in NSCs is related to the p38 MAP kinase signalling pathway but not to the transcriptional control of Nf-κB. (a) Transcriptional activity of NF-κB-dependent genes

measured in WT (n=6), R1KO or R2KO (n=3) cells transfected with a 5x κB-luciferase reporter plasmid and treated with TNF-α, R1 or R2 agonistic antibodies for 24h. **(b)** Quantification of phosphorylated levels of CREB, JNK, NF-κB, p38, ERK, AKT, p70S6K and STAT3 proteins relative to the total amount of each protein assessed in R2 agonist treated cells by Luminex®-based multiplex assay. The data is normalized to phosphorylated levels in untreated cells (n=2). **(c)** Representative western blot images illustrating the induction of the phosphorylated state of p38 after TNF-α or R2 agonist treatments.

In order to test whether p38 activation is required for TNFR2 to exert its effects on NSCs, we decided to use a specific pharmacological p38 inhibitor (SB203580) in combination with TNF-α or R2-agonist treatments. Neurosphere assay showed, as expected, that the presence of TNF-α diminished the number of neurospheres whereas TNFR2 agonist produced the opposite effect (Figure 33b). Moreover, the presence of SB203580 did not prevent TNF-α from being detrimental to the culture (Figure 33b). Conversely, under p38 inhibiting conditions, R2-agonist failed to increase neurosphere formation (Figure 33b). Furthermore, when these neurospheres were dissociated and plated again for a second round of neurosphere assay in the absence of any treatment, we observed that neither TNF-α nor R2-agonist pre-treated cells that had been incubated with p38 inhibitor, displayed the increased expansion potential that was observed in non-inhibited cultures (Figure 33c). Therefore, p38 activation seems to be required for TNFR2 to promote neurosphere expansion of NSCs *in vitro*.

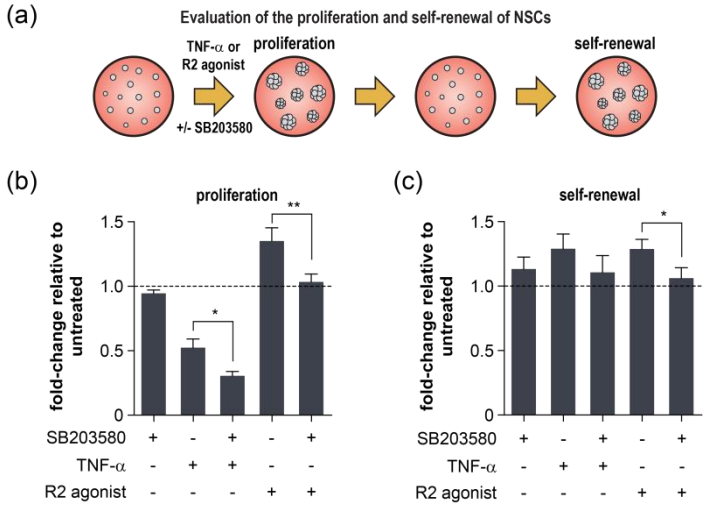

Figure 33. The activation of p38 mediates the TNFR2-induced expansion of neurosphere-forming cells. (a) Schematic representation of the experimental design. Neurosphere formation of single cells is evaluated first in the presence of TNF-α or R2 agonist combined with the p38 inhibitor SB203580 (proliferation) and then in a sequential assay by disaggregating the treated neurospheres and sub-culturing them in the absence of the factor (self-renewal). **(b)** Relative neurosphere formation of TNF-α and R2 agonist-treated cells in presence of SB203580 (n=5) and (**c**) assessment of subsequent neurosphere expansion potential of treated cells (n=8) showing that R2-induced positive effects, but not TNF-α detrimental ones on neurosphere formation, are abolished in the presence of the p38 inhibitor SB203580.

4. Effects of TNF-α in adult subependymal quiescent NSCs

4.1. *In vitro* properties of qNSCs

Our *in vitro* data indicated that TNFR2 signalling induced a subset of multipotent neurosphere-forming cells to self-renew. Our data also showed that mild peripheral signals, i.e. induced by an intra-peritoneal saline injection, caused in the SEZ a transient up-regulation of TNF-α and PGRN and a shift of quiescent NSCs towards an alert qNSC2 state without affecting the activated pool. The description of the transition from dormancy to an alert state in NSCs is relatively recent, and the subjacent molecular mechanisms that might be involved are largely unknown. Therefore, one possibility worth testing was that TNFR2 signalling could be promoting the transition from qNSC1 to qNSC2. However, it is currently unclear whether neurosphere cultures preserve NSCs in different states. It has been reported that isolated qNSC rarely form neurospheres under mitogenic stimulation (Codega et al., 2014; Mich et al., 2014). Nevertheless, it is worth noting that Mitch *et al.* defined the quiescent pool of NSCs as those $GLAST^{high}/EGFR^{-}$ cells, a fraction which actually corresponds to a dormant state. On the other hand, Codega *et al*. observed that some qNSCs can be activated *in vitro* and behave as colony forming multipotent cells, and that both states can be dynamically interconverted, maybe contributing to the heterogeneity of the neurosphere culture. However, they did not subdivide the quiescent NSCs into qNSC1 and qNSC2, so it remains unsolved if the activation they observed was affecting both populations. Actually, due to its

recent identification, we lack experimental evidences of the behaviour of alert qNSC2 *in vitro* and both scenarios, i.e. they either behave as quiescent cells or get activated and form neurospheres, seem equally plausible. Interestingly, G_{alert} MuSCs have been described as being prone to enter proliferation when challenged *in vitro* with mitogens (Rodgers et al., 2014).

We, therefore, sought to test whether the transient induction of qNSC2 following i.p. injection of saline translated *in vitro* into a higher number of neurospheres, reflecting an activation of qNSC2, or, conversely, had no impact on neurosphere formation, revealing that qNSC2 behave as quiescent cells also *in vitro*. Thus we injected mice with saline and performed primary SEZ cultures 24 hours later scoring the number of primary neurospheres after 7 DIV. We observed that SEZ homogenates obtained from saline-injected mice yielded more neurospheres than their naïve non-injected counterparts (Figure 34a), suggesting that qNSC2 had been activated under *in vitro* culture conditions of mitogenic stimulation and behaved as neurosphere-forming cells.

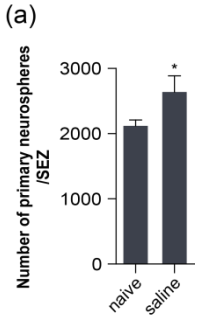

Figure 34. I.p. saline injection in vivo induces SEZ NSCs to form higher number of primary neurospheres when cultures under mitogenic stimulation. (a) Total number of SEZ-derived primary neurospheres obtained from naïve and saline-injected mice showing a higher proportion of cells that proliferate and give rise to neurospheres 24 h after the i.p. saline-injection (n=4).

To gain insight into this process and to directly study potential effects of TNFR2 activation on qNSCs, we returned to our magnetic separation of the Lin^- fraction, which is enriched in both quiescent qNSC1 and qNSC2 states along with aNSCs. Once isolated from naïve wild-type mice, we cultured Lin^- cells for 24h or 7 days in neurosphere growing medium supplemented with EGF and FGF in the

presence or not of R2-agonist. After 24h *in vitro*, we could observe many Lin⁻ cells that had started to divide and were already forming 2-3 cell aggregates. In line with our previous data, after 7 days in culture, we observed that treatment with R2-agonist induced Lin⁻cells to generate a higher number of neurospheres (Figure 35b).

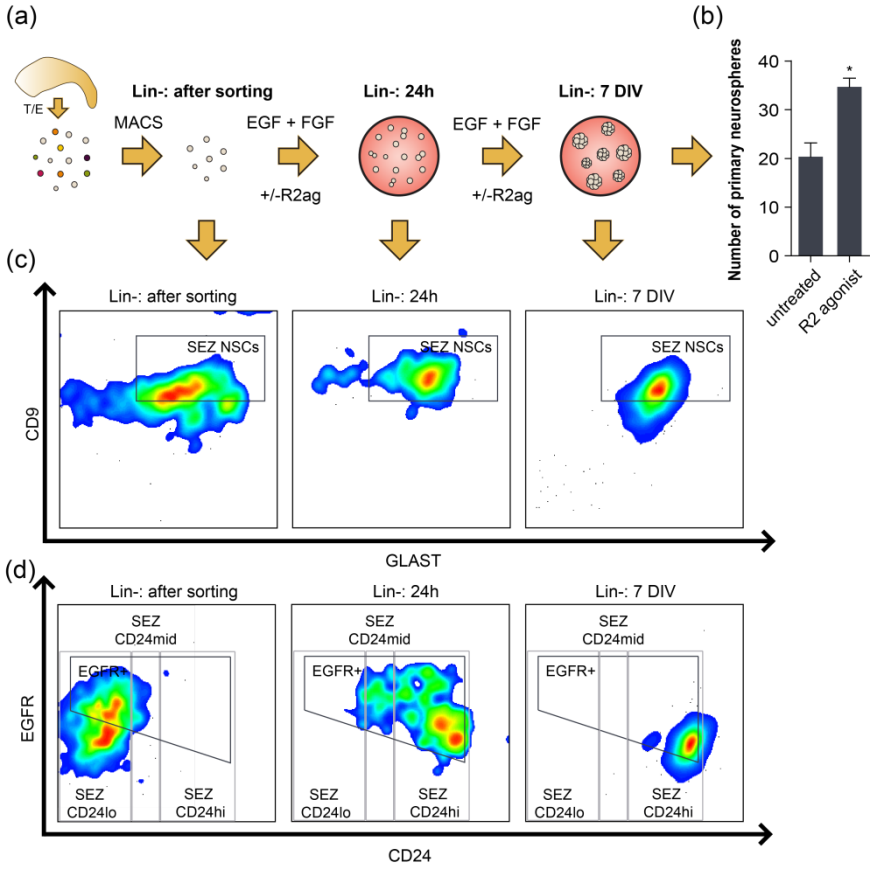

Figure 35. The specific stimulation of TNFR2 enhances neurosphere formation of isolated NSCs but culture conditions do not maintain the cell surface marker profile of SEZ NSCs. (a) Schematic representation of the experimental design. After dissociating SEZ samples, Lin⁻ cells are magnetically isolated and cultured in the presence of TNFR2 agonist. Recently isolated Lin⁻ or cultured under mitogenic stimulation for 24h or 7 days are analysed by flow cytometry and neurosphere formation. **(b)** The number of Lin⁻-derived primary neurospheres formed under culture conditions is increased in presence of R2 agonist (n=3). **(c,d)** Representative plots of Lin⁻ cells showing the evolution of NSC cell surface markers (GLAST, CD9, EGFR and CD24) under culture conditions. Note that after 24h and 7 days *in vitro*, none of the Lin⁻ cells maintains the expected marker expression profile displaying (**c**) homogeneous levels of GLAST and CD9, and (**d**) low but evident level of EGFR combined with high levels of CD24.

In an attempt to study the acute effect of TNFR2 stimulation, we collected cells after just 24h *in vitro* and labelled them with the whole set of cell surface markers that we used for the characterization of the different SEZ populations. Flow cytometry analysis indicated that all cells were still expressing GLAST and CD9 after 24h in culture (Figure 35c). However, instead of finding a great range of expression of CD24 and EGFR (from negative to high for both markers), virtually all cells in both treated and untreated samples, showed some level of CD24 and EGFR (Figure 35d). And even more, 7 days after plating, all cells from Lin^-derived neurospheres had GLAST and CD9 but expressed aberrantly higher levels of CD24 and homogeneous although lower than expected levels of EGFR (Figure 35c,d). This indicated that the expression of some of our classifying markers was highly sensitive to culturing conditions. Thus, classical *in vitro* culture conditions, despite maintaining stemness properties of NSCs, such as self-renewal and multipotency (Pastrana et al., 2011), seem to be forcing an artificial expression of progeny markers, precluding the analysis of the quiescence-activation dynamics based on the features seen *in vivo*.

Cytometry experiments had, therefore, evidenced that we could not directly identify the presence of quiescent cells once NSCs have been placed under *in vitro* culture conditions. In an attempt to visualize this population, we measured cell size and mitochondrial activity of NSCs in culture, since we had observed a positive correlation between these parameters along the quiescent, alert and active states *in vivo*. First, we disaggregated neurospheres derived from naïve or saline-injected mice, labelled them with MitoTracker and analysed them in a flow cytometer to detect changes in those parameters. We did not find clear differences in the size distribution between cells from naïve or saline-derived neurospheres (Figure 36a). However, we could clearly identify a small discrete population of cells displaying high mitochondrial activity and low cellular complexity in naïve cultures which was greatly increased in the saline-injected group (Figure 36b).

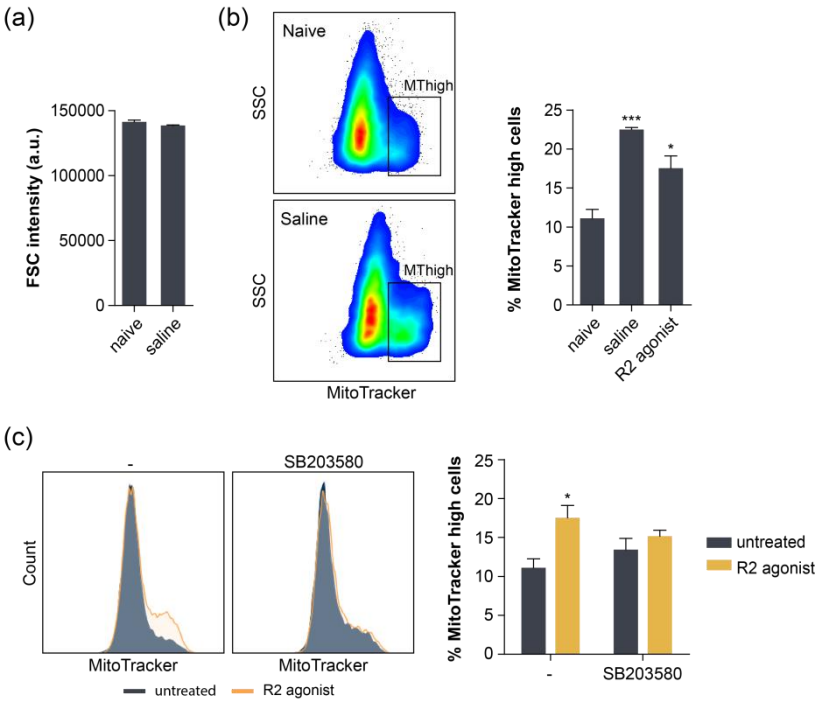

Figure 36. NSCs cultured *in vitro* contain a population of TNFR2-responsive cells that display enhanced mitochondrial activity. (a) Analysis of cell size by mean intensity of FSC parameter in naïve and saline-injected mice-derived cultures (n=4). (**b**) Representative FACS plots displaying MitoTracker and SSC intensity (left). Compared to naïve untreated cultures, the proportion of MitoTraker^{hi} cells in NSC cultures obtained from saline-injected mice and R2-agonist-treated naïve cultures is significantly increased (right) (n=4). **(c)** Representative histograms of Mitotracker intensity in untreated or R2 agonist treated cultures in the presence or not of the p38 inhibitor SB203580 (left) and the percentage of MitoTracker^{hi} cells in each condition (n=4). The presence of SB203580 completely abolishes the TNFR2-induced increase of MitoTracker^{hi} cells.

Additionally, we performed the same analysis on naïve cultures but specifically stimulating TNFR2 with an agonistic antibody during 4 days. Analysis of MitoTracker staining revealed that activation of TNFR2 reproduced the effect of the saline injection and led to an increment of cells with higher mitochondrial activity in the culture (Figure 36b). These data suggested that TNFR2 activation targets a population, which might be reminiscent of qNSCs, that does remain in the culture and can be followed *in vitro* by its increased mitochondrial activity. Finally,

we quantified the mitochondrial activity of R2-agonist-treated cells grown in presence of SB203580. In line with the previous result, we could observe that the increased number of cells with high mitochondrial activity promoted by the treatment with the specific R2-agonist completely disappeared when p38 was pharmacologically inhibited (Figure 36c). Although further characterization will be needed to clearly identify all the molecular mediators downstream of TNFR2 transduction signal and their role in regulating the quiescence-alert cycle of NSCs, our results demonstrate that p38 is an essential component of this pathway.

Previous experiments performed in our lab had evidenced that NSC cultures display proliferative heterogeneity and that a small population of cells that divide at an evident slower kinetics exists within the neurospheres. Interestingly, this slow-cycling population seems to be responsible for the long-term expansion and maintenance of the culture (S.R. Ferrón, unpublished data). Therefore, we decided to test whether this population might be targeted by TNFR2 stimulation. In order to track cells with different division kinetics, we used two different fluorescent probes (Cell Trace Far Red DDAO-SE -DDAO- and Cell Trace Oregon Green 488 Carboxy-DFFDA SE -DFFDA-). These molecules can enter passively through the plasma membrane of living cells, get retained intracellularly, and are progressively diluted during the successive rounds of division through their homogeneous distribution among daughter cells. SEZ dissociates were first loaded with the far red DDAO cell tracer and plated for primary neurosphere formation. After 10 days *in vitro*, the generated primary neurospheres were dissociated to analyse the intensity of DDAO in each single cell by flow cytometry. Compared to the initial load, all living cells displayed lower levels of DDAO evidencing that all cells had divided at least a few times. However, we could observe a wide range of tracer retention in the culture with cells displaying high levels of DDAO (close to the initial load level) whereas others showed intermediate intensity or complete dilution of the probe (Figure 37a). This situation reflected that, under culture conditions, most

of the cells go through multiple rounds of cell division while others only cycle a few times, despite the strong EGF-dependent mitogenic stimulation.

In this context, we decided to evaluate if TNFR2 stimulation targets the slow-cycling population. Thus, we submitted DDAO primary neurospheres to a second round of proliferation in the presence or not of TNFR2 agonistic antibody. To be able to assess cell division during the second round of culture, we labelled cells derived from DDAO neurospheres with green DFFDA, a second cell tracer conjugated with a different fluorophore. Then, double labelled cells were cultured for 3 days to allow dilution of both cell tracers in the presence or not of R2-agonist. As expected, after 3 days in culture, we could see that all cells had proliferated and had diluted to some extent the green DFFDA tracer (Figure 37b). Interestingly, after 2 rounds of culture and 13 days under mitogenic stimulation, we could still identify cells that retained different levels of the initial DDAO load (DDAO retaining-cells, DRCs) (Figure 37a) that, according to their slow cycling dynamics, also retained high levels of green DFFDA (Figure 37b). Of notice, R2-agonist treated cultures presented a remarkable increase in DRCs (Figure 37c). This might be the result of the treatment causing a proliferative arrest preventing the dilution of the probe; however, the TNFR2 increased DRC pool retained lower levels of the second cell tracer compared to the untreated DRCs (Figure 37d) revealing that TNFR2 activation had actually induced the proliferation of the DRC population, yet maintaining their slow-cycling kinetics.

These data evidenced that, under *in vitro* culture conditions, TNFR2 activation targets a subset of slow-cycling NSCs and promotes their expansion without changing their cell division kinetics, supporting the idea that TNFR2 promotes a quiescent state that, *in vitro*, behaves as a slow-proliferating cell.

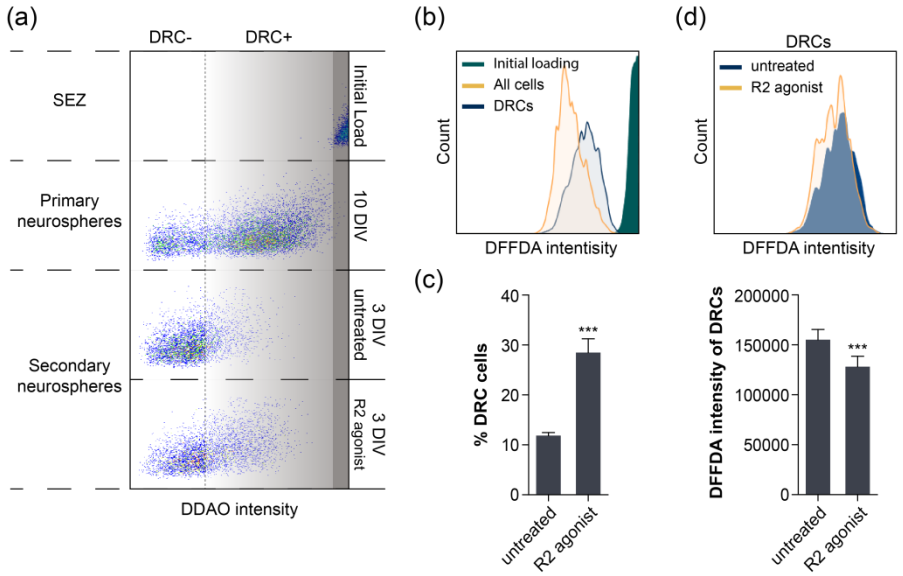

Figure 37. NSCs cultured *in vitro* contain a population of TNFR2-responsive cells that display slow cycling rate. (a) Representative FACS plots displaying far-red DDAO intensity of DDAO-loaded SEZ homogenates and the marker intensity present in the initial load, and in disaggregated neurosphere cells from primary or secondary formed neurospheres. Dashed vertical line indicates the threshold stablished to select DDAO-retaining cells (DRC^+). Secondary neurosphere were grown in the presence or not of R2-agonist during 3 days in vitro (DIV). **(b)** After 10 DIV, primary neurospheres were dissociated and loaded with green DFFDA and cultured for additional 3 DIV. The histograms are representative of DFFDA intensity in recently loaded cells or secondary neurospheres after 3 DIV. Note that DRCs show higher retention of DFFDA. **(c)** Quantification of DRC^+ cells present in untreated or R2-agonist-treated secondary neurospheres (n=6) showing a great enrichment upon TNFR2 stimulation. **(d)** Representative histogram displaying DFFDA intensity in the DRC^+ fraction in untreated or R2-agonist-treated cultures and the quantification of DFFDA mean intensity retained in DRCs after 3 DIV showing that the R2-mediated increment in DRC^+ is actually consequence of cell division (dilution of DFFDA)(n=6).

4.2. Direct actions of TNF-α in the alert state

Our *in vivo* experimental evidences pointed to inflammatory signals, such as TNF-α and PGRN, most probably acting through TNFR2, promoting the exit form quiescence and the acquisition of an alert qNSC2 state. Additionally, *in vitro* data had revealed the existence of a subpopulation of NSCs in the neurosphere cultures, which might retain some features of qNSCs and is specifically expanded by TNFR2 activation. However, so far we had not been able to visualize the qNSC1 to qNSC2 transition *in vitro*. We proposed that this might be accomplished by a specific activation of TNFR2 *in vivo* followed by cytometry analysis. Unfortunately, any

manipulation *in vivo*, such as intracerebral infusion of R2 agonist, would cause some level of inflammation potentially leading to confounding results. We, therefore, decided to set-up an intermediate approach consisting in the organotypic *ex vivo* culture of a whole SEZ, in trying to keep the NSC environment as intact as possible and maintain the qNSC population, at least for a short period of time. After dissection, SEZ whole-mounts were placed on a culture dish with the ependymal layer facing upwards and covered with neurosphere growing medium supplemented with EGF and FGF. We replaced regular EGF with fluorescent-labelled EGF-A488, to be able to detect EGFR positive cells without having to perform an extra starvation step to avoid ligand pre-occupation of the receptor. Each SEZ was cultured in the presence or not of TNFR2-agonist for 3h before tissue dissociation and labelling with SEZ populations marker panel, including MitoTracker for mitochondrial activity.

Flow cytometry analysis showed that, after 3h in culture, we were able to nicely identify each NSC linage, finding that the marker profile of each population did not differ from a recently-dissected control tissue (Figure 38a). However, compared to non-cultured tissue, we found a certain shift from qNSC1 to qNSC2, probably induced by the culture conditions (Figure 38b). Furthermore, in line with the idea that qNSC2 respond and adapt to the culture, we found that, compared to basal levels in the SEZ, they greatly increased their mitochondrial activity, more even than activated NSCs, as well as their cell size (Figure 38d,e).

Under these conditions, we could observe that qNSC1 remained mostly unaltered and displayed a similar mitochondrial activity and cell size than those directly obtained from the animal. According to our hypothesis, we could appreciate that the quiescent pool shifted from the dormant to the alert state upon TNFR2 stimulation while the activation/quiescence ratio remained unaltered (Figure 38b,c).

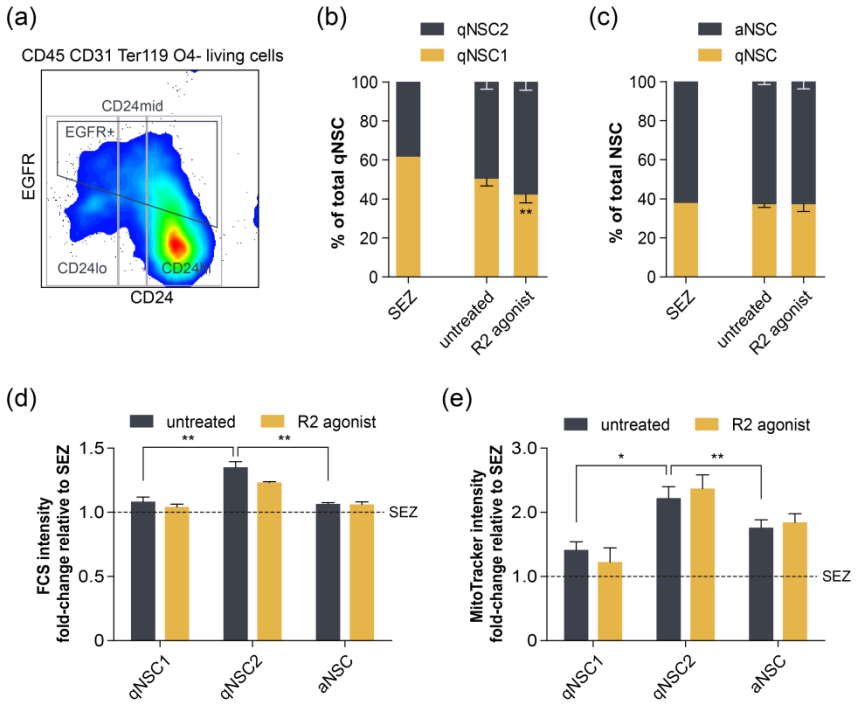

Figure 38. Organotypic *ex vivo* culture of SEZ tissue preserves the quiescence of NSCs and reveals that TNFR2 stimulation promotes the transition from dormant qNSC1 to alert qNSC2 state. (a) FACS strategy for NSC identification in organotypic *ex vivo* culture of a whole SEZ. Note that cultured SEZ maintain the NSC containing gate ($CD24^{lo}$ $EGFR^{+/-}$). **(b)** Evaluation of the proportion of qNSC displaying qNSC1 or qNSC2 state indicates that the presence of R2 agonist drives a shift to the alert state but (**c**) the proportion of aNSC is not altered upon TNFR2 activation (n=4). **(d,e)** Relative increase in cell size (FSC intensity) and mitochondrial activity (MitoTracker intensity) of qNSC1, qNSC2 and aNSC displayed under culture conditions respect to their average size in the 'naïve' SEZ. Note that qNSC2 are suffering a remarkable cell size and mitochondrial activity remodelling when cultured *in vitro* (n=4).

Discussion

The two major findings of the present thesis are (1) that adult NSCs in the SEZ niche can sense and respond to remote peripheral mild lesions and that (2) TNFR2 signalling is involved in this process and mediates positive effects of inflammation on NSC behaviour. The first finding is in line with recent data indicating that adult SCs of different systems can react to distant injuries, suggesting a homeostatic control of their activity at the organismal level. The second one increases our understanding of the role of inflammation in the neurogenic process. Although the most accepted view is that acute or chronic inflammation plays a negative role in neurogenesis, our data uncover concomitant beneficial effects of inflammatory cytokines in at least a fraction of NSCs.

Additionally, we have found that responding to either peripheral signals or acute inflammation, entails the transition of quiescent NSCs from a dormant to a primed pre-activation state. This alert qNSC2 state had remained undetected within the quiescent pool of NSCs until a couple of years ago, and very little is known about its behaviour and regulation. Here we provide new data uncovering the implication of TNFR2 signalling, most probably transduced intracellularly through p38, in the regulation of these qNSC2 cells, their behaviour *in vitro* and their role during regeneration and in response to injury. These previously undescribed effects add another piece of knowledge to the incipient research of regulation of quiescence/activation in NSCs.

The quest to find specific cell markers to unravel the unforeseen heterogeneity of adult NSCs.

In the absence of unique distinctive markers, the heterogeneity of adult SCs can only be revealed by the prospective isolation of the different proliferative states and subpopulations with combinations of labels. Understanding the heterogeneity of SCs has become in the last few years an obligated step in the journey to unravel the behaviour and regulation of these cellular entities. This heterogeneity comprises different levels of the SC biology, and has revealed that

we must undertake their study without disregarding that, instead of a specific cell type with singular characteristics, they behave as a dynamic network of interchangeable states showing distinctive regional identity, lineage commitment, self-renewal potential, gene expression programs and cell cycle dynamics (Biteau et al., 2011; Chaker et al., 2016; Dykstra et al., 2007; Li and Clevers, 2010; Ousset et al., 2012; Stange et al., 2013; Van Keymeulen et al., 2011). Therefore, the development of lineage-tracing and molecular strategies that allow the identification and isolation of all this variety of states and subpopulations is essential for the proper advance of our knowledge about SCs.

As the leading field in SCs, the HSC lineage is probably the best characterized SC system where several HSC types and intermediate states have been identified (Goodell et al., 2015; Tian and Zhang, 2016). This success has heavily relied in the availability of multiple surface markers that, in combination with FACS-based technologies, has allowed the isolation of discrete populations with common molecular features for their subsequent functional characterization (Tian and Zhang, 2016). The NSC field, however, has been limited for many years by the sparse availability of markers, especially cell surface proteins that would have enabled their isolation and further characterization. NSCs were initially defined and functionally characterized using *in vitro* criteria (Reynolds and Weiss, 1992) and later by ultrastructural, morphological and functional *in vivo* features (Doetsch et al., 1999a; Doetsch et al., 1997, 1999b). Since then, their identification has mainly relied upon the expression of cytoskeletal proteins such as the glial marker GFAP or Nestin, in combination with transcription factors such as Sox2 or proliferation markers such as ki67 and/or retention of nucleoside analogues. Of notice, none of these markers is compatible with the FACs separation of living cells, due to their intracellular localization, which has imposed the search for alternative strategies to circumvent this limitation.

The use of reporter transgenic mice such as *GFAP*::GFP provided the first reliable approach for FACS isolation of NSCs but, their glial nature required the combination with other markers in order to discriminate neurogenic from non-neurogenic astrocytes (Pastrana et al., 2009). It has not been until recently that a few laboratories have successfully isolated SEZ cells that display SC features using different combinations of both reporter expression mouse strains and/or surface markers. Moreover, the application of either bulk or single cell global transcriptomic assays to these isolated populations has led to the identification of different quiescent and proliferative states among NSCs, broadening our vision of their biology (Codega et al., 2014; Daynac et al., 2013; Giachino et al., 2014; Khatri et al., 2014; Llorens-Bobadilla et al., 2015; Mich et al., 2014).

In this thesis, we have developed a new strategy, based exclusively on the detection of surface markers, to allow the identification of SEZ NSCs at different quiescent and proliferative states, along with their more committed progeny until their transformation into OB neuroblasts. Analogously to the LSK-based strategy for HSC identification, which is based on the exclusion of eight differentiation markers (Lin+ cells) and the subsequent selection of c-Kit and Sca-1 positive HSC (Tian and Zhang, 2016), we first excluded non-neurogenic lineages using CD45, CD31, Ter119 and O4 to later perform a positive selection of $CD9^{+}$ neurogenic, $GLAST^{+}$ astrocytes. Although GFAP has been for years the gold standard for the identification of astroglial cells, the localization of GLAST in their membrane has overcome the need for reporter mouse strains, allowing the identification of living astrocytes in mice of any genetic background (Jungblut et al., 2012). However, both GFAP and GLAST are also expressed by non-neurogenic astrocytes, so inclusion of additional markers that distinguish NSCs from parenquimal astrocytes is compulsory. Prominin (CD133) has been found in primary cilium of NSCs (Cesetti et al., 2011; Pinto et al., 2008) and has been used in combination with GFAP to identify this population (Beckervordersandforth et al., 2010; Mirzadeh et al., 2008). Nonetheless, despite being quite specific, it appears to label only a subset of NSCs

(Codega et al., 2014). Hence, taking advantage of the single-cell RNA-Seq performed by Llorens-Bobadilla et al., we decided to include CD9, in combination with GLAST, to identify neurogenic astrocytes (Llorens-Bobadilla et al., 2015). It is worth noting that, despite the fact that its broad expression among different cell types might make it unsuitable as specific marker, we could observe that SEZ NSCs expressed much higher levels of this protein compared to non-neurogenic astrocytes from other areas such as the cortex or the striatum.

Despite being initially alleged as a progenitor marker, EGFR is now widely accepted as a marker of active NSCs (Codega et al., 2014; Daynac et al., 2013; Giachino et al., 2014; Khatri et al., 2014; Llorens-Bobadilla et al., 2015; Mich et al., 2014) that are consequently eliminated by anti-mitotic drugs. However, we found slight discrepancies with previous reports that associated CD24 mainly with neuroblasts, defining NSCs as a CD24 negative population (Codega et al., 2014; Daynac et al., 2013; Llorens-Bobadilla et al., 2015; Mich et al., 2014). Our data suggest instead that this marker starts being expressed in aNSCs and increases with the progression through the neurogenic lineage becoming the highest in PSA-NCAM$^+$ neuroblasts. Of notice, single-cell RNA-seq analysis also supports this idea and, similarly to Ascl1 expression that is already present in activated aNSCs, presence of Cd24a mRNA is detected increasingly in aNSCs, TAPs and neuroblasts (Llorens-Bobadilla et al., 2015). Similarly, the expression of GLAST in TAPs is also under debate. While others define TAPs as GLAST$^+$/EGFR$^+$ cells (Llorens-Bobadilla et al., 2015), we believe that CD24^{mid}/EGFR$^+$ TAPs are in the process of silencing astroglial features and can still show residual levels of GLAST. It is worth noting that the detection of surface markers is highly dependent on the chosen protocol for the enzymatic dissociation of the SEZ tissue. Most of the strategies for the disaggregation of neural tissue rely on a combination of mechanical dissociation along with an enzymatic digestion with papain or trypsin. During the development of our protocol, we could observe that GLAST and CD24 were highly sensitive to papain. Similarly, although trypsin is clearly gentler with both markers, the amount

of enzyme and the incubation time have a deep impact in the preservation of these antigens in the cell membrane. Therefore, protocols slightly more aggressive with these two markers might have led to the classification of low-expressing cells as negative.

We are aware that the ultimate validation of our marker panel and gating strategy will only be achieved by the molecular and cellular analysis of each FACS-separated population. However, we strongly believe that we provide enough evidences of its accuracy with the regeneration experiments, neurosphere formation assays, and analysis of the expected morphological and metabolic changes we performed over the course of this thesis.

The dilemma of being a quiescent cell *in vitro*

As previously mentioned, neurosphere cultures contain a heterogeneous population of cells as NSCs coexist with their progeny (different types of more committed progenitors and even differentiated cells). Moreover, NSCs unavoidably produce cell progeny *in vitro* and some of the highly proliferative committed progenitors or TAP cells appear also capable of forming neurospheres, albeit only for a few passages (Doetsch et al., 2002a; Reynolds and Rietze, 2005) Nonetheless, since neurospheres reproduce the defining characteristics of SC such as self-renewal, clonal long-term expansion and multipotency, their cell division in the culture must be self-maintaining and at least a small percentage of them should remain somehow equivalent to the NSCs found in the niche *in vivo*.

General protocols for the *in vitro* culture of mammalian cells rely on the presence in the culture medium of proliferative signals either in the form of different kinds of serum or by defined growth factors that act as mitogens. This fact imposes a strong pressure over the culture, selecting the most proliferative cells as the culture is successively passaged. Therefore, any kind of non-

proliferative cell will necessarily be negatively selected and under-represented or removed from the culture.

NSCs are no exception to this rule, and commonly used protocols include strong mitogenic stimulation with a combination of EFG and FGF2 (Belenguer et al., 2016). Consequently, it is conceivable that the quiescent population that would be initially present in the SEZ tissue homogenate might either be forced to activate and adapt to the culture conditions, or, conversely, remain quiescent and be progressively eliminated. As a matter of fact, it has been reported that isolated qNSC rarely form neurospheres *in vitro* (Codega et al., 2014; Mich et al., 2014) but that they can get activated contributing to the neurosphere forming pool of the culture (Codega et al., 2014). On the other hand, a different scenario where NSCs alternate between quiescent and active states during their time *in vitro* has also been proposed (Codega et al., 2014) and would justify the presence of qNSCs in the culture, even after several passages under strong mitogenic stimulation. This phenomenon, though, remains controversial and the characterization of the quiescent cells in the culture, if present, has not been done. Additionally, due to their recent discovery, few data are available about the specific behaviour of qNSC2 *in vitro*.

Most of the results we have obtained during this thesis can only be explained by *in vitro* culture conditions driving NSCs, at least qNSC2, to exit quiescence, start expressing EGFR and proliferate. This raises the question of whether these *in vitro* activated qNSC2 are functionally different form the aNSCs already present in the culture and if any of them retain the capacity of returning to quiescence. Be as it may, we have found that *in vitro* culture conditions have a profound impact on the expression of surface markers, specially GLAST, CD24 and EGFR, preventing us from unequivocally identify quiescent cells in the culture, at least by our cytometry-based assay. However, we could find evidences of heterogeneity among the NSC population *in vitro* that might reflect the presence of an adapted form of quiescent

NSC to the culture conditions or, alternatively, be the consequence of the returning of aNSCs to a more quiescent state after a few rounds of cell division in each passage. This is supported by the observation of a subset of cells displaying differential mitochondrial activity and the fact that cells with considerably slower cell cycle kinetics coexist in the culture among highly proliferative ones. Additionally, these populations seem to be targeted by TNFR2 stimulation leading to their expansion in the culture but without losing their particular characteristics. Together these evidences have prompted us to hypothesise that the expansion of the neurosphere forming cells that we observe after TNFR2 stimulation *in vitro*, is actually a consequence of TNFR2 targeting a subpopulation of quiescent cells that are adapted to the *in vitro* conditions and, hence, cannot behave as fully quiescent cells. This hypothesis would conciliate our *in vitro* and *in vivo* observations because TNFR2 seems to be promoting changes among the quiescent populations of NSCs *in vivo*, without necessarily leading to their activation, whereas, *in vitro,* incremented $EGFR^+$ symmetrical divisions and enhanced neurosphere formation rather suggest an activation signal.

The SEZ niche constitutes a complex environment where a great plethora of signals that actively regulate NSC stemness, quiescence and activation (Porlan et al., 2013b). Consequently, withdrawing them from their natural habitat and placing them *in vitro*, no matter how optimised the culture medium might be, will unquestionably affect their biology and behaviour. In line with this, the only method that we found to maintain quiescent cells *in vitro*, at least for a short period of time, was the organotypic *ex vivo* culture of the whole SEZ, and even so, we could appreciate slight sings of emerging activation in the control explants. This result evidences that key niche factors such as cell adhesion to components of the niche (Porlan et al., 2014) and especially hypoxic environment (Mohyeldin et al., 2010), among others, being absent from the culture conditions, might be necessary for the full expression of quiescence *in vitro*.

It is all about that alert quiescent state

Adult stem cells, regardless of their tissue localization, are known to alternate between a quiescent non proliferative state and an active, progeny-producing one. However, it has recently been reported that some adult quiescent SCs, such as HSCs or MuSCs, are found in a primed or alert state, non-cycling but prone to activation and that the probability of this state increases with mild and/or remote insults (Rodgers et al., 2014; Rodgers et al., 2017). As mentioned before, the potential existence of this intermediate state between quiescence and activation in the SEZ niche remained undetected until a couple of years ago when single-cell transcriptome analysis of isolated NSCs revealed their presence (Llorens-Bobadilla et al., 2015).

Analogously to other SC systems, the alert state of NSCs was initially defined molecularly as an intermediate state between dormancy and activation, suggesting a prone-to-activation state. However, aside from their molecular identity, very little is known about this pool of NSCs. For instance, although bioinformatics analysis suggests a linear qNSC1-qNSC2-aNSC progression during the NSC activation process, this has not been functionally tested and an alternative scenario where qNSC2 correspond to an accessory population that is only recruited and activated in the presence of specific signals, might also be plausible. Nevertheless, our data indicate that dormant qNSCs, at least in the functional scenarios we have analysed, acquire an intermediate alert qNSC2 phenotype before reaching full activation. Additionally, we could see that the transition to an alert state under mild non-pathological stimulation is a reversible process and primed qNSC2 can progressively return to dormancy without reaching activation. We have not explored all the variety of signals that might lead to NSC activation, but it would be interesting to analyse whether perturbations distinct in nature, intensity and/or duration might regulate differently the response of qNSCs. Additionally, it is not known whether different types of injury would trigger specific signalling pathways

and recruit specific subpopulations of qNSCs and if this will be reflected in the generation of functionally different cohorts of qNSC2. Curiously, in a zebrafish model, it has been observed that quiescent radial glia cells, equivalent to murine SEZ qNSCs, get activated upon injury, but that different types of stimuli target discrete subgroups of these cells (Than-Trong and Bally-Cuif, 2015). Similarly, the existence of stimulus-specific subpopulations of qNSCs in the murine hippocampus has also been described (Jhaveri et al., 2015). In the adult murine SEZ, NSCs display regional heterogeneity and it has been demonstrated that specific subtypes of OB neurons arise from definite subpopulations of NSCs with distinctive localization along the lateral ventricle wall (Kelsch et al., 2007; Lopez-Juarez et al., 2013; Merkle et al., 2014; Young et al., 2007). Although it has not been explored, it might be possible that stimulus-specificity and regional heterogeneity be intrinsic characteristics of dormant qNSC1 and that, once targeted for activation, transition through an alert qNSC2 state might be a common cellular mechanism. We have found that qNSC1 respond to inflammatory signals such as TNF-α and progranulin through TNFR2, but it would be interesting to know if what we observed is a general mechanism or if we just targeted a specific TNFR2 responsive subpopulation of quiescent NSCs. Further work will be required to address all these questions but the fact that MuSCs, HSCs, among other types of SCs, undergo a transition from G_0 to G_{alert} state in response to multiple types of distant injuries (Rodgers et al., 2014; Rodgers et al., 2017) suggests that this primed state might be a general mediator in the response to any kind of injury.

On the other hand, we consistently found that around one third of the quiescent NSCs in wild-type control SEZ tissue, were qNSC2. This might be the consequence of multiple local and/or systemic potentially damaging signals being constantly surveyed by qNSCs and/or other niche components such as microglia and endothelial cells, anticipating the need of an eventual rapid response by maintaining a pool of alert qNSC2. If that were the case, this would mean that the qNSC2 population could be a reflection of the general systemic health of an

individual at a specific moment. Conversely, the existence of a basal population of qNSC2 might reflect that there is a homeostatic equilibrium between dormant and active NSCs that entails the presence of a transitional pool of qNSC2. However, *in vivo* tracing experiments suggested that active NSCs are short-lived and actively divide generating multiple waves of progenitors before becoming exhausted (Calzolari et al., 2015), what would explain the decline in neurogenesis that is observed with aging (Shook et al., 2012). Although this work challenged the idea of active NSCs returning to quiescence *in vivo* after a period of proliferation, their data could not conclusively exclude the possible existence of a few $GFAP^+$ neurogenic cells that could do so. Moreover, they did not explore the possible role of qNSC2 in this process. We speculate that, after reaching activation, NSCs might divide giving rise to another active, proliferating aNSC and a daughter cell that might return to dormancy through an intermediate qNSC2 state. Interestingly, it has been reported that, although neurogenesis to the OB declines with age, and total number of NSCs, pinwheel units and NSCs per pinwheel is reduced, the percentage of actively mitotic NSCs increases (Shook et al., 2012). Therefore, it is tempting to hypothesise that aging involves the impairment of the reversible quiescence/activation cycle leading to the exhaustion of the quiescent NSC pool rather than the active one. Although we did not explore the behaviour of qNSC2 in aged animals, it would be really interesting to assess the role of these cells during aged-related neurogenesis decline.

Remote insults: no matter how far, NSCs know what is going on

Tissue specific SC harbour the ability to sense and respond to pathological situations, such as traumatic injury or ischemia, activating the production of committed progenitors that migrate to the damaged area and contribute to the reparation and return to homeostasis of the tissue (Kokaia and Lindvall, 2003, 2012). In the CNS, although regeneration is actively impaired by the formation of a reactive glial scar (Ohtake and Li, 2015) and the inhibiting properties of central

myelin (Boghdadi et al., 2017), among other factors, NSCs respond to a great variety of insults initiating a regenerative program that involves the activation of qNSCs (Barazzuol et al., 2017; Daynac et al., 2013; Llorens-Bobadilla et al., 2015; Pineda et al., 2013). The way that qNSCs respond to injury, however, is barely known and is now beginning to be examined. Additionally, the identification of the alert state of NSCs, adds a new level of complexity and raises the question of their specific role in homeostasis and during regeneration after injury. Interestingly, acute ischemia induces an IFNγ-dependent priming of dormant NSCs (Llorens-Bobadilla et al., 2015).

It is clear, however, that signals released by injured cells can travel long distances through the blood stream arriving to distant niches where local cells and resident or infiltrating immune cells react and eventually regulate SCs (Kizil et al., 2015). The CNS has been widely considered as an immune privileged organ due to the presence of the BBB. However, now it is well known that immune responses occur in the CNS driven by the activation of resident microglia, circulating immune cells and the production of cytokines, chemokines, neurotransmitters and ROS (Waisman et al., 2015). Furthermore, the SEZ is considered a specialized vascular niche with a "relaxed" BBB (Shen et al., 2008; Tavazoie et al., 2008) that may allow the crossing of some circulating factors including hormones, cytokines, metabolites and gases. For instance, heterochronic parabiosis models where young and old animals share the same blood, show that circulating factors can rejuvenate adult neurogenesis in the aged mouse (Katsimpardi et al., 2014). Moreover, SEZ endothelial cells are also activated by circulating inflammatory factors including LPS, IL-1β and TNF-α transmitting these signals to the CNS (Skelly et al., 2013). Therefore, even peripheral stimuli that do not trigger BBB dysfunction might trigger a systemic inflammatory response that could be, directly or indirectly, be transmitted to NSCs.

Along this thesis we have explored the response of NSCs to two clearly damaging insults such as systemic inflammation caused by LPS, and massive eradication of proliferative cells by TMZ. The first one is the most extended model of acute systemic inflammation and, although peripherally administered, some of the inflammatory mediators that it induces, either directly or indirectly, reach the CNS conveying the apparition of secondary neuroinflammation (Skelly et al., 2013). In the case of TMZ, although the existence of concomitant neuroinflammation associated with the massive cell loss it causes in the SEZ has not been previously reported, it is frequently observed in oncologic patients treated with chemotherapeutic agents (Vyas et al., 2014). In fact, we observed the up-regulation of TNF-α and PGRN in the SEZ tissue from TMZ injected mice. In line with previous reports, we observed that local neuroinflammation, in both scenarios, was accompanied by the shift of SEZ qNSC1 to an alert qNSC2 state. We cannot discard that signals other than inflammation are playing a role in this process, especially in the TMZ treatment since it is well-known that feedback signals from TAPS and neuroblasts regulate NSC behaviour (Aguirre et al., 2010; Kawaguchi et al., 2013). However, the fact that we could reproduce this effect by the specific *ex vivo* stimulation of TNFR2, common receptor to both molecules, suggests that in both scenarios the binding of TNFα and/or PGRN to TNFR2 is the subjacent mechanism that promotes the alert state.

During the aforementioned analysis, we came across to an unexpected result when we saw that a single IP injection of sterile saline, not only derived in mild neuroinflammation, but also induced a shift towards qNSC2, but not aNSCs, of the dormant NSC population that progressively returns to basal levels. Similar behaviour has been reported for HSCs or MuSCs, finding that they can respond to contralateral muscle or bone injury and to minor remote skin wound, moving to a G_{alert} state (Rodgers et al., 2014). However, we provide the first evidence that adult NSCs respond to mild non-threatening remote signals acquiring an alert quiescent state. Curiously, peripheral saline injection also induced mild neuroinflammation

characterized by up-regulated TNF-α and PGRN. Therefore, we propose that inflammation, and specifically TNFR2, plays a central role in the response of qNSCs to local or remote signals that may imply the production of new differentiated progeny. In this scenario, an additional level of regulation must be taken into account, since local or remote inflammatory signals are most probably being sensed, modulated and transferred to NSCs by other cellular component of the SEZ niche such as endothelial cells and microglia. Specifically, microglia, although disregarded for years as niche element, is now known to be a fundamental component regulating NSCs not only upon injury, but also in basal homeostatic conditions (Borsini et al., 2015; Sato, 2015; Sierra et al., 2010). Additionally, it has been described that microglia from the SEZ is unique in their activation state and functional properties (Goings et al., 2006; Ribeiro Xavier et al., 2015) and is found in close association with NSCs and their progeny (Solano Fonseca et al., 2016) Microglia activity has been related to both enhanced and decreased hippocampal neurogenesis (Ekdahl et al., 2003; Monje et al., 2003; Ziv et al., 2006). Moreover, changes in microglia with age have been associated with impaired subependymal neurogenesis (Solano Fonseca et al., 2016). Therefore, it would be interesting to assess whether microglia activation is a necessary step to initiate, modulate and/or extinguish the NSC response to remote stimuli that we have described in this thesis.

Inflammation: not as bad as they say. The central role of TNFR2 and p38.

Our data clearly indicate that TNF-α and PGRN positively regulate neurosphere proliferation and expansion through the signalling of a common receptor: TNFR2. Effects of PGRN on NSC have been previously suggested in hippocampal NPC (Nedachi et al., 2011) but the impact on adult NSCs and the implication of TNFR2 has not been previously tested. In contrast, several reports have implicated TNF-α in NSC proliferation, lineage commitment and neuroblast survival but their conclusions are largely contradictory showing both negative and

positive effects (Ben-Hur et al., 2003; Bernardino et al., 2008; Chen and Palmer, 2013; Iosif et al., 2008; Iosif et al., 2006; Keohane et al., 2010; Liu et al., 2005b; Widera et al., 2006a; Wong et al., 2004; Wu et al., 2000). Here, we have been able to dissect TNF-α negative and positive effects that concomitantly occur in different subset of neurosphere forming cells: some cells activate apoptosis and a cell-cycle arrest while others are activated to divide symmetrically. Although a few previous reports have suggested the differential role of each receptor in NSCs (Chen and Palmer, 2013; Iosif et al., 2008; Iosif et al., 2006), here we demonstrate with knock-out cells and specific agonistic antibodies that TNFR1 activation leads to detrimental effects in neurosphere survival and proliferation while TNFR2 activation promotes the expansion of the population of neurosphere forming cells. Furthermore, the fact that both effects occur at the same time in the culture, as reflected in the response of continuously treated cells, suggest a differential distribution of TNF-α receptors in different subset of cells. Thus, further analysis of the expression of each receptor along the NSC lineage will help to clarify the double-sided effects of TNF-α in neurogenesis. In line with our results, a few reports have also related TNFR2 signalling with SC emergence in other systems. For instance, TNFR2 is required for cardiac stem cells emergence upon TNF-α treatment in heart organ cultures promoting a cell-cycle entry (Al-Lamki et al., 2013). Additionally, embryonic HSC emergence is mediated by inflammatory signals and TNFR2 deficiency leads to lower numbers of HSCs and HSC defects (Espin-Palazon et al., 2014; He et al., 2015). Together suggest that instead of being a specific mechanism of neural tissue, TNFR2 may play a general role in the pre-activation of quiescent SCs.

The discovery of the G_{alert} state in NSCs is relatively recent, and the subjacent molecular mechanisms that might be involved are completely unknown. Here we have identified p38 as an essential component of TNFR2 signalling in NSCs and, hence, it emerges as a candidate for the transduction of external stimuli that regulate the exit from dormancy. The p38 MAPK pathway is involved in the

response to environmental stress and inflammatory cytokines but its activation leads to a multiple cellular processes including senescence, apoptosis, cell-cycle arrest, regulation of RNA splicing, tumour development or differentiation. Although we have not deepened in the complete mechanism so far, we can speculate with reported connections between p38 and other cell signalling components known to be relevant for quiescence emergence or alert transition. Interestingly, p38 translocates to the nucleus where it phosphorylates components of the policomb repressive complex 1 (PRC1) such as Bmi1 (Gaestel, 2006), which has been reported to be essential for qNSC maintenance (Mich et al., 2014). Furthermore, p38 activates MAPK-activated protein kinases (MAPKAPs) including MK2, with reported connections with components of the mTOR pathway, whose activation has been shown to be required for the transition of MuSCs from quiescence to G_{alert} (Rodgers et al., 2014; Rodgers et al., 2017). MK2 phosphorylates TSC1 and TSC2 inhibitors to activate 4E-BP1 phosphorylation resulting in the activation of protein translation (Gaestel, 2006), one of the functional defining features of the G_{alert} state. Therefore, it would be plausible that, likewise other SCs such as MuSCs, HSC and MSCs, mTOR, as a target of p38, could be also implicated in the regulation of the transition from dormancy to alert states (Rodgers et al., 2014; Rodgers et al., 2017).

Inflammation, evolution and the road to regeneration

Injury or disease triggers an inflammatory response that can either promote functional tissue regeneration or fast healing that may protect the organism at the expense of preserving the normal function and structure of the tissue. Regenerative responses are usually associated with resolution of inflammation whereas maintenance of the inflamed state often associates to wound healing and scar formation. Interestingly, non-mammalian vertebrates exhibit a great capacity to regenerate lost tissue, including the CNS. In the adult zebrafish, NSCs are capable of regenerating brain tissue after a traumatic injury through the activation

of injury-induced molecular programs and inflammation-related signaling (Kizil et al., 2012b; Kyritsis et al., 2012). In contrast, the neural tissue in mammals possesses a limited regenerative potential (Figure 39). Although neurogenesis is negatively impaired by neuroinflammatory processes, injury plays a double-sided role where detrimental effects are partially counteracted by a transient regenerative response triggered in part by NSCs (Kizil et al., 2015). Although it is currently unclear which stage is targeted by injury, the fact that TNF-α and progranulin predispose qNSCs to activation indicates that the dormant NSC could act as switch of the response to injury. In fact, the enriched expression of surface receptors described in qNSCs suggests that the quiescent pools are highly predisposed for injury response (Llorens-Bobadilla et al., 2015). We propose that the acquisition of a G_{alert} state represents an adaptive response of NSCs to the innate immune system that might reflect a reminiscent form of inflammation-induced regeneration seen in non-mammalian vertebrates. In regenerating vertebrates, initial phases of inflammation take place similarly to mammals, but prolonged inflammation does not occur (Kyritsis et al., 2012). In our model of peripheral saline injection, cytokine expression subsides a few days after the lesion suggesting that we have encountered a favorable scenario for the analysis of beneficial effects of inflammation.

Adult mammals appear to have gained a scar, fast wound healing response at the expense of regeneration capability. But because during prenatal development and early in life, mammals can exhibit some repair potential, one possibility is that regenerative genetic programs are present in some cells but turned off during development. Therefore, we could predict some beneficial pro-regenerative effects of inflammation that could rely on an adequate balance between cytokines and/or in selective responses on specific types of cells. Thus, pro-regenerative components of the immune response could still be maintained within the context of a more advanced immune system, like that of mammals, even if they are not easily apparent. To sum up, the elucidation of mechanisms that operate similarly in

regenerating and non-regenerating organisms can provide clues to boost SC-based regenerative potential in mammalian adult tissues.

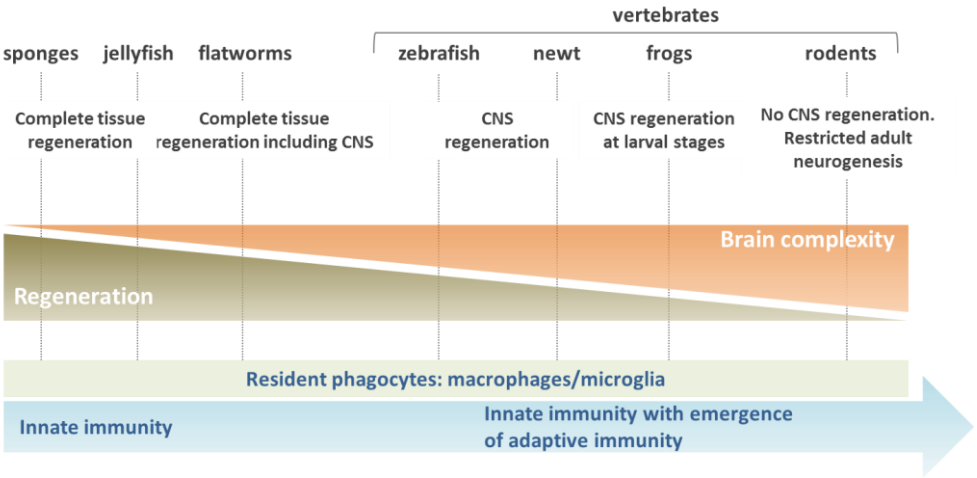

Figure 39. Schematic drawing showing the inverse coevolution of immune system and regenerative potential.

Conclusions

1. We have developed and tested in different scenarios, a new cytometry panel, based exclusively on the detection of surface markers, for the identification of SEZ NSCs in different quiescent (qNSC1 and qNSC2) and proliferative states, along with their more committed progeny.

2. In the adult SEZ, inflammatory signals such as TNF-α and progranulin drive dormant qNSC1 to exit quiescence but, before reaching full activation, they acquire a transient quiescent yet prone-to-activation alert qNSC2 state.

3. Mild peripheral insults, such as an intraperitoneal injection of sterile saline, induce the expression of inflammatory signals in the SEZ promoting the transition from qNSC1 to an alert qNSC2 that progressively returns to dormancy upon resolution of neuroinflammation.

4. TNF-α, acting through TNFR1, causes detrimental effects on NSC proliferation and survival whereas TNF-α and PGRN expand the population of multipotent NSCs *in vitro* maintaining stemness, through their binding to TNFR2.

5. TNFR2 signalling, most probably transduced intracellularly through p38, targets qNSC1 and prompts them to switch to an alert qNSC2.

6. In vitro culture conditions unavoidably force qNSCs to activation; however, a small fraction of cells in the culture that can be expanded by TNFR2 stimulation, retain some features reminiscent of the quiescent state found *in vivo*.

Bibliography

1. Adolf, B., Chapouton, P., Lam, C.S., Topp, S., Tannhauser, B., Strahle, U., Gotz, M., Bally-Cuif, L. (2006). 'Conserved and acquired features of adult neurogenesis in the zebrafish telencephalon'. *Dev Biol* 295, 278-293.
2. Aggarwal, B.B. (2000). 'Tumour necrosis factors receptor associated signalling molecules and their role in activation of apoptosis, JNK and NF-kappaB'. *Annals of the rheumatic diseases* 59 Suppl 1, i6-16.
3. Aggarwal, B.B., Gupta, S.C., Kim, J.H. (2012). 'Historical perspectives on tumor necrosis factor and its superfamily: 25 years later, a golden journey'. *Blood* 119, 651-665.
4. Aguirre, A., Rubio, M.E., Gallo, V. (2010). 'Notch and EGFR pathway interaction regulates neural stem cell number and self-renewal'. *Nature* 467, 323-327.
5. Aguzzi, A., Barres, B.A., Bennett, M.L. (2013). 'Microglia: scapegoat, saboteur, or something else?'. *Science* 339, 156-161.
6. Ahn, S., Joyner, A.L. (2005). 'In vivo analysis of quiescent adult neural stem cells responding to Sonic hedgehog'. *Nature* 437, 894-897.
7. Al-Lamki, R.S., Lu, W., Wang, J., Yang, J., Sargeant, T.J., Wells, R., Suo, C., Wright, P., Goddard, M., Huang, Q., Lebastchi, A.H., Tellides, G., Huang, Y., Min, W., Pober, J.S., Bradley, J.R. (2013). 'TNF, acting through inducibly expressed TNFR2, drives activation and cell cycle entry of c-Kit+ cardiac stem cells in ischemic heart disease'. *Stem Cells* 31, 1881-1892.
8. Alcantara Llaguno, S., Chen, J., Kwon, C.H., Jackson, E.L., Li, Y., Burns, D.K., Alvarez-Buylla, A., Parada, L.F. (2009). 'Malignant astrocytomas originate from neural stem/progenitor cells in a somatic tumor suppressor mouse model'. *Cancer cell* 15, 45-56.
9. Altman, J., Das, G.D. (1965). 'Autoradiographic and histological evidence of postnatal hippocampal neurogenesis in rats'. *J Comp Neurol* 124, 319-335.
10. Andreu-Agullo, C., Morante-Redolat, J.M., Delgado, A.C., Farinas, I. (2009). 'Vascular niche factor PEDF modulates Notch-dependent stemness in the adult subependymal zone'. *Nature neuroscience* 12, 1514-1523.
11. Anthony, T.E., Klein, C., Fishell, G., Heintz, N. (2004). 'Radial glia serve as neuronal progenitors in all regions of the central nervous system'. *Neuron* 41, 881-890.
12. Aurora, A.B., Olson, E.N. (2014). 'Immune modulation of stem cells and regeneration'. *Cell stem cell* 15, 14-25.
13. Banks, W.A., Erickson, M.A. (2010). 'The blood-brain barrier and immune function and dysfunction'. *Neurobiol Dis* 37, 26-32.
14. Barazzuol, L., Ju, L., Jeggo, P.A. (2017). 'A coordinated DNA damage response promotes adult quiescent neural stem cell activation'. *PLoS biology* 15, e2001264.

15. Barker, N., Bartfeld, S., Clevers, H. (2010). 'Tissue-resident adult stem cell populations of rapidly self-renewing organs'. *Cell stem cell* 7, 656-670.

16. Barker, N., Ridgway, R.A., van Es, J.H., van de Wetering, M., Begthel, H., van den Born, M., Danenberg, E., Clarke, A.R., Sansom, O.J., Clevers, H. (2009). 'Crypt stem cells as the cells-of-origin of intestinal cancer'. *Nature* 457, 608-611.

17. Bateman, A., Bennett, H.P. (2009). 'The granulin gene family: from cancer to dementia'. *Bioessays* 31, 1245-1254.

18. Bautch, V.L. (2011). 'Stem cells and the vasculature'. *Nature medicine* 17, 1437-1443.

19. Beckervordersandforth, R., Tripathi, P., Ninkovic, J., Bayam, E., Lepier, A., Stempfhuber, B., Kirchhoff, F., Hirrlinger, J., Haslinger, A., Lie, D.C., Beckers, J., Yoder, B., Irmler, M., Gotz, M. (2010). 'In vivo fate mapping and expression analysis reveals molecular hallmarks of prospectively isolated adult neural stem cells'. *Cell stem cell* 7, 744-758.

20. Belenguer, G., Domingo-Muelas, A., Ferron, S.R., Morante-Redolat, J.M., Farinas, I. (2016). 'Isolation, culture and analysis of adult subependymal neural stem cells'. *Differentiation; research in biological diversity* 91, 28-41.

21. Ben-Hur, T., Ben-Menachem, O., Furer, V., Einstein, O., Mizrachi-Kol, R., Grigoriadis, N. (2003). 'Effects of proinflammatory cytokines on the growth, fate, and motility of multipotential neural precursor cells'. *Mol Cell Neurosci* 24, 623-631.

22. Benner, E.J., Luciano, D., Jo, R., Abdi, K., Paez-Gonzalez, P., Sheng, H., Warner, D.S., Liu, C., Eroglu, C., Kuo, C.T. (2013). 'Protective astrogenesis from the SVZ niche after injury is controlled by Notch modulator Thbs4'. *Nature* 497, 369-373.

23. Berg, D.A., Belnoue, L., Song, H., Simon, A. (2013). 'Neurotransmitter-mediated control of neurogenesis in the adult vertebrate brain'. *Development* 140, 2548-2561.

24. Bernardino, L., Agasse, F., Silva, B., Ferreira, R., Grade, S., Malva, J.O. (2008). 'Tumor necrosis factor-alpha modulates survival, proliferation, and neuronal differentiation in neonatal subventricular zone cell cultures'. *Stem Cells* 26, 2361-2371.

25. Biteau, B., Hochmuth, C.E., Jasper, H. (2011). 'Maintaining tissue homeostasis: dynamic control of somatic stem cell activity'. *Cell stem cell* 9, 402-411.

26. Bjornsson, C.S., Apostolopoulou, M., Tian, Y., Temple, S. (2015). 'It takes a village: constructing the neurogenic niche'. *Developmental cell* 32, 435-446.

27. Boghdadi, A.G., Teo, L., Bourne, J.A. (2017). 'The Involvement of the Myelin-Associated Inhibitors and Their Receptors in CNS Plasticity and Injury'. *Molecular neurobiology*.

28. Bogoyevitch, M.A., Ngoei, K.R., Zhao, T.T., Yeap, Y.Y., Ng, D.C. (2010). 'c-Jun N-terminal kinase (JNK) signaling: recent advances and challenges'. *Biochimica et biophysica acta* 1804, 463-475.

29. Bond, A.M., Ming, G.L., Song, H. (2015). 'Adult Mammalian Neural Stem Cells and Neurogenesis: Five Decades Later'. *Cell stem cell* 17, 385-395.

30. Borsini, A., Zunszain, P.A., Thuret, S., Pariante, C.M. (2015). 'The role of inflammatory cytokines as key modulators of neurogenesis'. *Trends in neurosciences* 38, 145-157.

31. Brancho, D., Tanaka, N., Jaeschke, A., Ventura, J.J., Kelkar, N., Tanaka, Y., Kyuuma, M., Takeshita, T., Flavell, R.A., Davis, R.J. (2003). 'Mechanism of p38 MAP kinase activation in vivo'. *Genes & development* 17, 1969-1978.

32. Brinster, R.L., Zimmermann, J.W. (1994). 'Spermatogenesis following male germ-cell transplantation'. *Proceedings of the National Academy of Sciences of the United States of America* 91, 11298-11302.

33. Brouwers, N., Sleegers, K., Engelborghs, S., Maurer-Stroh, S., Gijselinck, I., van der Zee, J., Pickut, B.A., Van den Broeck, M., Mattheijssens, M., Peeters, K., Schymkowitz, J., Rousseau, F., Martin, J.J., Cruts, M., De Deyn, P.P., Van Broeckhoven, C. (2008). 'Genetic variability in progranulin contributes to risk for clinically diagnosed Alzheimer disease'. *Neurology* 71, 656-664.

34. Butovsky, O., Ziv, Y., Schwartz, A., Landa, G., Talpalar, A.E., Pluchino, S., Martino, G., Schwartz, M. (2006). 'Microglia activated by IL-4 or IFN-gamma differentially induce neurogenesis and oligodendrogenesis from adult stem/progenitor cells'. *Mol Cell Neurosci* 31, 149-160.

35. Cabal-Hierro, L., Lazo, P.S. (2012). 'Signal transduction by tumor necrosis factor receptors'. *Cellular signalling* 24, 1297-1305.

36. Calzolari, F., Michel, J., Baumgart, E.V., Theis, F., Gotz, M., Ninkovic, J. (2015). 'Fast clonal expansion and limited neural stem cell self-renewal in the adult subependymal zone'. *Nature neuroscience* 18, 490-492.

37. Candelario, K.M., Shuttleworth, C.W., Cunningham, L.A. (2013). 'Neural stem/progenitor cells display a low requirement for oxidative metabolism independent of hypoxia inducible factor-1alpha expression'. *J Neurochem* 125, 420-429.

38. Carpentier, P.A., Palmer, T.D. (2009). 'Immune influence on adult neural stem cell regulation and function'. *Neuron* 64, 79-92.

39. Carswell, E.A., Old, L.J., Kassel, R.L., Green, S., Fiore, N., Williamson, B. (1975). 'An endotoxin-induced serum factor that causes necrosis of tumors'.

Proceedings of the National Academy of Sciences of the United States of America 72, 3666-3670.

40. Cesetti, T., Fila, T., Obernier, K., Bengtson, C.P., Li, Y., Mandl, C., Holzl-Wenig, G., Ciccolini, F. (2011). 'GABAA receptor signaling induces osmotic swelling and cell cycle activation of neonatal prominin+ precursors'. *Stem Cells* 29, 307-319.
41. Codega, P., Silva-Vargas, V., Paul, A., Maldonado-Soto, A.R., Deleo, A.M., Pastrana, E., Doetsch, F. (2014). 'Prospective identification and purification of quiescent adult neural stem cells from their in vivo niche'. *Neuron* 82, 545-559.
42. Colak, D., Mori, T., Brill, M.S., Pfeifer, A., Falk, S., Deng, C., Monteiro, R., Mummery, C., Sommer, L., Gotz, M. (2008). 'Adult neurogenesis requires Smad4-mediated bone morphogenic protein signaling in stem cells'. *The Journal of neuroscience : the official journal of the Society for Neuroscience* 28, 434-446.
43. Conboy, I.M., Rando, T.A. (2012). 'Heterochronic parabiosis for the study of the effects of aging on stem cells and their niches'. *Cell Cycle* 11, 2260-2267.
44. Chaker, Z., Aid, S., Berry, H., Holzenberger, M. (2015). 'Suppression of IGF-I signals in neural stem cells enhances neurogenesis and olfactory function during aging'. *Aging Cell* 14, 847-856.
45. Chaker, Z., Codega, P., Doetsch, F. (2016). 'A mosaic world: puzzles revealed by adult neural stem cell heterogeneity'. *Wiley interdisciplinary reviews. Developmental biology* 5, 640-658.
46. Chang, L., Karin, M. (2001). 'Mammalian MAP kinase signalling cascades'. *Nature* 410, 37-40.
47. Chen, Z., Palmer, T.D. (2013). 'Differential roles of TNFR1 and TNFR2 signaling in adult hippocampal neurogenesis'. *Brain, behavior, and immunity* 30, 45-53.
48. Choi, H.R., Byun, S.Y., Kwon, S.H., Park, K.C. (2015). 'Niche interactions in epidermal stem cells'. *World journal of stem cells* 7, 495-501.
49. Daniel, R., He, Z., Carmichael, K.P., Halper, J., Bateman, A. (2000). 'Cellular localization of gene expression for progranulin'. *J Histochem Cytochem* 48, 999-1009.
50. Daynac, M., Chicheportiche, A., Pineda, J.R., Gauthier, L.R., Boussin, F.D., Mouthon, M.A. (2013). 'Quiescent neural stem cells exit dormancy upon alteration of GABAAR signaling following radiation damage'. *Stem Cell Res* 11, 516-528.
51. Daynac, M., Tirou, L., Faure, H., Mouthon, M.A., Gauthier, L.R., Hahn, H., Boussin, F.D., Ruat, M. (2016). 'Hedgehog Controls Quiescence and Activation of Neural Stem Cells in the Adult Ventricular-Subventricular Zone'. *Stem cell reports* 7, 735-748.

52. De Muynck, L., Van Damme, P. (2011). 'Cellular effects of progranulin in health and disease'. *J Mol Neurosci* 45, 549-560.

53. Deierborg, T., Roybon, L., Inacio, A.R., Pesic, J., Brundin, P. (2010). 'Brain injury activates microglia that induce neural stem cell proliferation ex vivo and promote differentiation of neurosphere-derived cells into neurons and oligodendrocytes'. *Neuroscience* 171, 1386-1396.

54. del Toro, R., Mendez-Ferrer, S. (2013). 'Autonomic regulation of hematopoiesis and cancer'. *Haematologica* 98, 1663-1666.

55. Delgado, A.C., Ferron, S.R., Vicente, D., Porlan, E., Perez-Villalba, A., Trujillo, C.M., D'Ocon, P., Farinas, I. (2014). 'Endothelial NT-3 delivered by vasculature and CSF promotes quiescence of subependymal neural stem cells through nitric oxide induction'. *Neuron* 83, 572-585.

56. Denis-Donini, S., Caprini, A., Frassoni, C., Grilli, M. (2005). 'Members of the NF-kappaB family expressed in zones of active neurogenesis in the postnatal and adult mouse brain'. *Brain research. Developmental brain research* 154, 81-89.

57. Dexter, T.M., Moore, M.A., Sheridan, A.P. (1977). 'Maintenance of hemopoietic stem cells and production of differentiated progeny in allogeneic and semiallogeneic bone marrow chimeras in vitro'. *The Journal of experimental medicine* 145, 1612-1616.

58. Dhawan, J., Rando, T.A. (2005). 'Stem cells in postnatal myogenesis: molecular mechanisms of satellite cell quiescence, activation and replenishment'. *Trends in cell biology* 15, 666-673.

59. Doetsch, F. (2003). 'The glial identity of neural stem cells'. *Nature neuroscience* 6, 1127-1134.

60. Doetsch, F., Alvarez-Buylla, A. (1996). 'Network of tangential pathways for neuronal migration in adult mammalian brain'. *Proceedings of the National Academy of Sciences of the United States of America* 93, 14895-14900.

61. Doetsch, F., Caille, I., Lim, D.A., Garcia-Verdugo, J.M., Alvarez-Buylla, A. (1999a). 'Subventricular zone astrocytes are neural stem cells in the adult mammalian brain'. *Cell* 97, 703-716.

62. Doetsch, F., Garcia-Verdugo, J.M., Alvarez-Buylla, A. (1997). 'Cellular composition and three-dimensional organization of the subventricular germinal zone in the adult mammalian brain'. *The Journal of neuroscience : the official journal of the Society for Neuroscience* 17, 5046-5061.

63. Doetsch, F., Garcia-Verdugo, J.M., Alvarez-Buylla, A. (1999b). 'Regeneration of a germinal layer in the adult mammalian brain'. *Proceedings of the National Academy of Sciences of the United States of America* 96, 11619-11624.

64. Doetsch, F., Petreanu, L., Caille, I., Garcia-Verdugo, J.M., Alvarez-Buylla, A. (2002a). 'EGF converts transit-amplifying neurogenic precursors in the adult brain into multipotent stem cells'. *Neuron* 36, 1021-1034.

65. Doetsch, F., Verdugo, J.M., Caille, I., Alvarez-Buylla, A., Chao, M.V., Casaccia-Bonnefil, P. (2002b). 'Lack of the cell-cycle inhibitor p27Kip1 results in selective increase of transit-amplifying cells for adult neurogenesis'. *The Journal of neuroscience : the official journal of the Society for Neuroscience* 22, 2255-2264.

66. Dykstra, B., Kent, D., Bowie, M., McCaffrey, L., Hamilton, M., Lyons, K., Lee, S.J., Brinkman, R., Eaves, C. (2007). 'Long-term propagation of distinct hematopoietic differentiation programs in vivo'. *Cell stem cell* 1, 218-229.

67. Ekdahl, C.T., Claasen, J.H., Bonde, S., Kokaia, Z., Lindvall, O. (2003). 'Inflammation is detrimental for neurogenesis in adult brain'. *Proceedings of the National Academy of Sciences of the United States of America* 100, 13632-13637.

68. Ellis, P., Fagan, B.M., Magness, S.T., Hutton, S., Taranova, O., Hayashi, S., McMahon, A., Rao, M., Pevny, L. (2004). 'SOX2, a persistent marker for multipotential neural stem cells derived from embryonic stem cells, the embryo or the adult'. *Dev Neurosci* 26, 148-165.

69. Escos, A., Risco, A., Alsina-Beauchamp, D., Cuenda, A. (2016). 'p38gamma and p38delta Mitogen Activated Protein Kinases (MAPKs), New Stars in the MAPK Galaxy'. *Frontiers in cell and developmental biology* 4, 31.

70. Espin-Palazon, R., Stachura, D.L., Campbell, C.A., Garcia-Moreno, D., Del Cid, N., Kim, A.D., Candel, S., Meseguer, J., Mulero, V., Traver, D. (2014). 'Proinflammatory signaling regulates hematopoietic stem cell emergence'. *Cell* 159, 1070-1085.

71. Faustman, D.L., Davis, M. (2013). 'TNF Receptor 2 and Disease: Autoimmunity and Regenerative Medicine'. *Frontiers in immunology* 4, 478.

72. Ferri, A.L., Cavallaro, M., Braida, D., Di Cristofano, A., Canta, A., Vezzani, A., Ottolenghi, S., Pandolfi, P.P., Sala, M., DeBiasi, S., Nicolis, S.K. (2004). 'Sox2 deficiency causes neurodegeneration and impaired neurogenesis in the adult mouse brain'. *Development* 131, 3805-3819.

73. Ferron, S.R., Charalambous, M., Radford, E., McEwen, K., Wildner, H., Hind, E., Morante-Redolat, J.M., Laborda, J., Guillemot, F., Bauer, S.R., Farinas, I., Ferguson-Smith, A.C. (2011). 'Postnatal loss of Dlk1 imprinting in stem cells and niche astrocytes regulates neurogenesis'. *Nature* 475, 381-385.

74. Fleming, H.E., Janzen, V., Lo Celso, C., Guo, J., Leahy, K.M., Kronenberg, H.M., Scadden, D.T. (2008). 'Wnt signaling in the niche enforces hematopoietic stem cell quiescence and is necessary to preserve self-renewal in vivo'. *Cell stem cell* 2, 274-283.

75. Fuchs, E., Tumbar, T., Guasch, G. (2004). 'Socializing with the neighbors: stem cells and their niche'. *Cell* 116, 769-778.

76. Fuentealba, L.C., Rompani, S.B., Parraguez, J.I., Obernier, K., Romero, R., Cepko, C.L., Alvarez-Buylla, A. (2015). 'Embryonic Origin of Postnatal Neural Stem Cells'. *Cell* 161, 1644-1655.

77. Furutachi, S., Matsumoto, A., Nakayama, K.I., Gotoh, Y. (2013). 'p57 controls adult neural stem cell quiescence and modulates the pace of lifelong neurogenesis'. *EMBO J* 32, 970-981.

78. Furutachi, S., Miya, H., Watanabe, T., Kawai, H., Yamasaki, N., Harada, Y., Imayoshi, I., Nelson, M., Nakayama, K.I., Hirabayashi, Y., Gotoh, Y. (2015). 'Slowly dividing neural progenitors are an embryonic origin of adult neural stem cells'. *Nature neuroscience* 18, 657-665.

79. Gaestel, M. (2006). 'MAPKAP kinases - MKs - two's company, three's a crowd'. *Nature reviews. Molecular cell biology* 7, 120-130.

80. Gaestel, M. (2015). 'MAPK-Activated Protein Kinases (MKs): Novel Insights and Challenges'. *Frontiers in cell and developmental biology* 3, 88.

81. Giachino, C., Basak, O., Lugert, S., Knuckles, P., Obernier, K., Fiorelli, R., Frank, S., Raineteau, O., Alvarez-Buylla, A., Taylor, V. (2014). 'Molecular diversity subdivides the adult forebrain neural stem cell population'. *Stem Cells* 32, 70-84.

82. Ginhoux, F., Greter, M., Leboeuf, M., Nandi, S., See, P., Gokhan, S., Mehler, M.F., Conway, S.J., Ng, L.G., Stanley, E.R., Samokhvalov, I.M., Merad, M. (2010). 'Fate mapping analysis reveals that adult microglia derive from primitive macrophages'. *Science* 330, 841-845.

83. Godbout, J.P., Chen, J., Abraham, J., Richwine, A.F., Berg, B.M., Kelley, K.W., Johnson, R.W. (2005). 'Exaggerated neuroinflammation and sickness behavior in aged mice following activation of the peripheral innate immune system'. *FASEB J* 19, 1329-1331.

84. Goings, G.E., Kozlowski, D.A., Szele, F.G. (2006). 'Differential activation of microglia in neurogenic versus non-neurogenic regions of the forebrain'. *Glia* 54, 329-342.

85. Gonzalez-Perez, O., Quinones-Hinojosa, A., Garcia-Verdugo, J.M. (2010). 'Immunological control of adult neural stem cells'. *Journal of stem cells* 5, 23-31.

86. Goodell, M.A., Nguyen, H., Shroyer, N. (2015). 'Somatic stem cell heterogeneity: diversity in the blood, skin and intestinal stem cell compartments'. *Nature reviews. Molecular cell biology* 16, 299-309.

87. He, Q., Zhang, C., Wang, L., Zhang, P., Ma, D., Lv, J., Liu, F. (2015). 'Inflammatory signaling regulates hematopoietic stem and progenitor cell emergence in vertebrates'. *Blood* 125, 1098-1106.

88. He, Z., Ong, C.H., Halper, J., Bateman, A. (2003). 'Progranulin is a mediator of the wound response'. *Nature medicine* 9, 225-229.

89. Hoglinger, G.U., Rizk, P., Muriel, M.P., Duyckaerts, C., Oertel, W.H., Caille, I., Hirsch, E.C. (2004). 'Dopamine depletion impairs precursor cell proliferation in Parkinson disease'. *Nature neuroscience* 7, 726-735.

90. Hsieh, J. (2012). 'Orchestrating transcriptional control of adult neurogenesis'. *Genes & development* 26, 1010-1021.

91. Imayoshi, I., Sakamoto, M., Ohtsuka, T., Takao, K., Miyakawa, T., Yamaguchi, M., Mori, K., Ikeda, T., Itohara, S., Kageyama, R. (2008). 'Roles of continuous neurogenesis in the structural and functional integrity of the adult forebrain'. *Nature neuroscience* 11, 1153-1161.

92. Iosif, R.E., Ahlenius, H., Ekdahl, C.T., Darsalia, V., Thored, P., Jovinge, S., Kokaia, Z., Lindvall, O. (2008). 'Suppression of stroke-induced progenitor proliferation in adult subventricular zone by tumor necrosis factor receptor 1'. *Journal of cerebral blood flow and metabolism : official journal of the International Society of Cerebral Blood Flow and Metabolism* 28, 1574-1587.

93. Iosif, R.E., Ekdahl, C.T., Ahlenius, H., Pronk, C.J., Bonde, S., Kokaia, Z., Jacobsen, S.E., Lindvall, O. (2006). 'Tumor necrosis factor receptor 1 is a negative regulator of progenitor proliferation in adult hippocampal neurogenesis'. *The Journal of neuroscience : the official journal of the Society for Neuroscience* 26, 9703-9712.

94. Jakubs, K., Bonde, S., Iosif, R.E., Ekdahl, C.T., Kokaia, Z., Kokaia, M., Lindvall, O. (2008). 'Inflammation regulates functional integration of neurons born in adult brain'. *The Journal of neuroscience : the official journal of the Society for Neuroscience* 28, 12477-12488.

95. Jhaveri, D.J., O'Keeffe, I., Robinson, G.J., Zhao, Q.Y., Zhang, Z.H., Nink, V., Narayanan, R.K., Osborne, G.W., Wray, N.R., Bartlett, P.F. (2015). 'Purification of neural precursor cells reveals the presence of distinct, stimulus-specific subpopulations of quiescent precursors in the adult mouse hippocampus'. *The Journal of neuroscience : the official journal of the Society for Neuroscience* 35, 8132-8144.

96. Jungblut, M., Tiveron, M.C., Barral, S., Abrahamsen, B., Knobel, S., Pennartz, S., Schmitz, J., Perraut, M., Pfrieger, F.W., Stoffel, W., Cremer, H., Bosio, A. (2012). 'Isolation and characterization of living primary astroglial cells using the new GLAST-specific monoclonal antibody ACSA-1'. *Glia* 60, 894-907.

97. Kang, W., Hebert, J.M. (2012). 'A Sox2 BAC transgenic approach for targeting adult neural stem cells'. *PloS one* 7, e49038.

98. Katsimpardi, L., Litterman, N.K., Schein, P.A., Miller, C.M., Loffredo, F.S., Wojtkiewicz, G.R., Chen, J.W., Lee, R.T., Wagers, A.J., Rubin, L.L. (2014). 'Vascular and neurogenic rejuvenation of the aging mouse brain by young systemic factors'. *Science* 344, 630-634.

99. Kawaguchi, D., Furutachi, S., Kawai, H., Hozumi, K., Gotoh, Y. (2013). 'Dll1 maintains quiescence of adult neural stem cells and segregates asymmetrically during mitosis'. *Nat Commun* 4, 1880.

100. Kelsch, W., Mosley, C.P., Lin, C.W., Lois, C. (2007). 'Distinct mammalian precursors are committed to generate neurons with defined dendritic projection patterns'. *PLoS biology* 5, e300.

101. Keohane, A., Ryan, S., Maloney, E., Sullivan, A.M., Nolan, Y.M. (2010). 'Tumour necrosis factor-alpha impairs neuronal differentiation but not proliferation of hippocampal neural precursor cells: Role of Hes1'. *Mol Cell Neurosci* 43, 127-135.

102. Kessenbrock, K., Frohlich, L., Sixt, M., Lammermann, T., Pfister, H., Bateman, A., Belaaouaj, A., Ring, J., Ollert, M., Fassler, R., Jenne, D.E. (2008). 'Proteinase 3 and neutrophil elastase enhance inflammation in mice by inactivating antiinflammatory progranulin'. *The Journal of clinical investigation* 118, 2438-2447.

103. Khatri, P., Obernier, K., Simeonova, I.K., Hellwig, A., Holzl-Wenig, G., Mandl, C., Scholl, C., Wolfl, S., Winkler, J., Gaspar, J.A., Sachinidis, A., Ciccolini, F. (2014). 'Proliferation and cilia dynamics in neural stem cells prospectively isolated from the SEZ'. *Scientific reports* 4, 3803.

104. Kim, E.J., Ables, J.L., Dickel, L.K., Eisch, A.J., Johnson, J.E. (2011). 'Ascl1 (Mash1) defines cells with long-term neurogenic potential in subgranular and subventricular zones in adult mouse brain'. *PloS one* 6, e18472.

105. Kim, E.J., Leung, C.T., Reed, R.R., Johnson, J.E. (2007). 'In vivo analysis of Ascl1 defined progenitors reveals distinct developmental dynamics during adult neurogenesis and gliogenesis'. *The Journal of neuroscience : the official journal of the Society for Neuroscience* 27, 12764-12774.

106. Kimura, W., Xiao, F., Canseco, D.C., Muralidhar, S., Thet, S., Zhang, H.M., Abderrahman, Y., Chen, R., Garcia, J.A., Shelton, J.M., Richardson, J.A., Ashour, A.M., Asaithamby, A., Liang, H., Xing, C., Lu, Z., Zhang, C.C., Sadek, H.A. (2015). 'Hypoxia fate mapping identifies cycling cardiomyocytes in the adult heart'. *Nature* 523, 226-230.

107. Kippin, T.E., Kapur, S., van der Kooy, D. (2005a). 'Dopamine specifically inhibits forebrain neural stem cell proliferation, suggesting a novel effect of antipsychotic drugs'. *The Journal of neuroscience : the official journal of the Society for Neuroscience* 25, 5815-5823.

108. Kippin, T.E., Martens, D.J., van der Kooy, D. (2005b). 'p21 loss compromises the relative quiescence of forebrain stem cell proliferation leading to exhaustion of their proliferation capacity'. *Genes & development* 19, 756-767.

109. Kizil, C., Kaslin, J., Kroehne, V., Brand, M. (2012a). 'Adult neurogenesis and brain regeneration in zebrafish'. *Developmental neurobiology* 72, 429-461.

110. Kizil, C., Kyritsis, N., Brand, M. (2015). 'Effects of inflammation on stem cells: together they strive?'. *EMBO Rep* 16, 416-426.

111. Kizil, C., Kyritsis, N., Dudczig, S., Kroehne, V., Freudenreich, D., Kaslin, J., Brand, M. (2012b). 'Regenerative neurogenesis from neural progenitor cells requires injury-induced expression of Gata3'. *Developmental cell* 23, 1230-1237.

112. Knobloch, M., Jessberger, S. (2017). 'Metabolism and neurogenesis'. *Current opinion in neurobiology* 42, 45-52.

113. Kokaia, Z., Lindvall, O. (2003). 'Neurogenesis after ischaemic brain insults'. *Current opinion in neurobiology* 13, 127-132.

114. Kokaia, Z., Lindvall, O. (2012). 'Stem cell repair of striatal ischemia'. *Progress in brain research* 201, 35-53.

115. Kokovay, E., Goderie, S., Wang, Y., Lotz, S., Lin, G., Sun, Y., Roysam, B., Shen, Q., Temple, S. (2010). 'Adult SVZ lineage cells home to and leave the vascular niche via differential responses to SDF1/CXCR4 signaling'. *Cell stem cell* 7, 163-173.

116. Kokovay, E., Wang, Y., Kusek, G., Wurster, R., Lederman, P., Lowry, N., Shen, Q., Temple, S. (2012). 'VCAM1 is essential to maintain the structure of the SVZ niche and acts as an environmental sensor to regulate SVZ lineage progression'. *Cell stem cell* 11, 220-230.

117. Kriegstein, A., Alvarez-Buylla, A. (2009). 'The glial nature of embryonic and adult neural stem cells'. *Annual review of neuroscience* 32, 149-184.

118. Kuhn, H.G., Eisch, A.J., Spalding, K., Peterson, D.A. (2016). 'Detection and Phenotypic Characterization of Adult Neurogenesis'. *Cold Spring Harbor perspectives in biology* 8, a025981.

119. Kyritsis, N., Kizil, C., Brand, M. (2014). 'Neuroinflammation and central nervous system regeneration in vertebrates'. *Trends in cell biology* 24, 128-135.

120. Kyritsis, N., Kizil, C., Zocher, S., Kroehne, V., Kaslin, J., Freudenreich, D., Iltzsche, A., Brand, M. (2012). 'Acute inflammation initiates the regenerative response in the adult zebrafish brain'. *Science* 338, 1353-1356.

121. Lalli, G. (2014). 'Extracellular signals controlling neuroblast migration in the postnatal brain'. *Adv Exp Med Biol* 800, 149-180.

122. Lapouge, G., Youssef, K.K., Vokaer, B., Achouri, Y., Michaux, C., Sotiropoulou, P.A., Blanpain, C. (2011). 'Identifying the cellular origin of squamous skin

tumors'. *Proceedings of the National Academy of Sciences of the United States of America* 108, 7431-7436.

123. Lee, S.Y., Reichlin, A., Santana, A., Sokol, K.A., Nussenzweig, M.C., Choi, Y. (1997). 'TRAF2 is essential for JNK but not NF-kappaB activation and regulates lymphocyte proliferation and survival'. *Immunity* 7, 703-713.

124. Li, L., Candelario, K.M., Thomas, K., Wang, R., Wright, K., Messier, A., Cunningham, L.A. (2014). 'Hypoxia inducible factor-1alpha (HIF-1alpha) is required for neural stem cell maintenance and vascular stability in the adult mouse SVZ'. *The Journal of neuroscience : the official journal of the Society for Neuroscience* 34, 16713-16719.

125. Li, L., Clevers, H. (2010). 'Coexistence of quiescent and active adult stem cells in mammals'. *Science* 327, 542-545.

126. Li, L., Xie, T. (2005). 'Stem cell niche: structure and function'. *Annual review of cell and developmental biology* 21, 605-631.

127. Lim, D.A., Tramontin, A.D., Trevejo, J.M., Herrera, D.G., Garcia-Verdugo, J.M., Alvarez-Buylla, A. (2000). 'Noggin antagonizes BMP signaling to create a niche for adult neurogenesis'. *Neuron* 28, 713-726.

128. Liu, H.K., Belz, T., Bock, D., Takacs, A., Wu, H., Lichter, P., Chai, M., Schutz, G. (2008). 'The nuclear receptor tailless is required for neurogenesis in the adult subventricular zone'. *Genes & development* 22, 2473-2478.

129. Liu, X., Wang, Q., Haydar, T.F., Bordey, A. (2005a). 'Nonsynaptic GABA signaling in postnatal subventricular zone controls proliferation of GFAP-expressing progenitors'. *Nature neuroscience* 8, 1179-1187.

130. Liu, Y.P., Lin, H.I., Tzeng, S.F. (2005b). 'Tumor necrosis factor-alpha and interleukin-18 modulate neuronal cell fate in embryonic neural progenitor culture'. *Brain Res* 1054, 152-158.

131. Livneh, Y., Adam, Y., Mizrahi, A. (2014). 'Odor processing by adult-born neurons'. *Neuron* 81, 1097-1110.

132. London, A., Cohen, M., Schwartz, M. (2013). 'Microglia and monocyte-derived macrophages: functionally distinct populations that act in concert in CNS plasticity and repair'. *Frontiers in cellular neuroscience* 7, 34.

133. Lopez-Juarez, A., Howard, J., Ullom, K., Howard, L., Grande, A., Pardo, A., Waclaw, R., Sun, Y.Y., Yang, D., Kuan, C.Y., Campbell, K., Nakafuku, M. (2013). 'Gsx2 controls region-specific activation of neural stem cells and injury-induced neurogenesis in the adult subventricular zone'. *Genes & development* 27, 1272-1287.

134. Lun, M.P., Monuki, E.S., Lehtinen, M.K. (2015). 'Development and functions of the choroid plexus-cerebrospinal fluid system'. *Nat Rev Neurosci* 16, 445-457.

135. Lledo, P.M., Valley, M. (2016). 'Adult Olfactory Bulb Neurogenesis'. *Cold Spring Harbor perspectives in biology* 8.

136. Llorens-Bobadilla, E., Martin-Villalba, A. (2016). 'Adult NSC diversity and plasticity: the role of the niche'. *Current opinion in neurobiology* 42, 68-74.

137. Llorens-Bobadilla, E., Zhao, S., Baser, A., Saiz-Castro, G., Zwadlo, K., Martin-Villalba, A. (2015). 'Single-Cell Transcriptomics Reveals a Population of Dormant Neural Stem Cells that Become Activated upon Brain Injury'. *Cell stem cell* 17, 329-340.

138. MacEwan, D.J. (2002). 'TNF receptor subtype signalling: differences and cellular consequences'. *Cellular signalling* 14, 477-492.

139. Malatesta, P., Hartfuss, E., Gotz, M. (2000). 'Isolation of radial glial cells by fluorescent-activated cell sorting reveals a neuronal lineage'. *Development* 127, 5253-5263.

140. Marchetti, L., Klein, M., Schlett, K., Pfizenmaier, K., Eisel, U.L. (2004). 'Tumor necrosis factor (TNF)-mediated neuroprotection against glutamate-induced excitotoxicity is enhanced by N-methyl-D-aspartate receptor activation. Essential role of a TNF receptor 2-mediated phosphatidylinositol 3-kinase-dependent NF-kappa B pathway'. *The Journal of biological chemistry* 279, 32869-32881.

141. Marques-Torrejon, M.A., Porlan, E., Banito, A., Gomez-Ibarlucea, E., Lopez-Contreras, A.J., Fernandez-Capetillo, O., Vidal, A., Gil, J., Torres, J., Farinas, I. (2013). 'Cyclin-dependent kinase inhibitor p21 controls adult neural stem cell expansion by regulating Sox2 gene expression'. *Cell stem cell* 12, 88-100.

142. Marshall, C.A., Novitch, B.G., Goldman, J.E. (2005). 'Olig2 directs astrocyte and oligodendrocyte formation in postnatal subventricular zone cells'. *The Journal of neuroscience : the official journal of the Society for Neuroscience* 25, 7289-7298.

143. McKhann, G.M., Albert, M.S., Grossman, M., Miller, B., Dickson, D., Trojanowski, J.Q., Work Group on Frontotemporal, D., Pick's, D. (2001). 'Clinical and pathological diagnosis of frontotemporal dementia: report of the Work Group on Frontotemporal Dementia and Pick's Disease'. *Arch Neurol* 58, 1803-1809.

144. Menn, B., Garcia-Verdugo, J.M., Yaschine, C., Gonzalez-Perez, O., Rowitch, D., Alvarez-Buylla, A. (2006). 'Origin of oligodendrocytes in the subventricular zone of the adult brain'. *The Journal of neuroscience : the official journal of the Society for Neuroscience* 26, 7907-7918.

145. Mercier, F. (2016). 'Fractones: extracellular matrix niche controlling stem cell fate and growth factor activity in the brain in health and disease'. *Cellular and molecular life sciences : CMLS* 73, 4661-4674.

146. Merkle, F.T., Fuentealba, L.C., Sanders, T.A., Magno, L., Kessaris, N., Alvarez-Buylla, A. (2014). 'Adult neural stem cells in distinct microdomains generate previously unknown interneuron types'. *Nature neuroscience* 17, 207-214.

147. Merkle, F.T., Tramontin, A.D., Garcia-Verdugo, J.M., Alvarez-Buylla, A. (2004). 'Radial glia give rise to adult neural stem cells in the subventricular zone'. *Proceedings of the National Academy of Sciences of the United States of America* 101, 17528-17532.

148. Mich, J.K., Signer, R.A., Nakada, D., Pineda, A., Burgess, R.J., Vue, T.Y., Johnson, J.E., Morrison, S.J. (2014). 'Prospective identification of functionally distinct stem cells and neurosphere-initiating cells in adult mouse forebrain'. *eLife* 3, e02669.

149. Mirzadeh, Z., Merkle, F.T., Soriano-Navarro, M., Garcia-Verdugo, J.M., Alvarez-Buylla, A. (2008). 'Neural stem cells confer unique pinwheel architecture to the ventricular surface in neurogenic regions of the adult brain'. *Cell stem cell* 3, 265-278.

150. Miyata, T., Kawaguchi, A., Okano, H., Ogawa, M. (2001). 'Asymmetric inheritance of radial glial fibers by cortical neurons'. *Neuron* 31, 727-741.

151. Mohyeldin, A., Garzon-Muvdi, T., Quinones-Hinojosa, A. (2010). 'Oxygen in stem cell biology: a critical component of the stem cell niche'. *Cell stem cell* 7, 150-161.

152. Molofsky, A.V., Pardal, R., Iwashita, T., Park, I.K., Clarke, M.F., Morrison, S.J. (2003). 'Bmi-1 dependence distinguishes neural stem cell self-renewal from progenitor proliferation'. *Nature* 425, 962-967.

153. Molofsky, A.V., Slutsky, S.G., Joseph, N.M., He, S., Pardal, R., Krishnamurthy, J., Sharpless, N.E., Morrison, S.J. (2006). 'Increasing p16INK4a expression decreases forebrain progenitors and neurogenesis during ageing'. *Nature* 443, 448-452.

154. Monje, M.L., Toda, H., Palmer, T.D. (2003). 'Inflammatory blockade restores adult hippocampal neurogenesis'. *Science* 302, 1760-1765.

155. Montgomery, S.L., Bowers, W.J. (2012). 'Tumor necrosis factor-alpha and the roles it plays in homeostatic and degenerative processes within the central nervous system'. *Journal of neuroimmune pharmacology : the official journal of the Society on NeuroImmune Pharmacology* 7, 42-59.

156. Moore, K.A., Ema, H., Lemischka, I.R. (1997). 'In vitro maintenance of highly purified, transplantable hematopoietic stem cells'. *Blood* 89, 4337-4347.

157. Moreno-Estelles, M., Diaz-Moreno, M., Gonzalez-Gomez, P., Andreu, Z., Mira, H. (2012). 'Single and dual birthdating procedures for assessing the response of adult neural stem cells to the infusion of a soluble factor using halogenated thymidine analogs'. *Current protocols in stem cell biology* Chapter 2, Unit 2D 10.

158. Morrens, J., Van Den Broeck, W., Kempermann, G. (2012). 'Glial cells in adult neurogenesis'. *Glia* 60, 159-174.

159. Morrison, S.J., Spradling, A.C. (2008). 'Stem cells and niches: mechanisms that promote stem cell maintenance throughout life'. *Cell* 132, 598-611.

160. Murayama, A., Matsuzaki, Y., Kawaguchi, A., Shimazaki, T., Okano, H. (2002). 'Flow cytometric analysis of neural stem cells in the developing and adult mouse brain'. *Journal of neuroscience research* 69, 837-847.

161. Nait-Oumesmar, B., Decker, L., Lachapelle, F., Avellana-Adalid, V., Bachelin, C., Baron-Van Evercooren, A. (1999). 'Progenitor cells of the adult mouse subventricular zone proliferate, migrate and differentiate into oligodendrocytes after demyelination'. *Eur J Neurosci* 11, 4357-4366.

162. Nam, H.S., Benezra, R. (2009). 'High levels of Id1 expression define B1 type adult neural stem cells'. *Cell stem cell* 5, 515-526.

163. Nedachi, T., Kawai, T., Matsuwaki, T., Yamanouchi, K., Nishihara, M. (2011). 'Progranulin enhances neural progenitor cell proliferation through glycogen synthase kinase 3beta phosphorylation'. *Neuroscience* 185, 106-115.

164. Nimmerjahn, A., Kirchhoff, F., Helmchen, F. (2005). 'Resting microglial cells are highly dynamic surveillants of brain parenchyma in vivo'. *Science* 308, 1314-1318.

165. Noctor, S.C., Flint, A.C., Weissman, T.A., Dammerman, R.S., Kriegstein, A.R. (2001). 'Neurons derived from radial glial cells establish radial units in neocortex'. *Nature* 409, 714-720.

166. Ohtake, Y., Li, S. (2015). 'Molecular mechanisms of scar-sourced axon growth inhibitors'. *Brain Res* 1619, 22-35.

167. Orford, K.W., Scadden, D.T. (2008). 'Deconstructing stem cell self-renewal: genetic insights into cell-cycle regulation'. *Nature reviews. Genetics* 9, 115-128.

168. Ortega, F., Berninger, B., Costa, M.R. (2013a). 'Primary culture and live imaging of adult neural stem cells and their progeny'. *Methods Mol Biol* 1052, 1-11.

169. Ortega, F., Gascon, S., Masserdotti, G., Deshpande, A., Simon, C., Fischer, J., Dimou, L., Chichung Lie, D., Schroeder, T., Berninger, B. (2013b). 'Oligodendrogliogenic and neurogenic adult subependymal zone neural stem cells constitute distinct lineages and exhibit differential responsiveness to Wnt signalling'. *Nature cell biology* 15, 602-613.

170. Ottone, C., Krusche, B., Whitby, A., Clements, M., Quadrato, G., Pitulescu, M.E., Adams, R.H., Parrinello, S. (2014). 'Direct cell-cell contact with the vascular niche maintains quiescent neural stem cells'. *Nature cell biology* 16, 1045-1056.

171. Ousset, M., Van Keymeulen, A., Bouvencourt, G., Sharma, N., Achouri, Y., Simons, B.D., Blanpain, C. (2012). 'Multipotent and unipotent progenitors

contribute to prostate postnatal development'. *Nature cell biology* 14, 1131-1138.

172. Paez-Gonzalez, P., Asrican, B., Rodriguez, E., Kuo, C.T. (2014). 'Identification of distinct ChAT(+) neurons and activity-dependent control of postnatal SVZ neurogenesis'. *Nature neuroscience* 17, 934-942.

173. Parras, C.M., Galli, R., Britz, O., Soares, S., Galichet, C., Battiste, J., Johnson, J.E., Nakafuku, M., Vescovi, A., Guillemot, F. (2004). 'Mash1 specifies neurons and oligodendrocytes in the postnatal brain'. *EMBO J* 23, 4495-4505.

174. Pastrana, E., Cheng, L.C., Doetsch, F. (2009). 'Simultaneous prospective purification of adult subventricular zone neural stem cells and their progeny'. *Proceedings of the National Academy of Sciences of the United States of America* 106, 6387-6392.

175. Pastrana, E., Silva-Vargas, V., Doetsch, F. (2011). 'Eyes wide open: a critical review of sphere-formation as an assay for stem cells'. *Cell stem cell* 8, 486-498.

176. Petkau, T.L., Neal, S.J., Orban, P.C., MacDonald, J.L., Hill, A.M., Lu, G., Feldman, H.H., Mackenzie, I.R., Leavitt, B.R. (2010). 'Progranulin expression in the developing and adult murine brain'. *J Comp Neurol* 518, 3931-3947.

177. Philips, T., De Muynck, L., Thu, H.N., Weynants, B., Vanacker, P., Dhondt, J., Sleegers, K., Schelhaas, H.J., Verbeek, M., Vandenberghe, R., Sciot, R., Van Broeckhoven, C., Lambrechts, D., Van Leuven, F., Van Den Bosch, L., Robberecht, W., Van Damme, P. (2010). 'Microglial upregulation of progranulin as a marker of motor neuron degeneration'. *J Neuropathol Exp Neurol* 69, 1191-1200.

178. Picard-Riera, N., Decker, L., Delarasse, C., Goude, K., Nait-Oumesmar, B., Liblau, R., Pham-Dinh, D., Baron-Van Evercooren, A. (2002). 'Experimental autoimmune encephalomyelitis mobilizes neural progenitors from the subventricular zone to undergo oligodendrogenesis in adult mice'. *Proceedings of the National Academy of Sciences of the United States of America* 99, 13211-13216.

179. Pineda, J.R., Daynac, M., Chicheportiche, A., Cebrian-Silla, A., Sii Felice, K., Garcia-Verdugo, J.M., Boussin, F.D., Mouthon, M.A. (2013). 'Vascular-derived TGF-beta increases in the stem cell niche and perturbs neurogenesis during aging and following irradiation in the adult mouse brain'. *EMBO molecular medicine* 5, 548-562.

180. Pinto, L., Mader, M.T., Irmler, M., Gentilini, M., Santoni, F., Drechsel, D., Blum, R., Stahl, R., Bulfone, A., Malatesta, P., Beckers, J., Gotz, M. (2008). 'Prospective isolation of functionally distinct radial glial subtypes--lineage and transcriptome analysis'. *Mol Cell Neurosci* 38, 15-42.

181. Pluchino, S., Muzio, L., Imitola, J., Deleidi, M., Alfaro-Cervello, C., Salani, G., Porcheri, C., Brambilla, E., Cavasinni, F., Bergamaschi, A., Garcia-Verdugo, J.M., Comi, G., Khoury, S.J., Martino, G. (2008). 'Persistent inflammation alters the function of the endogenous brain stem cell compartment'. *Brain* 131, 2564-2578.

182. Ponti, G., Obernier, K., Guinto, C., Jose, L., Bonfanti, L., Alvarez-Buylla, A. (2013). 'Cell cycle and lineage progression of neural progenitors in the ventricular-subventricular zones of adult mice'. *Proceedings of the National Academy of Sciences of the United States of America* 110, E1045-1054.

183. Porlan, E., Marti-Prado, B., Morante-Redolat, J.M., Consiglio, A., Delgado, A.C., Kypta, R., Lopez-Otin, C., Kirstein, M., Farinas, I. (2014). 'MT5-MMP regulates adult neural stem cell functional quiescence through the cleavage of N-cadherin'. *Nature cell biology* 16, 629-638.

184. Porlan, E., Morante-Redolat, J.M., Marques-Torrejon, M.A., Andreu-Agullo, C., Carneiro, C., Gomez-Ibarlucea, E., Soto, A., Vidal, A., Ferron, S.R., Farinas, I. (2013a). 'Transcriptional repression of Bmp2 by p21(Waf1/Cip1) links quiescence to neural stem cell maintenance'. *Nature neuroscience* 16, 1567-1575.

185. Porlan, E., Perez-Villalba, A., Delgado, A.C., Ferron, S.R. (2013b). 'Paracrine regulation of neural stem cells in the subependymal zone'. *Archives of biochemistry and biophysics* 534, 11-19.

186. Qin, L., Wu, X., Block, M.L., Liu, Y., Breese, G.R., Hong, J.S., Knapp, D.J., Crews, F.T. (2007). 'Systemic LPS causes chronic neuroinflammation and progressive neurodegeneration'. *Glia* 55, 453-462.

187. Rafii, S., Butler, J.M., Ding, B.S. (2016). 'Angiocrine functions of organ-specific endothelial cells'. *Nature* 529, 316-325.

188. Ramirez-Castillejo, C., Sanchez-Sanchez, F., Andreu-Agullo, C., Ferron, S.R., Aroca-Aguilar, J.D., Sanchez, P., Mira, H., Escribano, J., Farinas, I. (2006). 'Pigment epithelium-derived factor is a niche signal for neural stem cell renewal'. *Nature neuroscience* 9, 331-339.

189. Redzic, Z.B., Preston, J.E., Duncan, J.A., Chodobski, A., Szmydynger-Chodobska, J. (2005). 'The choroid plexus-cerebrospinal fluid system: from development to aging'. *Curr Top Dev Biol* 71, 1-52.

190. Reynolds, B.A., Rietze, R.L. (2005). 'Neural stem cells and neurospheres--re-evaluating the relationship'. *Nat Methods* 2, 333-336.

191. Reynolds, B.A., Weiss, S. (1992). 'Generation of neurons and astrocytes from isolated cells of the adult mammalian central nervous system'. *Science* 255, 1707-1710.

192. Ribeiro Xavier, A.L., Kress, B.T., Goldman, S.A., Lacerda de Menezes, J.R., Nedergaard, M. (2015). 'A Distinct Population of Microglia Supports Adult Neurogenesis in the Subventricular Zone'. *The Journal of neuroscience : the official journal of the Society for Neuroscience* 35, 11848-11861.

193. Rios, M., Williams, D.A. (1990). 'Systematic analysis of the ability of stromal cell lines derived from different murine adult tissues to support maintenance of hematopoietic stem cells in vitro'. *Journal of cellular physiology* 145, 434-443.

194. Rodgers, J.T., King, K.Y., Brett, J.O., Cromie, M.J., Charville, G.W., Maguire, K.K., Brunson, C., Mastey, N., Liu, L., Tsai, C.R., Goodell, M.A., Rando, T.A. (2014). 'mTORC1 controls the adaptive transition of quiescent stem cells from G0 to G(Alert)'. *Nature* 510, 393-396.

195. Rodgers, J.T., Schroeder, M.D., Ma, C., Rando, T.A. (2017). 'HGFA Is an Injury-Regulated Systemic Factor that Induces the Transition of Stem Cells into GAlert'. *Cell reports* 19, 479-486.

196. Romero-Grimaldi, C., Moreno-Lopez, B., Estrada, C. (2008). 'Age-dependent effect of nitric oxide on subventricular zone and olfactory bulb neural precursor proliferation'. *J Comp Neurol* 506, 339-346.

197. Rossi, L., Lin, K.K., Boles, N.C., Yang, L., King, K.Y., Jeong, M., Mayle, A., Goodell, M.A. (2012). 'Less is more: unveiling the functional core of hematopoietic stem cells through knockout mice'. *Cell stem cell* 11, 302-317.

198. Rumman, M., Dhawan, J., Kassem, M. (2015). 'Concise Review: Quiescence in Adult Stem Cells: Biological Significance and Relevance to Tissue Regeneration'. *Stem Cells* 33, 2903-2912.

199. Sabio, G., Davis, R.J. (2014). 'TNF and MAP kinase signalling pathways'. *Seminars in immunology* 26, 237-245.

200. Sato, K. (2015). 'Effects of Microglia on Neurogenesis'. *Glia* 63, 1394-1405.

201. Sawamoto, K., Wichterle, H., Gonzalez-Perez, O., Cholfin, J.A., Yamada, M., Spassky, N., Murcia, N.S., Garcia-Verdugo, J.M., Marin, O., Rubenstein, J.L., Tessier-Lavigne, M., Okano, H., Alvarez-Buylla, A. (2006). 'New neurons follow the flow of cerebrospinal fluid in the adult brain'. *Science* 311, 629-632.

202. Schofield, R. (1978). 'The relationship between the spleen colony-forming cell and the haemopoietic stem cell'. *Blood cells* 4, 7-25.

203. Schwartz, M. (2010). '"Tissue-repairing" blood-derived macrophages are essential for healing of the injured spinal cord: from skin-activated macrophages to infiltrating blood-derived cells?'. *Brain, behavior, and immunity* 24, 1054-1057.

204. Schwartz, M., London, A., Shechter, R. (2009). 'Boosting T-cell immunity as a therapeutic approach for neurodegenerative conditions: the role of innate immunity'. *Neuroscience* 158, 1133-1142.

205. Schwartz, M., Shechter, R. (2010). 'Systemic inflammatory cells fight off neurodegenerative disease'. *Nature reviews. Neurology* 6, 405-410.

206. Seri, B., Garcia-Verdugo, J.M., McEwen, B.S., Alvarez-Buylla, A. (2001). 'Astrocytes give rise to new neurons in the adult mammalian hippocampus'. *The Journal of neuroscience : the official journal of the Society for Neuroscience* 21, 7153-7160.

207. Sethi, G., Sung, B., Aggarwal, B.B. (2008). 'TNF: a master switch for inflammation to cancer'. *Frontiers in bioscience : a journal and virtual library* 13, 5094-5107.

208. Shaulian, E., Karin, M. (2002). 'AP-1 as a regulator of cell life and death'. *Nature cell biology* 4, E131-136.

209. Shen, Q., Goderie, S.K., Jin, L., Karanth, N., Sun, Y., Abramova, N., Vincent, P., Pumiglia, K., Temple, S. (2004). 'Endothelial cells stimulate self-renewal and expand neurogenesis of neural stem cells'. *Science* 304, 1338-1340.

210. Shen, Q., Wang, Y., Kokovay, E., Lin, G., Chuang, S.M., Goderie, S.K., Roysam, B., Temple, S. (2008). 'Adult SVZ stem cells lie in a vascular niche: a quantitative analysis of niche cell-cell interactions'. *Cell stem cell* 3, 289-300.

211. Shin, J., Berg, D.A., Zhu, Y., Shin, J.Y., Song, J., Bonaguidi, M.A., Enikolopov, G., Nauen, D.W., Christian, K.M., Ming, G.L., Song, H. (2015). 'Single-Cell RNA-Seq with Waterfall Reveals Molecular Cascades underlying Adult Neurogenesis'. *Cell stem cell* 17, 360-372.

212. Shook, B.A., Manz, D.H., Peters, J.J., Kang, S., Conover, J.C. (2012). 'Spatiotemporal changes to the subventricular zone stem cell pool through aging'. *The Journal of neuroscience : the official journal of the Society for Neuroscience* 32, 6947-6956.

213. Sierra, A., Encinas, J.M., Deudero, J.J., Chancey, J.H., Enikolopov, G., Overstreet-Wadiche, L.S., Tsirka, S.E., Maletic-Savatic, M. (2010). 'Microglia shape adult hippocampal neurogenesis through apoptosis-coupled phagocytosis'. *Cell stem cell* 7, 483-495.

214. Silva-Vargas, V., Maldonado-Soto, A.R., Mizrak, D., Codega, P., Doetsch, F. (2016). 'Age-Dependent Niche Signals from the Choroid Plexus Regulate Adult Neural Stem Cells'. *Cell stem cell* 19, 643-652.

215. Skelly, D.T., Hennessy, E., Dansereau, M.A., Cunningham, C. (2013). 'A systematic analysis of the peripheral and CNS effects of systemic LPS, IL-1beta, [corrected] TNF-alpha and IL-6 challenges in C57BL/6 mice'. *PloS one* 8, e69123.

216. Smith, K.R., Damiano, J., Franceschetti, S., Carpenter, S., Canafoglia, L., Morbin, M., Rossi, G., Pareyson, D., Mole, S.E., Staropoli, J.F., Sims, K.B., Lewis, J., Lin, W.L., Dickson, D.W., Dahl, H.H., Bahlo, M., Berkovic, S.F. (2012). 'Strikingly different clinicopathological phenotypes determined by progranulin-mutation dosage'. *Am J Hum Genet* 90, 1102-1107.

217. Sohn, J., Orosco, L., Guo, F., Chung, S.H., Bannerman, P., Mills Ko, E., Zarbalis, K., Deng, W., Pleasure, D. (2015). 'The subventricular zone continues to generate corpus callosum and rostral migratory stream astroglia in normal adult mice'. *The Journal of neuroscience : the official journal of the Society for Neuroscience* 35, 3756-3763.

218. Solano Fonseca, R., Mahesula, S., Apple, D.M., Raghunathan, R., Dugan, A., Cardona, A., O'Connor, J., Kokovay, E. (2016). 'Neurogenic Niche Microglia Undergo Positional Remodeling and Progressive Activation Contributing to Age-Associated Reductions in Neurogenesis'. *Stem cells and development* 25, 542-555.

219. Spassky, N., Merkle, F.T., Flames, N., Tramontin, A.D., Garcia-Verdugo, J.M., Alvarez-Buylla, A. (2005). 'Adult ependymal cells are postmitotic and are derived from radial glial cells during embryogenesis'. *The Journal of neuroscience : the official journal of the Society for Neuroscience* 25, 10-18.

220. Stange, D.E., Koo, B.K., Huch, M., Sibbel, G., Basak, O., Lyubimova, A., Kujala, P., Bartfeld, S., Koster, J., Geahlen, J.H., Peters, P.J., van Es, J.H., van de Wetering, M., Mills, J.C., Clevers, H. (2013). 'Differentiated Troy+ chief cells act as reserve stem cells to generate all lineages of the stomach epithelium'. *Cell* 155, 357-368.

221. Stolp, H.B., Turnquist, C., Dziegielewska, K.M., Saunders, N.R., Anthony, D.C., Molnar, Z. (2011). 'Reduced ventricular proliferation in the foetal cortex following maternal inflammation in the mouse'. *Brain* 134, 3236-3248.

222. Takeda, H., Koso, H., Tessarollo, L., Copeland, N.G., Jenkins, N.A. (2013). 'Musashi1-CreER(T2) : a new cre line for conditional mutagenesis in neural stem cells'. *Genesis* 51, 128-134.

223. Tavazoie, M., Van der Veken, L., Silva-Vargas, V., Louissaint, M., Colonna, L., Zaidi, B., Garcia-Verdugo, J.M., Doetsch, F. (2008). 'A specialized vascular niche for adult neural stem cells'. *Cell stem cell* 3, 279-288.

224. Tesz, G.J., Guilherme, A., Guntur, K.V., Hubbard, A.C., Tang, X., Chawla, A., Czech, M.P. (2007). 'Tumor necrosis factor alpha (TNFalpha) stimulates Map4k4 expression through TNFalpha receptor 1 signaling to c-Jun and activating transcription factor 2'. *The Journal of biological chemistry* 282, 19302-19312.

225. Than-Trong, E., Bally-Cuif, L. (2015). 'Radial glia and neural progenitors in the adult zebrafish central nervous system'. *Glia* 63, 1406-1428.

226. Thomas, K., Engler, A.J., Meyer, G.A. (2015). 'Extracellular matrix regulation in the muscle satellite cell niche'. *Connective tissue research* 56, 1-8.

227. Tian, C., Zhang, Y. (2016). 'Purification of hematopoietic stem cells from bone marrow'. *Annals of hematology* 95, 543-547.

228. Tian, H., Biehs, B., Warming, S., Leong, K.G., Rangell, L., Klein, O.D., de Sauvage, F.J. (2011). 'A reserve stem cell population in small intestine renders Lgr5-positive cells dispensable'. *Nature* 478, 255-259.

229. Till, J.E., Mc, C.E. (1961). 'A direct measurement of the radiation sensitivity of normal mouse bone marrow cells'. *Radiation research* 14, 213-222.

230. Tong, C.K., Chen, J., Cebrian-Silla, A., Mirzadeh, Z., Obernier, K., Guinto, C.D., Tecott, L.H., Garcia-Verdugo, J.M., Kriegstein, A., Alvarez-Buylla, A. (2014). 'Axonal control of the adult neural stem cell niche'. *Cell stem cell* 14, 500-511.

231. Tournier, C., Dong, C., Turner, T.K., Jones, S.N., Flavell, R.A., Davis, R.J. (2001). 'MKK7 is an essential component of the JNK signal transduction pathway activated by proinflammatory cytokines'. *Genes & development* 15, 1419-1426.

232. Tramontin, A.D., Garcia-Verdugo, J.M., Lim, D.A., Alvarez-Buylla, A. (2003). 'Postnatal development of radial glia and the ventricular zone (VZ): a continuum of the neural stem cell compartment'. *Cereb Cortex* 13, 580-587.

233. Turrin, N.P., Gayle, D., Ilyin, S.E., Flynn, M.C., Langhans, W., Schwartz, G.J., Plata-Salaman, C.R. (2001). 'Pro-inflammatory and anti-inflammatory cytokine mRNA induction in the periphery and brain following intraperitoneal administration of bacterial lipopolysaccharide'. *Brain Res Bull* 54, 443-453.

234. Urban, N., van den Berg, D.L., Forget, A., Andersen, J., Demmers, J.A., Hunt, C., Ayrault, O., Guillemot, F. (2016). 'Return to quiescence of mouse neural stem cells by degradation of a proactivation protein'. *Science* 353, 292-295.

235. Van Damme, P., Van Hoecke, A., Lambrechts, D., Vanacker, P., Bogaert, E., van Swieten, J., Carmeliet, P., Van Den Bosch, L., Robberecht, W. (2008). 'Progranulin functions as a neurotrophic factor to regulate neurite outgrowth and enhance neuronal survival'. *J Cell Biol* 181, 37-41.

236. Van Keymeulen, A., Rocha, A.S., Ousset, M., Beck, B., Bouvencourt, G., Rock, J., Sharma, N., Dekoninck, S., Blanpain, C. (2011). 'Distinct stem cells contribute to mammary gland development and maintenance'. *Nature* 479, 189-193.

237. Venere, M., Han, Y.G., Bell, R., Song, J.S., Alvarez-Buylla, A., Blelloch, R. (2012). 'Sox1 marks an activated neural stem/progenitor cell in the hippocampus'. *Development* 139, 3938-3949.

238. Voog, J., Jones, D.L. (2010). 'Stem cells and the niche: a dynamic duo'. *Cell stem cell* 6, 103-115.

239. Vyas, D., Laput, G., Vyas, A.K. (2014). 'Chemotherapy-enhanced inflammation may lead to the failure of therapy and metastasis'. *OncoTargets and therapy* 7, 1015-1023.

240. Wagers, A.J. (2012). 'The stem cell niche in regenerative medicine'. *Cell stem cell* 10, 362-369.

241. Waisman, A., Liblau, R.S., Becher, B. (2015). 'Innate and adaptive immune responses in the CNS'. *The Lancet. Neurology* 14, 945-955.

242. Wajant, H., Pfizenmaier, K., Scheurich, P. (2003). 'Tumor necrosis factor signaling'. *Cell death and differentiation* 10, 45-65.

243. Wang, B.C., Liu, H., Talwar, A., Jian, J. (2015). 'New discovery rarely runs smooth: an update on progranulin/TNFR interactions'. *Protein & cell* 6, 792-803.

244. Weissman, I.L. (2000). 'Stem cells: units of development, units of regeneration, and units in evolution'. *Cell* 100, 157-168.

245. Widera, D., Mikenberg, I., Elvers, M., Kaltschmidt, C., Kaltschmidt, B. (2006a). 'Tumor necrosis factor alpha triggers proliferation of adult neural stem cells via IKK/NF-kappaB signaling'. *BMC Neurosci* 7, 64.

246. Widera, D., Mikenberg, I., Kaltschmidt, B., Kaltschmidt, C. (2006b). 'Potential role of NF-kappaB in adult neural stem cells: the underrated steersman?'. *International journal of developmental neuroscience : the official journal of the International Society for Developmental Neuroscience* 24, 91-102.

247. Wolf, S.A., Steiner, B., Wengner, A., Lipp, M., Kammertoens, T., Kempermann, G. (2009). 'Adaptive peripheral immune response increases proliferation of neural precursor cells in the adult hippocampus'. *FASEB J* 23, 3121-3128.

248. Wong, G., Goldshmit, Y., Turnley, A.M. (2004). 'Interferon-gamma but not TNF alpha promotes neuronal differentiation and neurite outgrowth of murine adult neural stem cells'. *Experimental neurology* 187, 171-177.

249. Wu, H., Coskun, V., Tao, J., Xie, W., Ge, W., Yoshikawa, K., Li, E., Zhang, Y., Sun, Y.E. (2010). 'Dnmt3a-dependent nonpromoter DNA methylation facilitates transcription of neurogenic genes'. *Science* 329, 444-448.

250. Wu, J.P., Kuo, J.S., Liu, Y.L., Tzeng, S.F. (2000). 'Tumor necrosis factor-alpha modulates the proliferation of neural progenitors in the subventricular/ventricular zone of adult rat brain'. *Neuroscience letters* 292, 203-206.

251. Yeh, W.C., Shahinian, A., Speiser, D., Kraunus, J., Billia, F., Wakeham, A., de la Pompa, J.L., Ferrick, D., Hum, B., Iscove, N., Ohashi, P., Rothe, M., Goeddel, D.V., Mak, T.W. (1997). 'Early lethality, functional NF-kappaB activation, and increased sensitivity to TNF-induced cell death in TRAF2-deficient mice'. *Immunity* 7, 715-725.

252. Young, K.M., Fogarty, M., Kessaris, N., Richardson, W.D. (2007). 'Subventricular zone stem cells are heterogeneous with respect to their embryonic origins and neurogenic fates in the adult olfactory bulb'. *The Journal of neuroscience : the official journal of the Society for Neuroscience* 27, 8286-8296.

253. Young, K.M., Mitsumori, T., Pringle, N., Grist, M., Kessaris, N., Richardson, W.D. (2010). 'An Fgfr3-iCreER(T2) transgenic mouse line for studies of neural stem cells and astrocytes'. *Glia* 58, 943-953.

254. Youssef, K.K., Van Keymeulen, A., Lapouge, G., Beck, B., Michaux, C., Achouri, Y., Sotiropoulou, P.A., Blanpain, C. (2010). 'Identification of the cell lineage at the origin of basal cell carcinoma'. *Nature cell biology* 12, 299-305.

255. Zhang, J.M., An, J. (2007). 'Cytokines, inflammation, and pain'. *International anesthesiology clinics* 45, 27-37.

256. Zheng, W., Nowakowski, R.S., Vaccarino, F.M. (2004). 'Fibroblast growth factor 2 is required for maintaining the neural stem cell pool in the mouse brain subventricular zone'. *Dev Neurosci* 26, 181-196.

257. Zhu, J., Nathan, C., Jin, W., Sim, D., Ashcroft, G.S., Wahl, S.M., Lacomis, L., Erdjument-Bromage, H., Tempst, P., Wright, C.D., Ding, A. (2002). 'Conversion of proepithelin to epithelins: roles of SLPI and elastase in host defense and wound repair'. *Cell* 111, 867-878.

258. Ziegler, A.N., Schneider, J.S., Qin, M., Tyler, W.A., Pintar, J.E., Fraidenraich, D., Wood, T.L., Levison, S.W. (2012). 'IGF-II promotes stemness of neural restricted precursors'. *Stem Cells* 30, 1265-1276.

259. Ziv, Y., Ron, N., Butovsky, O., Landa, G., Sudai, E., Greenberg, N., Cohen, H., Kipnis, J., Schwartz, M. (2006). 'Immune cells contribute to the maintenance of neurogenesis and spatial learning abilities in adulthood'. *Nature neuroscience* 9, 268-275.

260. Zonis, S., Pechnick, R.N., Ljubimov, V.A., Mahgerefteh, M., Wawrowsky, K., Michelsen, K.S., Chesnokova, V. (2015). 'Chronic intestinal inflammation alters hippocampal neurogenesis'. *J Neuroinflammation* 12, 65.

Resumen

Introducción

Células madre adultas: unidades funcionales de la homeostasis y la reparación tisular. Las células madre (SCs, del inglés *Stem Cell*) adultas son células únicas con capacidad de perpetuarse (auto-renovación) mientras producen nuevas células diferenciadas propias de cada tejido (multipotencia) y representan el componente esencial para el mantenimiento de la homeostasis y la reparación de tejidos en organismos multicelulares. En condiciones homeostáticas, las SCs son células relativamente quiescentes que se dividen infrecuentemente para producir nuevas SCs y células de ciclo rápido no auto-renovantes, o progenitores de rápida amplificación (TAPs, del inglés *Transit Amplifying Cells*) que proliferarán durante un número discreto de ciclos para terminar diferenciandose en células funcionales de cada tejido en particular. Este proceso requiere un equilibrio finamente regulado entre auto-renovación, proliferación y diferenciación celular para garantizar el correcto reemplazo de células dañadas y al mismo tiempo limitar situaciones patológicas como el cáncer.

En las últimas décadas, se han identificado multitud de poblaciones de SCs residiendo en muy diversos tejidos y su caracterización ha puesto de manifiesto la existencia de una notable diversidad en cuanto a los marcadores de identificación, el grado de multipotencialidad o su dinámica proliferativa. En realidad, las SCs representan un conjunto de células individuales en diferentes estados proliferativos (quiescentes o activos) con distintas predisposiciones en la respuesta a estímulos externos.

La quiescencia es un estado del ciclo celular no proliferativo reversible (G_o) y, a diferencia de células post-mitóticas, las SCs quiescentes mantienen la capacidad de re-entrar en ciclo y proliferar. Actualmente se conoce que esta condición no es un proceso celular inactivo por defecto sino que más bien representa un estado activamente regulado por multiples señales del nicho que les rodea. Además, en distintos tejidos, se ha visto que después de una lesión esta población es capaz de

aumenta drásticamente su proliferación mostrando una enorme capacidad regenerativa. Recientemente se ha descrito en músculo y en tejido hematopoyetico que las SCs quiescentes son capaces de responder a una lesión distante mostrando propiedades de un estado pre-activado. Este estado quiescente en alerta (G_{alert}), como se ha definido, y comparado con el estado inactivo (G_o), muestra una mayor predisposición a entrar en proliferación, una entrada acelerada en el ciclo celular, una mayor actividad mitocondrial y un tamaño ligeramente más grande. Además, los perfiles globales de transcripción sugieren que representa un estado intermedio entre G_o y las SC activas. Estas poblaciones de SCs parecen adoptar este estado en respuesta a las lesiones remotas cuyo impacto en la fisiología del tejido no es suficiente para promover su activación. Estos datos han demostrado que las SCs también experimentan transiciones dinámicas entre las distintas fases funcionales de quiescencia e indican que las SCs quiescentes adoptan un estado adaptativo en respuesta a señales que pueden ser producidas en regiones remotas del organismo, sugiriendo la existencia de un control homeostático global de las SCs adultas. Sin embargo, la relevancia de la regulación de esta transición en homeostasis y regeneración tisular o la naturaleza de los reguladores que controlan la adquisición de un estado alerta o un estado inactivo no se conocen todavía.

Células madre neurales (NSCs) subependimales y neurogénesis adulta. En el cerebro adulto de los mamíferos se detecta neurogénesis en dos "nichos neurogénicos": el giro dentado (SGZ) y la zona subependimaria o ventricular-subventricular (SEZ o V-SVZ). Las células madre neurales (NSCs, del inglés *Neural Stem Cells*) de la SEZ y su progenie están distribuidos a lo largo de las paredes laterales delos ventrículos laterales y son responsables de la producción continua de nuevas neuronas destinadas al bulbo olfactorio (OB). Este proceso sigue una progresión jerárquica en la que las NSCs multipotentes, identificadas inicialmente como células de tipo B1, tras activarse, dan lugar a TAPs o células de tipo C que se

dividen unas pocas veces más antes de convertirse en neuroblastos migratorios o células de tipo A.

Las NSCs adultas o células tipo B1 son células gliales derivadas de la glia radial embrionaria que comparten características ultraestructurales y moleculares con otros astrocitos cerebrales como la expresión de los marcadores GFAP, GLAST y BLBP. Una vez aisladas de la SEZ, las NSCs pueden ser cultivadas *in vitro* en presencia de factor de crecimiento epidérmico (EGF) o fibroblástico básico (FGF2). En estas condiciones, las NSCs proliferan activamente y pueden ser cultivadas de forma prácticamente ilimitada. Además son capaces de diferenciarse a neuronas, oligodendrocitos y astrocitos, lo que demuestra su multipotencialidad.

En los últimos años, varios trabajos han demostrado la co-existencia de NSCs que difieren en el grado de actividad dentro de su relativa quiescencia encontrándose NSCs en estado "durmiente" (G_0) o NSCs quiescentes (qNSCs) y, por otra parte, NSCs en estado "activado" (aNSCs, en ciclo activo, aunque lento). Además, el análisis del perfil de expresión de NSCs a nivel individual, tanto en condiciones homeostáticas como en condiciones de daño cerebral, han sugerido la existencia de células quiescentes en un estado 'alerta' (qNSC2) o competentes para la activación en respuesta a distintas señales, diferenciándose del resto de quiescentes en estado durmiente (qNSC1). Sin embargo, todavía se desconoce si la transición al estado alerta es reversible y cuál es su posible implicación en el mantenimiento del reservorio de NSCs. Una adecuada renovación tisular, tanto en homeostasis como tras una lesión, depende de un equilibrio finamente regulado entre quiescencia y activación, auto-renovación, proliferación y diferenciación de las SCs. En los nichos neurogénicos adultos se han descrito múltiples factores, tanto determinantes intrínsecos de las propias NSCs como señales externas provenientes del nicho, que participan en el control la función de las NSCs, como son interacciones directas con células mesenquimales, vasculares, neuronales,

gliales o inflamatorias, factores solubles producidos por éstas, señales de la matriz extracelular o parámetros físicos como la disponibilidad de oxígeno.

Regulación de las NSCs adultas por el sistema inmune innato. Actualmente no existe duda de que la neuroinflamación, tanto en situaciones agudas como crónicas, afecta de múltiples maneras a las NSCs. Las SCs adultas en distintos tejidos pueden ser activadas por lesión para producir progenie y contribuir a la reparación del tejido, aunque actualmente se desconoce en profundidad cuáles son los factores desencadenantes y los reguladores moleculares de esta activación. Los organismos vivos están constantemente expuestos a una variedad de estímulos internos y externos y algunos de ellos pueden clasificarse como señales de peligro. Cuando se detectan tales señales, se pone en marcha una respuesta compleja que está dirigida por un lado a eliminar dichas señales de peligro y, por otro, a restaurar la homeostasis de los tejidos. Esta respuesta se conoce como inflamación y es parte del sistema inmune innato presente en todos los metazoos. En vertebrados, la activación del sistema inmune en respuesta a una lesión ha evolucionado para promover el sellado de heridas y cicatrices protegiendo el tejido dañado de mamíferos homeotermos adultos de la invasión de patógenos de una manera muy rápida y eficiente. Sin embargo, esta refinada respuesta inmune adaptativa conlleva la pérdida de regeneración epimórfica característica de los vertebrados de sangre fría. A pesar de esta pérdida de capacidad regenerativa, las SCs residentes en los tejidos de mamíferos adultos mantienen cierto recambio celular a través de la producción de nuevas células y podrían, por lo tanto, ser consideradas como contrapartidas naturales de las células implicadas en la regeneración previa a la evolución.

Las células madre adultas son sensibles a su nicho ya que se comportan integrando acciones de reguladores intrínsecos en respuesta a las señales que emanan tanto de su microambiente más inmediato así como de la circulación. Se ha demostrado que la inflamación es capaz de actuar sobre varios nichos de SCs, pero la

observación tanto de efectos perjudiciales como beneficiosos mantiene en controversia el papel preciso de la inflamación en el mantenimiento y la regeneración de los tejidos. En el caso del sistema nervioso central, en particular, existe evidencia experimental acumulada en la última década que indica que la inflamación puede desempeñar un papel negativo en la neurogénesis de mamíferos adultos. En cambio, en el cerebro de vertebrados no mamíferos existen NSCs que son capaces de regenerar el tejido cerebral después de una lesión traumática a través de la activación de programas moleculares inducidos por la propia lesión y la señalización relacionada con inflamación.

El factor de necrosis tumoral alfa (*TNF-α*, del inglés *Tumor Necrosis Factor alpha*) y progranulina (PGRN): TNF-α es una proteína caracterizada inicialmente como citoquina pro-inflamatoria implicada en la respuesta inmune innata. Sin embargo, en los últimos años se ha descrito que es una proteína multifuncional con múltiples actividades en diferentes sistemas. En el cerebro adulto, TNF-α es producida por microglía y macrofagos infiltrantes pero también por astrocitos y neuronas tras un proceso de daño. Se expresa inicialmente en forma de proteína precursora transmembrana de tipo II (tm-TNF-α o pro-TNF-α) la cual es cortada proteolíticamente en la membrana celular por la metaloproteasa TACE (del inglés *TNF-α Converting Enzyme*) para dar lugar a la forma soluble homotrimerica sTNF-α. Ambos ligandos son biológicamente activos e interaccionan con dos receptores trans-membrana glicosilados, TNF-Receptor 1 (TNFR1) and TNF-Receptor 2 (TNFR2). La unión de TNF-alfa con TNFR1 generalmente induce apoptosis y citotoxicidad mientras que la activación de TNFR2 se ha asociado con protección celular y proliferación. TNFR1, a diferencia de TNFR2, presenta un dominio de muerte celular (TRADD, del inglés *TNF Receptor-Asociated Death Domain*) el cual permite el reclutamiento de caspasas y la consiguiente inducción de apoptosis. Además, la unión del Factor Asociado a Receptor TNF 2 en ambos receptores (TRAF2, del inglés *TNF Receptor-Asociated Factor 2*) resulta en la activación de RIP (del inglés

Receptor Interacting Protein) y la inducción de las vías de señalización NFkB, p38, JNK y ceramida/esfingomielinasa.

TNFR2 puede ser activado también por progranulina (PGRN), una glicoproteína de secreción que, en el sistema nervioso central adulto, está presente en neuronas y microglía. Además, la expresión de PGRN aumenta dramáticamente cuando la microglía se activa por lesión. Una vez es secretada, PGRN puede ser cortada en siete péptidos de granulina (GRN) y una paragranulina que contiene una mitad de la granulina por metaloproteinasas tales como MMP-9, MMP-14 y ADAMTS-7, o las proteasas de serina como elastasa y proteinasa 3. Curiosamente, tanto PGRN como las GRNs constituyentes muestran actividad biológica; PGRN actúa como factor anti-inflamatorio y antagoniza los efectos del TNF-α a través de TNFR2 mientras que las GRN liberadas promueven inflamación.

Objetivos

En la mayoría de los tejidos, las células madre adultas parecen coexistir en dos estados de activación, pero la transición entre estos estados, así como su regulación, siguen siendo ampliamente desconocidas. Además, algunas células madre adultas parecen responder a lesiones remotas de maneras que no se entienden completamente. En este trabajo se propone la hipótesis de que las NSCs adultas reaccionan a señales inflamatorias generadas en la periferia mediante la modificación de su estado de activación dentro del ciclo de quiescencia de células madre.

Los objetivos específicos propuestos para probar esta hipótesis son:

1.- Desarrollo de un protocolo basado en citometría de flujo para la identificación y análisis de NSCs de la zona subependimaria así como de su progenie.

2.- Caracterización del ciclo celular quiescente en NSCs durante regeneración y en respuesta a inflamación.

3.- Análisis de los efectos de los mediadores inflamatorios TNF-α y progranulina y su receptor común TNFR2 en NSCs.

Metodología

Cepas: se han utilizado ratones como modelo de experimentación para la obtención y estudio de las NSCs de la SEZ. A lo largo del trabajo se han usado cepas de varios fondos genéticos: C57Bl6 (silvestre o Wild-type), tnfrsf1a-/- (TNFR1 KO), tnfrsf1b-/- (TNFR2 KO) y tnfrsf1a-/-;tnfrsf1b-/- (TNFR DKO).

Inmunohistoquímica y análisis *in vivo*: para realizar las detecciones de retención de análogos de timidina en células de división lenta en el cerebro adulto (LRCs), los ratones recibieron siete inyecciones intraperitoneales de CldU a una dosis de 50 µg/g de peso corporal del animal cada dos horas, y se sacrificaron 28 días después. 1h antes del sacrificio, se inyectó también intraperitonealmente una dosis de 10 mg/ml de IdU para la detección de células en proliferación. Posteriormente, los ratones se perfundieron intracardíacamente con paraformaldehído 4% (PFA) en tampón fosfato 0.1M, pH 7.4 (PB). Después de toda la noche en PFA, los cerebros se lavaron con PB durante 2 horas y el tejido se procesó en un vibratomo. La detección de CldU e IdU se realizó mediante inmunofluorescencia con anticuerpos específicos. Para la detección de células $GFAP^+$, $EGFR^+$ o $Ki67^+$ se usaron anticuerpos primarios específicos y posteriormente se utilizaron los secundarios fluorescentes correspondientes. Para el análisis de cadenas de DCX en wholemount, el tejido fresco recién diseccionado se fijó en PFA 4% durante 24h. Tras permeabilizar y bloquear con 10% FBS y 0.5% TX-100, las cadenas de neuroblastos se analizaron mediante inmuhistoquímica con un anticuerpo específico para DCX y sus correspondientes anticuerpos secundarios.

Citometría de flujo en muestras de SEZ: para el estudio de los distintos estados de las NSCs y su progenie se ha puesto a punto un protocolo de detección por citometría de flujo. Tras disección de la SEZ, el tejido se disgregó primero

enzimáticamente con Tripsina/EDTA y después mecánicamente con pipeta de vidrio pulida. El homogenado de tejido se filtró por 40 µm y se incubó con el kit de eliminación de muerte celular (Miltenyi). Tras separación magnética con columnas MS (Miltenyi), la fracción eluida se incubó con anticuerpos primarios marcados para la detección de las distintas poblaciones residentes en la SEZ: CD45-BUV395, CD31-BUV395, Ter119-BUV395, CD24-PerCP-Cy5.5 (BD), O4-biotin, Glast-APC, CD9-Vio770 (Miltenyi) y EGF-Alexa488 (Invitrogen). Las células muertas se descartaron por la incorporación de Dapi. Las muestras marcadas se analizaron en un equipo LSR Fortessa (BD).

Separación magnética de células Lin^- (MACS®): por otra parte se ha puesto a punto la obtención de muestras de tejido enriquecidas en NSCs. Previamente, tras disociar las muestras de SEZ y filtrarlas, las muestras se incubaron con anticuerpos biotinilados contra CD45, CD31, Ter119, CD24 y O4. Posteriormente, las muestras se incubaron con 30 µl de micropartículas magnéticas anti-biotina (Miltenyi). Las muestras marcadas magnéticamente se cargaron en una columna MS previamente equilibrada en un separador magnético OctoMACS®. La fracción eluida se recogió como fracción Lin^- y la fracción retenida Lin^+ se eluyó una vez separada la columna del imán.

Inducción de inflamación: para la activación de inflamación sistémica se inyectaron intraperitonealmente 5mg/kg de LPS (Sigma-Aldrich). A distintos tiempos se sacrificaron un grupo de animales para el análisis del proceso de inflamación cerebral en tejido mediante la expresión de citoquinas pro-inflamatorias (extracción de mRNA). Para el análisis *in vivo* de la neurogénesis se realizaron técnicas inmunohistoquímicas y de análisis por citometría 24h después de la inyección de LPS. Como control se utilizaron ratones pinchados con suero salino 0.9% y ratones no inyectados (naive). Además, ratones pinchados con suero salino esteril y naive se analizaron a los 3 y 6 días por citometría para analizar el estado NSCs quiescentes al resolverse la inflamación periférica.

Paradigma de regeneración: para la estimulación de la regeneración de la SEZ se inyectó el antimitótico temozolomida (TMZ) a 100 mg/kg/día en salino al 25% DMSO o vehículo durante 3 días de manera consecutiva. A los 3 y a los 35 días se evaluó los efectos de la lesión en SEZ y la reaparición de las distintas poblaciones mediante citometría, formación de esferas primarias y la presencia de cadenas de neuroblastos (DCX+) por inmunohistoquímica en wholemounts.

Cultivo y ensayos celulares en NSCs: ver metodología del grupo de investigación detallada en Belenguer et al., 2016. A partir del establecimiento de cultivos primarios de NSCs, se realizaron ensayos de proliferación y auto-renovación mediante ensayo de neuroesferas, además de estudios de ciclo celular por tinción con ioduro de propidio y de viabilidad celular mediante ensayo enzimático MTS o detección de la actividad caspasa 3 por inmunocitoquímica. La expansión de NSCs en cultivo se analizó mediante inmunocitoquímica para EGFR en células recién divididas y mediante el análisis de la capacidad diferenciativa de clones aislados. Durante los experimentos con cultivos de NSCs, se han utilizado distintos reactivos como TNF-α recombinante murino (R&D) y anticuerpos agonistas específicos para TNFR1 (R&D) y TNFR2 (Hycult Biotech). Además, para ensayos de rutas de señalización se ha utilizado el inhibidor específico de la ruta de p38, SB203580.

Medios condicionados por microglía activada: se han utilizado células de la línea de microglía para el acondicionamiento del medio de NSCs. Previamente, se estimularon las células a un estado pro-inflamatorio M0 con 250 ng / ml de LPS. El medio de NSCs condicionado por microglía se incubó con 2,5 µg / ml de anticuerpo anti-TNF-α o con un anticuerpo no relacionado a la misma concentración para la inmunodepleción específica de TNF-α mediante la unión a Dynabeads® magnéticas acopladas a Protein G y separación usando un imán DYNAL® (Invitrogen). El medio condicionado resultante se diluyó 1: 4 en medio NSCs fresco para el tratamiento de cultivos de NSCs en un ensayo de neuroesferas.

Evaluación de la dinámica de proliferación celular por dilución de marcadores fluorescentes: homogenados celulares obtenidos a partir la SEZ se marcaron el trazador fluorescente permeable DDAO-SE (Thermo Fischer, nº cat. C34553). Después de 10 días, las neurosferas primarias resultantes fueron disociadas para una segunda ronda de carga usando el trazador fluorescente Oregon Green 488 Carboxy- DFFDA-SE (Thermo Fischer, cat. C34555). Después de 3 días en cultivo, se disociaron las neurosferas secundarias y se midió la intensidad de fluorescencia de cada marcador celular en un citómetro de flujo FACS Fortessa (BD).

Medida de actividad mitocondrial: células individuales se tiñeron con la sonda fluorescente MitoTrackerTM Orange CM-H2TMRos y la actividad mitocondrial se determinó mediante análisis de la intensidad fluorescente por citometría de flujo en FACS Fortessa (BD).

Análisis de expresión génica por ARN: se obtuvieron muestras de ARN a partir de SEZ o de células aisladas utilizando el Kit de Tejido de ARN simple Maxwell® 16 LEV (Promega, nº de cat. AS1280) y se convirtió a ADNc por RT-PCR utilizando el kit PrimeScript™ RT-PCR Kit (Clontech, cat. no. RR014B). El análisis de expresión génica se evaluó mediante PCR en tiempo real usando 5-10 ng de ADNc, sondas Taqman específicas (Applied Biosystems) y el kit de amplificación Premix Ex TaqTM (Probe qPCR) (Clontech, nº de cat. RR390A). La PCR en tiempo real se realizó en un dispositivo Step One Plus (Applied Biosystems). El nivel de expresión de cada gen se obtuvo por cuantificación relativa (2e-ΔΔCt) utilizando la expresión constitutiva de genes Gapdh y 18S como controles endógenos.

Ensayos de activación de la vía de NFκB: se introdujo en las células un plásmido reportero de luciferasa de la vía NFκB (5xkB-luc) junto con un reportero control de luciferasa de Renila, mediante electroporación con un Nucleofector (II)® (Amaxa Biosystems) y el Kit de Nucleofección de NSCs de ratón (Mouse NSC Nucleofector Kit; Amaxa Biosystems). Para las determinaciones, tras la estimulación con el factor TNF-alfa o agonistas específicos para cada receptor, se lisaron las células y se

analizó la expresión del reportero mediante el Dual Luciferase Assay System Kit, de Promega. Los extractos celulares se obtuvieron mediante lisis en Passive Lysis Buffer (Promega). La actividad luciferasa se determinó mediante un equipo Victor®3 (Perkin Elmer) en placas de 96 con 20 µl del lisado celular por pocillo, tras añadir solución Stop & Glo (Promega) y usando la actividad luciferasa de Renila como control positivo.

Determinaciones de la actividad de vías de señalización mediante western blot y Milliplex®: se realizaron extracciones de proteínas de NSCs en cultivo crecidas durante 1h utilizando el tampón de lisis MILLIPLEX MAP (Millipore, cat no. 43-040). Por una parte se midió el estado fosforilado y la cantidad total de CREB, JNK, NF-κB, p38, AKT, p70S6K y STAT3 con el kit de señalización de multiplex MILLIPLEX® MAP 9-plex Phosphoprotein (Millipore, nº de cat .: 48- 680MAG) y el kit de señalización MILLIPLEX® MAP 9-plex Multi-Path Magnetic Bead Signaling Total (Millipore, nº de catálogo: 48-681MAG) siguiendo las instrucciones del fabricante. Además se realizó una detección por western blot de la actividad de p38 utilizando anticuerpos específicos de las formas totales y fosforiladas y anticuerpos secundarios conjugados con HRP y el sistema de detección quimioluminiscente (ECL; Amersham).

Resultados

Este trabajo ha abordado la posibilidad de que las células madre neurales adultas del cerebro de roedor puedan responder positivamente a ciertas señales inflamatorias, una reacción que parece ser oscurecida por los efectos perjudiciales más dramáticos de las citoquinas inflamatorias en la neurogénesis.

Para ello, previamente hemos puesto a punto y validado una estrategia de identificación de NSCs y su progenie en la SEZ y en el OB mediante la utilización de marcadores de superficie. Tras una exclusión de marcadores CD45, CD31, Ter119, CD24 y O4, las NSC, los TAPs y neuroblastos son identificados en base a GLAST, CD9

y CD24. Hemos encontrado, en concordancia con un trabajo anterior, que la elevada expresión de CD9 distingue las NSCs de astrocitos no neurogénicos dentro de la población GLAST+. Por otro lado, contrariamente a lo que se había descrito, observamos que las NSCs pueden mostrar un cierto nivel de expresión de CD24, marcador que siempre se había asociado a neuroblastos. Proponemos que durante la transición de NSCs hacia neuroblasto, las células comienzan a expresar CD24, incrementando progresivamente su expresión en al convertirse en TAPs, llegando a la máxima expresión en neurobñastos. Finalmente, la presencia de EGFR dentro de la población de NSCs GLAST+/CD9+ permite diferenciar entre estados activados y quiescentes.

La identificación de distintos estados quiescentes (qNSC1 y qNSC2) nos ha permitido además determinar que el estado alerta de las qNSCs representa un estado intermedio reversible entre latencia y activación. Además, este estado muestra propiedades de pre-activación como son un mayor tamaño, la predisposición a formar neuroesferas y el aumento de actividad mitocondrial cuando son cultivadas *in vitro*. En este trabajo hemos observado que las NSCs adquieren este estado incluso tras un pinchazo intraperitoneal de suero salino estéril pero, a diferencia de una inflamación sistémica mediada por LPS o durante un proceso de regeneración inducida por TMZ, donde las NSCs sufren además un proceso de activación, en este caso las qNSC2 no llegan a activarse volviendo progresivamente a su estado basal. Curiosamente, en respuesta a estos estímulos que tienen en común la movilización del reservorio de qNSCs, ya sea para activarse (inyecciones de TMZ y LPS) o simplemente para adquirir un fenotipo alerta transitorio (inyección salina), se observa un aumento de los mediadores inflamatorios TNF-α y PGRN en la SEZ sugiriendo que ambos podrían actuar como factores de nicho regulando estos procesos.

Ensayos en cultivos de NSCs muestran que TNF-α, a través de su unión a TNFR1, reduce la proliferación y viabilidad de las NSCs. Sin embargo, la unión tanto de TNF-

α como de progranulina a TNFR2 modula la auto-renovación de las NSCs, promoviendo divisiones simétricas y expandiendo una población de NSCs multipotentes que mantienen propiedades de ciclo lento y una actividad mitocondrial alta. Además, esta señalización de TNFR2 en NSCs está relacionada con la vía de señalización p38 MAP quinasa, pero no con el control transcripcional de Nf-κB, y dicha activación media la expansión de NSCs inducida por TNFR2. Sin embargo, análisis de cultivos organotípicos de SEZ *ex vivo*, el cual hemos descubierto que preserva la quiescencia de NSCs, revela que la estimulación TNFR2 promueve la transición de un estado qNSC1 latente a un estado qNSC2 de alerta.

En este trabajo hemos encontrado que las NSCs pueden detectar y responder a las lesiones periféricas remotas y que la señalización TNFR2, en respuesta a las citoquinas TNF-α y progranulina, participa en este proceso y media efectos positivos de la inflamación en el comportamiento de las NSCs y la neurogenesis. El primer hallazgo es congruente con datos recientes que indican que las células madre adultas de diferentes sistemas pueden reaccionar a lesiones lejanas, lo que sugiere un control homeostático de su actividad a nivel organizacional. El segundo aumenta nuestra comprensión del papel de la inflamación en el proceso neurogénico. Aunque la opinión más aceptada es que la inflamación aguda o crónica juega un papel negativo en la neurogénesis, nuestros datos revelan efectos beneficiosos concomitantes de citoquinas inflamatorias en al menos una fracción de células madre neurales.

Además, hemos encontrado que la respuesta a señales periféricas o inflamación aguda, implica la transición de NSC quiescentes de un estado inactivo a un estado de pre-activación. Este estado de alarma qNSC2 no se conocía hasta hace un par de años, y por lo tanto, se sabe muy poco sobre su comportamiento y regulación. En este trabajo se proporcionan nuevos datos que revelan la implicación de la señalización de TNFR2, muy probablemente a través de la transducción intracelular de p38, en la regulación de estas células qNSC2, su comportamiento *in vitro* y su

papel durante la regeneración y en respuesta a lesión. Estos efectos previamente desconocidos añaden una pieza más a la incipiente investigación de la regulación de la quiescencia / activación en NSCs.

Conclusiones

1. Hemos desarrollado y probado en diferentes escenarios, un nuevo panel de citometría de flujo, basado exclusivamente en la detección de marcadores de superficie, para la identificación de células madre neurales de la zona subependimaria en diferentes estados de quiescencia (qNSC1 y qNSC2) y proliferación, así como de su progenie más comprometida.

2. En la zona subependimaria adulta, señales inflamatorias tales como TNF-α y progranulina promueven una salida del estado quiescente qNSC1 pero, como paso previo a la activación completa, adquieren un estado transitorio de alerta qNSC2 que presenta mayor predisposición a la activación.

3. Daños periféricos leves, como una inyección intraperitoneal de solución salina estéril, inducen la expresión de señales inflamatorias en la zona subependimaria promoviendo la transición de un estado durmiente qNSC1 a un estado alerta qNSC2, el cual regresa progresivamente al estado latente tras la resolución de la neuroinflamación.

4. TNF-α, a través de TNFR1, produce efectos perjudiciales sobre la proliferación y supervivencia de las células madre neurales, mientras que TNF-α y PGRN expanden la población de células madre neurales multipotentes *in vitro*, manteniendo sus propiedades, a través de su unión a TNFR2.

5. La señalización mediada por TNFR2, muy probablemente a través de la transducción intracelular por p38, actúa sobre las células madre neurales en estado qNSC1 promoviendo un cambio al estado alerta qNSC2.

6. Las condiciones del cultivo *in vitro* promueven la activación forzosa de las qNSCs; sin embargo, una pequeña fracción de células del cultivo, la cual puede expandirse mediante la estimulación de TNFR2, conserva algunas características que recuerdan al estado quiescente encontrado *in vivo*.